

RADAR AND MULTISPECTRAL IMAGE FUSION OPTIONS FOR IMPROVED LAND
COVER CLASSIFICATION


by

Erwin J. Villiger
A Dissertation
Submitted to the
Graduate Faculty
of
George Mason University
in Partial Fulfillment of
The Requirements for the Degree
of
Doctor of Philosophy
Environmental Science and Public Policy

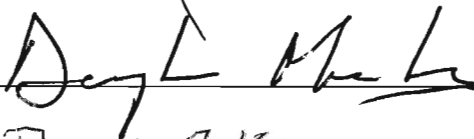
Committee:



Dr. Barry N. Haack,
Dissertation Director



Dr. Allan Falconer,
Committee Member



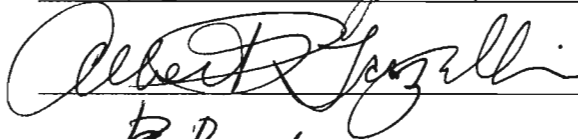
Dr. Douglas Muchoney,
Committee Member




Dr. Donald Kelso,
Committee Member



Dr. R. Christian Jones,
Department Chairperson



Dr. Albert P. Torzilli,
Program Director



Dr. Peter Becker, Associate
Dean for Graduate Studies,
College of Science



Dr. Vikas Chandhoke, Dean,
College of Science

Date: April 24, 2008

Spring Semester 2008
George Mason University
Fairfax, VA

Radar and Multispectral Image Fusion Options for Improved Land Cover
Classification

A dissertation submitted in partial fulfillment of the requirements for the degree
of Doctor of Philosophy at George Mason University

By

Erwin J. Villiger
Master of Science
George Mason University, 1996

Director: Barry N. Haack, Professor
Department of Geography

Spring Semester 2008
George Mason University
Fairfax, VA

Copyright 2008, Erwin J. Villiger
All Rights Reserved

ACKNOWLEDGEMENT

I would like to thank my committee members for their guidance, wisdom, support, and most specifically their patience with me in pursuing this research. Dr. Barry Haack, a scholar and a gentleman, I consider my mentor and a model of professional and intellectual bearing.

Neal Sealy with Media Enterprises Ltd, the citizens of Staniard Creek, North Andros Island, and the Bahamas Environmental Research Center, provided significant support and a base of operations for the field work portion of this project. Dr. Ted Bradley was instrumental in identifying appropriate study sites and his knowledge of the flora of Andros Island was invaluable.

Data for this project was provided through funding from the United States National Aeronautical and Space Administration Application Development and Research Opportunity program under Grant Numbers NAGW 4970 and NAG5 4140.

TABLE OF CONTENTS

	Page
List of Tables.....	vi
List of Figures.....	viii
Abbreviations.....	x
Abstract.....	xii
1. Introduction	1
2. State of the Research.....	12
Remote Sensing Concepts.....	12
Multispectral Imagery (MSI) Land Cover Assessment	17
Radar (SAR) Remote Sensing Concepts.....	22
SAR Wavelength	24
Incident Angle	25
Look Direction.....	26
Number of Looks	28
Pixel Spacing and Resolution.....	29
Polarization.....	30
Vegetation Analysis with Radar	31
Speckle Reduction.....	40
Assessment of Texture in Radar Imagery	48
Analysis Using Angle of Incidence	51
Time-Series Analysis	54
MSI and SAR Image Fusion.....	61
Discussion	77
3. Methodology.....	80
Research Objectives	80
Study Site.....	81
Pinelands	83
Coppice.....	85
Rockland.....	86

Saw Grass Marsh	87
Mangrove	88
Differentiation of Cover types.....	89
Datasets	90
Remotely Sensed Data.....	90
Multispectral (MSI) Imagery	91
Synthetic Aperture Radar (SAR) Imagery	92
Geocover Ortho Imagery	95
Ground Truth	95
Cartographic Datasets	96
Analysis Process.....	97
TM Image Processing	98
SAR Image Processing.....	99
SAR Speckle Suppression Algorithms	100
SAR Processing Paths.....	102
TM Processing Paths.....	104
4. Results.....	108
Processing of Landsat TM.....	108
Processing of Unfiltered SAR.....	113
Collection Modes	119
Seasonality	123
Seasonal and Multitemporal Combinations.....	124
SAR Speckle Suppression	129
SAR Texture	139
SAR Texture in Speckle Suppressed Datasets	149
Landsat TM Fused with Unfiltered SAR	156
Landsat TM Fused with Speckle Suppressed SAR	159
Landsat TM Fused with SAR Texture.....	162
Various Combinations.....	167
5. Discussion and Future Research.....	181
Discussion	181
Future Research.....	187
Conclusion	191
References	193

LIST OF TABLES

Table	Page
2.1 SAR Bands.....	24
3.1 Acquired RADARSAT Standard Beam Modes	94
3.2 Calibration and Validation Sites	96
4.1 Classification Results of Landsat TM.....	109
4.2 Contingency Table for Wet TM Classification Results	110
4.3 Contingency Table for Combined Dry TM and Wet TM	111
4.4 Unfiltered SAR Classification Accuracy Results	114
4.5 Contingency Table SAR 0510	115
4.6 Contingency Table SAR 0517	116
4.7 Summary Statistics for 21 SAR datasets	118
4.8 Classification Accuracy by Incident Angle	120
4.9 Classification Accuracy by Look Direction	122
4.10 Average Accuracy by Season	123
4.11 Best Scene Accuracy for Each Season.....	124
4.12 Multitemporal Dataset Classification Accuracy	125
4.13 Multitemporal Dry Season Contingency Table	127
4.14 Multitemporal Wet Season Contingency Table.....	127
4.15 Multitemporal Combined SAR Contingency Table.....	128
4.16 Average Total Classification Accuracy by Speckle Suppression Filter	130
4.17 SAR 0418 Dataset Unfiltered	133
4.18 SAR 0418 Dataset Filtered with GM at 11x11 kernel	133
4.19 SAR 0416 Frost 9x9.....	135
4.20 SAR 0510 Frost 9x9.....	136
4.21 Average Classification Results for Speckle Suppressed Multitemporal SAR (21 scenes)	137
4.22 Average Classification Accuracy of Variance Texture Measure	140
4.23 Multitemporal SAR Classification Accuracy by Variance (21 scenes)	146
4.24 SAR 0418 Unfiltered	150
4.25 Classification Accuracy for SAR 0418, Speckle Suppressed	150
4.26 SAR 0418 Speckle Suppressed Gamma-MAP 7x7.....	151

4.27	Classification Accuracy for SAR 0418, Texture Measure	151
4.28	SAR 0418 Variance Texture Measure with 9x9 kernel.....	152
4.29	SAR 0418, Speckle Suppression followed by Variance Texture.....	153
4.30	SAR 0418 GM 7x7 followed by Variance Texture Measure at 9x9.....	155
4.31	TM and Unfiltered SAR Classification Results.....	157
4.32	Average Classification Accuracy by Season Combination	157
4.33	Fused TM and Speckle Suppressed SAR Average Accuracy Results ...	159
4.34	Classification Results for Dry TM and SAR 1203	161
4.35	Fused TM and SAR Texture Measure Average Accuracy Results	163
4.36	SAR 0418 as Three-banded Image (Unfiltered, GM7, VAR11)	169
4.37	SAR 0418 Process Combinations with Dry TM	170
4.38	SAR 1203 as Three-banded Image (Unfiltered, GM7, VAR11)	173
4.39	SAR 1203 Process Combinations with Dry TM	174
4.40	DryTM, and All SAR Processed at GM09	180

LIST OF FIGURES

Figure	Page
2.1 Electromagnetic Spectrum.....	13
2.2 Spectral Curve for Green Vegetation	14
2.3 Example Spectral Curves for Different Cover Types.....	15
2.4 Example Sampling Regions for 5-banded MSI.....	15
2.5 SAR Incident Angle	25
2.6 The Multi-look Effect.....	28
2.7 The Neighborhood Filter Process	42
3.1 Andros Island, The Bahamas.....	81
3.2 Pinelands Cover Type	84
3.3 Coppice Cover Type	85
3.4 Rockland Cover Type.....	86
3.5 Saw Grass Cover Type	87
3.6 Mangrove Cover Type	88
3.7 Landsat Thematic Mapper Imagery Bands 7,4,2.....	92
3.8 RADARSAT Standard Beam Mode 3 Descending.....	94
3.9 Image Processing Paths.....	103
4.1 Total Classification Accuracy for Unfiltered SAR.....	117
4.2 Average Classification Accuracy for Speckle Suppressed SAR.....	131
4.3 Average Classification Results for Speckle Suppressed Multitemporal SAR (21 scenes).....	138
4.4 Average Classification Accuracy of Variance Texture Measure	140
4.5 SAR Classification Accuracy for Variance with a 15x15 Kernel	142
4.6 Comparative Average Texture Classification Accuracy by System Mode and Kernel Size	143
4.7 Comparative Average Texture Classification Accuracy by Angle of Incidence and Kernel Size.....	145
4.8 Accuracy Results of Texture Measure for Multitemporal SAR (21 scenes).....	146
4.9 Classification Accuracy of Land Cover Classes for Multitemporal SAR by Texture Kernel (21 scenes).....	148
4.10 SAR 0418 Speckle Suppressed followed by Variance Texture Measure	154

4.11	Fused TM and Speckle Suppressed SAR, Average Accuracy Results ...	161
4.12	Fused TM and SAR Texture Measure Average Accuracy Results	163
4.13	Fused TM and SAR Texture Measure by Collection Mode	164
4.14	Fused TM and SAR Texture Measure by Incident Angle	165
4.15	Comparative Average Classification of TM/SAR Texture	166
4.16	Unfiltered SAR 0418 and Filtered SAR 0418 Datasets	168
4.17	Unfiltered SAR 1203 Coupled with Filtered SAR 1203 Datasets	171
4.18	Multitemporal SAR GM09 Classified as Multiband Images	175
4.19	DryTM B1-B4, Combined with SAR Couple (Unfiltered, GM09)	177
4.20	Dataset Selection Using Transformed Divergence.....	179

LIST OF ABBREVIATIONS

AVHRR	Advanced Very High Resolution Radiometer
BERC	Bahamas Environmental Research Center
CCA	Canonical correlation analysis
DN	Digital number
EMS	Electromagnetic Spectrum
ERS	European Remote Sensing
ETM+	Enhanced Thematic Mapper + (Landsat)
FR	Frost speckle suppression filter
GM	Gamma-MAP speckle suppression filter
GPS	Global Positioning System
GSD	Ground sample distance
HH	Horizontal/Horizontal
HV	Horizontal/Vertical
IR	Infrared Imagery
IHS	Intensity, Hue, Saturation
JERS	Japanese Earth Resources Satellite
LAI	Leaf area index
MAP	Maximum A Posteriori
MLC	Maximum Likelihood Classifier
MS	Multispectral
MSI	Multispectral Imagery
MSS	Multispectral Scanner (Landsat)
NDVI	Normalized Difference Vegetation Index
OPS	Optical Sensor (JERS)
Pan	Panchromatic
PCA	Principal Components Analysis
RGB	Red, Green, Blue
RMS	Root Mean Square
SAR	Synthetic Aperture RADAR
SIR-A	Shuttle Imaging Radar-A
SIR-B	Shuttle Imaging Radar-B
SIR-C	Shuttle Imagine Radar-C
SPOT	Satellite pour l'Observation de la Terre

ST	Standard beam
TC	Tasseled Cap
TM	Thematic Mapper (Landsat)
UTM	Universal Transverse Mercator
VAR	Variance texture measure
VH	Vertical/horizontal
VV	Vertical/Vertical
WGS	World Geodetic System

ABSTRACT

RADAR AND MULTISPECTRAL IMAGE FUSION OPTIONS FOR IMPROVED LAND COVER CLASSIFICATION

Erwin J. Villiger, Ph.D.

George Mason University, 2008

Dissertation Director: Dr. Barry N. Haack

Investigators engaged in research utilizing remotely-sensed data are increasingly faced with a plethora of data sources and platforms that exploit different portions of the electromagnetic spectrum. Considerable efforts have focused on the application of these sources to the development of a better understanding of lithosphere, biosphere, and atmospheric systems. Many of these efforts have concentrated on the use of single sensors. More recently, some research efforts have turned to the fusion of sources in an effort to determine if different sensors and platforms can be combined to more effectively analyze or model the systems in question.

This study evaluates multisensor integration of Synthetic Aperture Radar (SAR) with Multispectral Imagery (MSI) data for land cover analysis and

vegetation mapping. Three principle analytical issues are addressed in this investigation: the value of SAR collected at different incident angles, preclassification processing alternatives to improve fusion classification results, and the value of cross-season (dry and wet) data integration in a subtropical climate.

The study site for this research is Andros Island, the largest island in The Bahamas archipelago. Andros has a number of distinct plant communities ranging from saltwater marsh and mangroves to pine stands and hardwood coppices. Despite the island's size and proximity to the United States, it is largely uninhabited and has large expanses of minimally disturbed landscapes.

An empirical assessment of SAR filtering techniques, namely speckle suppression and texture analysis at various window sizes, is utilized to determine the most appropriate technique to apply when integrating SAR and MSI for land cover characterization. Multiple RADARSAT-1 SAR images were collected at various incident angles for wet and dry season conditions over the region of interest. Two Landsat Thematic Mapper-5 MSI datasets were also collected to coincide with the time periods of the SAR images.

A land cover classification process applied to the dry season and wet season MSI data achieved a total classification accuracy of 80.6% and 80.7% respectively. When combined into a single multiseason dataset the MSI data

resulted in a total classification accuracy of 87.3%. SAR proved to be a valuable source of information especially when processed as a time series and with a speckle suppression algorithm applied. A 21-scene multitemporal SAR dataset achieved a total classification accuracy of 65.8%. When a classification was applied to the multitemporal dataset following speckle suppression, the resulting total classification accuracy was as high as 83.8% depending on the speckle algorithm and kernel applied.

While texture measures have been successfully utilized for integrating SAR and MSI data, in this study speckle suppression proved to be significantly more valuable. SAR collection parameters such as look direction (ascending or descending orbit) and incident angle did not prove to contain uniquely valuable characteristics. The highest total classification accuracy achieved involved a combination of two MSI datasets and a multitemporal SAR dataset processed to suppress speckle using a Gamma- Maximum A Posteriori (MAP) filter with a 9x9 kernel.

This study sought to investigate processing alternatives when fusing SAR and MSI data. While not all of the results met with expectations, this study does determine that SAR and MSI are complementary data sources. A combination of SAR and MSI provide unique and valuable results that can not be achieved by each variable used independently.

1.0 INTRODUCTION

Land managers are often faced with the task of answering questions about our earth without having the most relevant or accurate information at hand. The science of Remote Sensing has developed into a very important source of current and accurate data that can be used for improved analysis and understanding of land cover and natural processes related to it.

Over the past three decades an increasing number of sources of remotely sensed data have become available. This diversity of satellite and airborne sources has collected data using a variety of sensors obtaining information from different portions of the electromagnetic spectrum (EMS) and at a great variety of scales and resolutions. Other sensor specific variables further contribute to a substantial volume of remotely sensed data much of which has not yet been fully evaluated. One goal of current research is to evaluate specific datasets to improve our understanding of natural processes. A further goal is to investigate the value of complementary data from different sources used in tandem to provide improved characterizations of land surface phenomena. It is increasingly important to understand how data from different systems can be

used in a complementary, integrated, or in some instances as a surrogate for direct single sensor observation. This allows us to characterize the earth's surface in the most effective manner using integrated datasets to answer specific questions, problems, or issues for a given regions.

There is a great volume of valuable research that has been published in scientific journals documenting the value and application of remotely sensed data to a wide variety of earth resource related issues. However, much of this research has focused on a select number of individual sensors and data collected from specific portions of the EMS. The results of many of these efforts have determined that remotely sensed data are a very valuable source of information about our earth and can be a very important tool for land managers under many circumstances (Jensen, 1996). There are limitations to its value, however, depending on the application, geographic location, and specific sensor related issues such as spatial and spectral resolution. Furthermore, research often identifies ideal conditions for a given application of remotely sensed data. Unfortunately, ideal conditions do not always translate into operational systems that can consistently provide expected results.

Despite the great volume of data that is now available and the substantial research efforts applied against it, there are some very specific and potentially valuable issues regarding remotely sensed data that have not been thoroughly

investigated. One specific area where further research is needed is in the integration of data from different sensors to derive new or improved information concerning a given area of the earth.

Multispectral optical imagery collected by satellite has been successfully used for land cover analysis since the early 1970's with the launch of what became known as Landsat-1. This satellite was followed by a series of comparable, though improved upon, platforms that have provided a consistent source of multispectral data for over 30 years. The subsequent launch of complementary platforms such as the French SPOT, Indian IRS, Japanese JERS and NASA EOS related satellites has resulted in the availability of a variety of high quality visible and near-visible, such as Infrared (IR), imagery.

The advent of satellite based active microwave or Synthetic Aperture Radar (SAR) platforms has added a further dimension to the data available for characterizing surface phenomena. SEASAT, ERS-1 and 2, JERS-1, and the Canadian RADARSAT platforms have provided consistent and valuable sources of information from portions of the EMS that are complementary to those imaged by multispectral imagery (MSI) platforms (Plaut, et al., 1999). One significant benefit from these platforms is their all-weather and cloud penetration capabilities. However, they are not simple data sources to use. MSI imaging systems rely on principles that are similar to the functioning of the human eye,

with reflected energy measured by the imaging sensor. While MSI platforms do extend into nonvisible wavelengths, such as the infrared, the principles remain largely the same, and they are therefore easier to understand and apply to specific problems. The physics of active microwave, or radar (SAR), energy are much more complex, less easily understood, and by extension, more difficult to apply to traditional land resource issues (Rany, 1998).

Unlike MSI remote-sensing systems, SAR are active imaging systems. Instead of relying in a passive sense on measurements of the sun's reflected energy to develop a digital image of a region, as is the case with MSI sensors, a SAR system provides its own energy source. The sensor emits microwave pulses and then measures the return signal. Depending on a number of factors peculiar to the platform, an image is constructed based upon the returning signal which has traveled to the surface of the earth, interacted in some fashion, and returned to the sensor. Some of the factors that need to be considered with radar include wavelength, incident angle, and polarization (Lewis and Henderson, 1998). These and a number of additional variables combine to create added complexity to the use and application of microwave remote sensing or SAR.

Understanding the utility of SAR imagery requires an understanding of these variables and their practical implications when applied to different types of land surface materials. The complexity of the data does not detract from its

utility. The goal of an image scientist is to use these variables and the unique qualities of SAR data to acquire a better characterization of the surface of the Earth.

The purpose of this research was to investigate different processing alternatives and SAR image parameters to maximize the value of SAR when integrated with MSI imagery for land cover assessment over a subtropical landscape. MSI imagery is well accepted as a tool for vegetation and land cover analysis. As a result, the primary focus of this project is on SAR collection parameters and filtering alternatives to determine the utility of SAR when integrated with MSI. The factors affecting SAR image collection impact the information content of the resulting image datasets. Assessing the impact of these parameters on information content will provide a better appreciation of appropriate collection parameters for given applications. How a SAR image is processed can also impact its usability. Prior research identified two processes that can enhance the information content of SAR data and result in improved land cover characterization, namely texture analysis (Hsu, 1973) and speckle suppression (Schistad and Jain, 1992).

One of the valuable attributes of SAR imagery is its reaction to the physical characteristics of materials and surfaces that it images. Smoother surfaces will result in a different returned signal than rougher or irregular

surfaces. This fact may be exploited for the purpose of discriminating land cover by allowing one to assess the relative smoothness or roughness of a particular land cover class through the analysis of SAR texture (Hsu, 1973). Surface materials with similar physical characteristics and under similar conditions will have similar texture values, while those with different characteristics and under different conditions will result in different texture values. One attribute of SAR imagery that can confound the measurement of texture is the presence of speckle (Schistad and Jain, 1992).

Remote sensing SAR systems create a radar image with coherent radiation backscatter back from a given area on the ground, the ground sample distance or a resolution cell. Multiple echoes of energy are returned from the same cell though slightly out of phase due to differences in surface conditions and the presence of scatterers such as buildings. Speckle results from the fact that the returned echoes are measured collectively and, depending on the phase shift, the measured value may be higher or lower than a pure signal would return. Speckle could be considered to be a random field of artificial return signal that either enhances or suppresses the true return signal. SAR imagery typically has a grainy appearance as a result of this phenomenon. Speckle is essentially a false component of texture in SAR images that must be removed or suppressed to accurately assess the texture present in an image. There is a balance required in

this process however. Suppressing speckle too much may degrade underlying texture while insufficiently suppressing speckle results in artificial texture being present (Rany, 1998). A number of processes have been developed to deal with this issue. Increasing the number of samples, or number of looks, taken for each cell measured may mitigate this characteristic but such processing reduces the spatial resolution of the data in the process. Speckle suppression is often still required for a variety of reasons to improve image interpretability. When attempting to measure variations in texture in a SAR image, the goal of speckle suppression is to minimize the impact of speckle while preserving texture features across the image.

A number of different algorithms have been developed to suppress speckle and to measure texture in an image. The primary techniques involve looking at individual pixel values relative to their surrounding or neighboring pixels. For speckle suppression, individual pixel values may be reduced or enhanced to more closely conform to the values found in surrounding pixels. This process reduces variation in pixel values across an image and will reduce texture, ideally false texture. Texture measures use a similar technique to quantify variability in neighborhoods. Areas that have greater variability are assessed as having greater texture and result from a rougher surface; lower variability results from a smoother surface. Maximizing the value of texture in a

SAR dataset involves using appropriate processing techniques to suppress speckle while preserving and still being able to quantify texture.

This project engages in an empirical investigation of speckle suppression and texture measure algorithms to assess the most appropriate combination to use when integrating MSI and SAR imagery for land cover classification. Prior research has determined that the Variance measure of texture provides the greatest contribution for the purposes of discriminating different cover types (Anys and He, 1995; Pierce et al., 1998; Haack et al., 1998; 2000; Haack and Bechdol, 1999; and Herold et al., 2005). As a result, this research will solely investigate the application of the Variance texture measure for integration with MSI for land cover assessment. However, the most appropriate window size at which to apply the Variance measure, especially in the face of speckle suppression processing, has not been definitively determined. A number of speckle suppression techniques have been developed and published in the literature. The most appropriate algorithm to use for a given situation depends on the intended use of the SAR dataset. Five speckle suppression algorithms were selected for this analysis ranging from a simple median, or pixel averaging, filter to more complex multi-zone neighborhood analysis filters. These five are representative of the most common filter classes found in the literature (Durand et al., 1987).

A comprehensive image dataset was compiled for the purposes of this research. It includes 21 SAR images from the Canadian RADARSAT-1 satellite and two MSI image datasets from the U.S. Landsat 5 satellite system. The datasets span an extended period of time covering wet-season and dry-season periods for the study site and the SAR images represent multiple incident angles from two different look directions for each period. This combination permitted the investigation of the impact of seasonality and SAR incident angle on land cover classification results as well as a basis for investigating combinations of filtering processes to maximize SAR's contribution to the accuracy of land cover classification.

The methodology for this study follows a model described by Pohl (1996) and is similar to that successfully employed by Haack et al. (1998) in East Africa. The basic procedure involved performing a digital classification using standard processing techniques applied to spatially coregistered sets of optical and radar spaceborne data, all resampled to the same pixel size. Spectral signatures were extracted for the various land cover types using supervised training sites established during field visits. After signature extraction, a Maximum Likelihood Classifier (MLC) was employed to classify the dataset and a contingency table compiled for accuracy assessment. The contingency tables

were created from a separate set of validation sites also identified during field visits.

The results of this study are a comparison of the accuracy assessments from various classifications for individual land cover types and for all types combined for overall classification accuracy. Multiple data combinations and statistical manipulations of the data have been examined. The processes implemented depended on the data source (SAR or TM) and included comparisons of the original sensor data independently and in combination.

The study site selected for this project is the northern extent of Andros Island, the largest island in The Bahamas. The island contains a variety of distinctive plant communities that have been minimally fragmented due to a low population density with most citizens concentrated in small communities along the east coast. North Andros Island lies 24.5 degrees north of the equator and exhibits a classic tropical wet and dry season. Plant communities range from coastal mudflat and dune communities to mangrove, scrub/brush, and pine stands or hardwood coppices in inland and highland regions.

The structural differences and minimally disturbed state of these plant communities coupled with the systematic wet/dry seasonality of the region made this an ideal location for the pursuit of the variables investigated in this project. While the results of this research are not independently conclusive, they

do support the thesis that a significant benefit is achieved by the integration of SAR and MSI imagery over most temperate and tropical landscapes with vegetation communities consisting of moderate biomass volumes.

Chapter 2 discusses some basic principles of MSI and SAR imagery that provide important context for understanding the basis of this research. There is also a thorough review of published research related to the different variables investigated in this study. Chapter 3 describes the methodology applied as well as the principle datasets, land cover categories, and study site for this research. In Chapter 4 the results of the analysis are presented. Chapter 5 contains a discussion of the results as well as suggestions for future research.

2.0 STATE OF THE RESEARCH

2.1 REMOTE SENSING CONCEPTS

Remote Sensing is essentially the process of observing and recording information concerning an object or phenomenon without being in direct contact with that object or phenomenon. The human eye is an excellent example of a remote sensing instrument. It collects reflected light from our surroundings allowing the brain to reconstruct an image of our environment. The photographic process mimics this by actually capturing the level of reflected light on film, allowing for the recording of conditions at that moment in time. Both photographic film and the human optic nerves are sensitive to electromagnetic energy (Figure 2.1) in what has become known as the “visible” portion of the EMS. While the visible portion of the EMS provides a great deal of information about ones surroundings there is even more value to be gained from information found outside of this region.

The science of Remote Sensing uses a variety of advanced instruments to measure energy from expanded portions of the EMS. These instruments may be ground-based, on airborne platforms, or mounted on satellites in orbit. The data

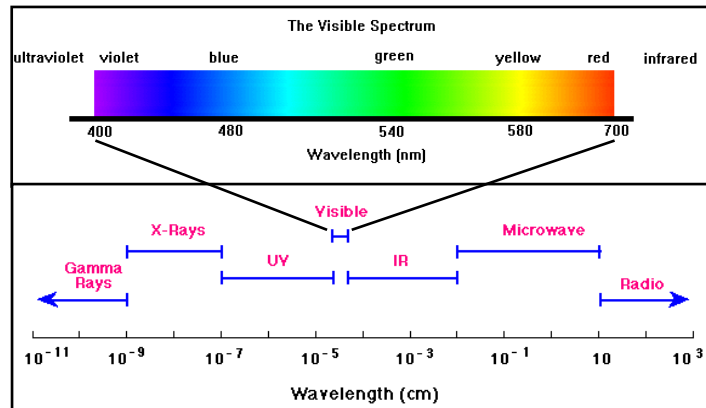


Figure 2.1: Electromagnetic Spectrum (after Saxby, 2002)

they collect are very diverse and can be used for many different pursuits from meteorological analysis to natural resource exploration. A significant research base has established the value of Remote Sensing for characterizing atmospheric and surface conditions and processes and these instruments prove to be one of the most cost effective means of recording quantitative information about our earth. In recent decades the advent of satellite based sensors has extended our ability to record information remotely to the entire earth and beyond.

The EMS proves to be so valuable because different portions of the EMS react consistently to surface or atmospheric phenomena in specific and

predictable ways. A single surface material will exhibit a variable response across the EMS that is unique and is typically referred to as a spectral curve.

Figure 2.2 provides an example of a typical EMS response to green vegetation. In

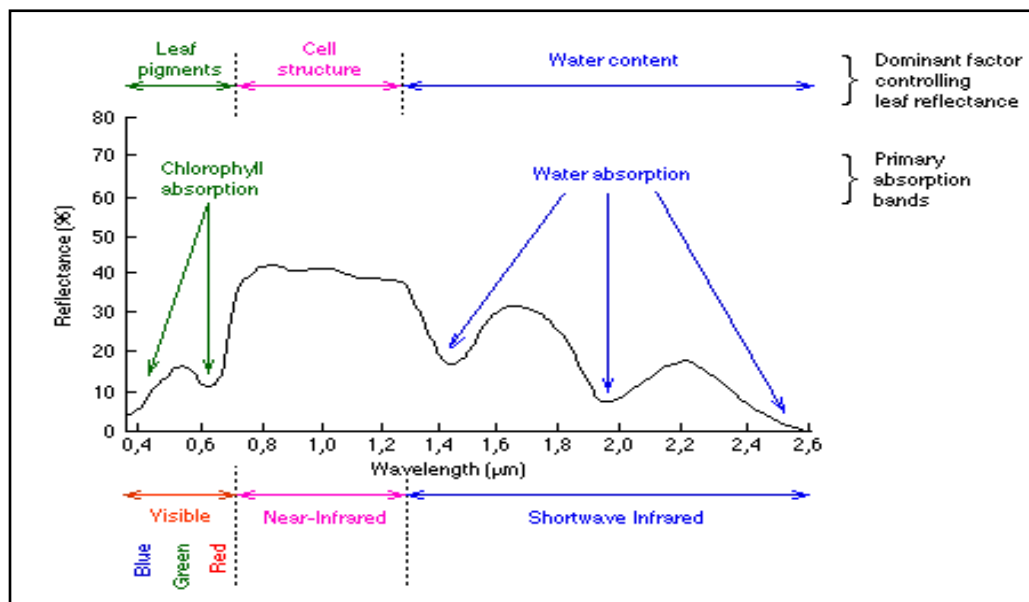


Figure 2.2: Spectral Curve for Green Vegetation (after Hoffer, 1978)

essence a particular object or material, such as vegetation, has a consistent EMS response that is different from that of another object of different material, composition, or surface character, such as water (Figure 2.3). These consistent responses can be measured and used to develop a unique “signature” for their respective object or material. Essentially, an expected and measurable response to the EMS is obtained. Remote Sensing capitalizes on this fact by measuring electromagnetic energy from different portions of the EMS and recording them, thus allowing for their comparison.

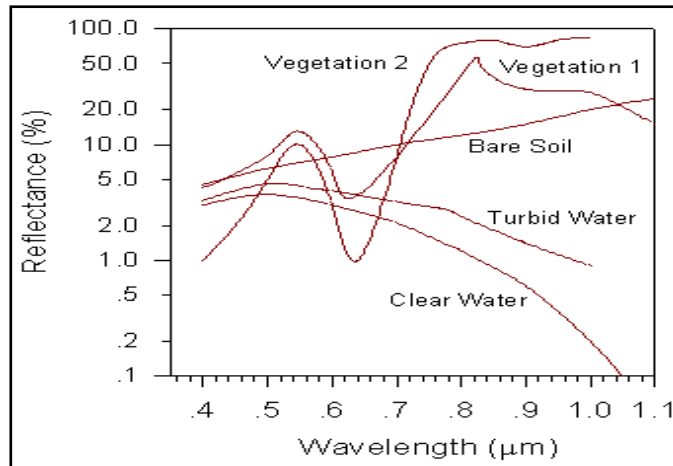


Figure 2.3: Example Spectral Curves for Different Cover Types (Liew, 2001)

RS sensors typically sample a selection of specific wavelengths or portions of the EMS to collect a series of measurements of a single object or area across its spectrum. The regions that are sampled are often referred to as bands (Figure 2.4) since the sensors typically record energy in relatively narrow ranges of the EMS. As an example, a sensor that collects data from the visible and infrared

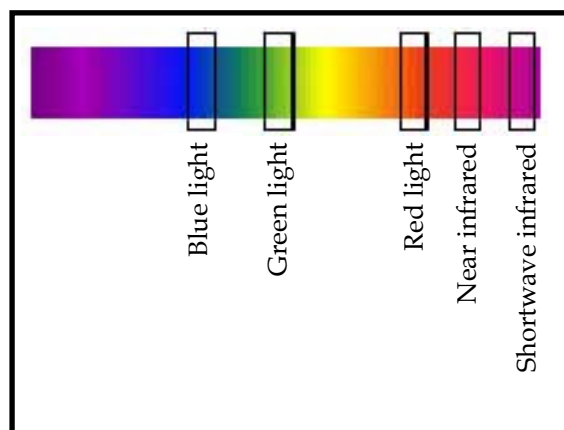


Figure 2.4: Example Sampling Regions for 5-banded MSI

portions (MSI or optical systems) of the EMS may have three bands that collect values from the blue, green, and red portions of the visible spectrum as well as a number of bands that record data from the infrared portion of the spectrum. A greater number of bands mean that more portions of the spectrum are recorded and greater discrimination can be applied to determining what a particular surface material or object is. Sensors that collect up to 16 bands of data are typically referred to as multispectral sensors while those that collect a greater number (typically up to 256) are referred to as hyperspectral.

Interpreting the data collected by MSI or hyperspectral sensors is not a simple science. There are considerable complicating factors that affect the type of information that can be collected and how it may be applied, from atmospheric interference, to sensor limitations and, most importantly, data volume. One of the primary goals of research in Remote Sensing is to find the optimum sensor parameters and collection conditions to maximize the information content of the data collected. One of the goals of this research is to identify some of these parameters and processing options to allow for more informed tasking and consistent results with regard to the application of remotely sensed data.

2.2 MULTISPECTRAL IMAGERY (MSI) LAND COVER ASSESSMENT

The main objective of MSI remote sensing is the acquisition of information about surface materials or objects. The information that can be collected is driven by the chemical composition, surface material and condition, and location of a target. Depending on chemical composition and surface condition, different portions of energy in the EMS are transmitted, absorbed, or reflected. The combinations of this phenomenon are largely unique to the materials' composition. A specific pattern of measured reflectance along the EMS can be used as a signature to identify the composition of a material without chemical testing or even coming into direct contact with it.

This phenomenon has been used in a number of ways to characterize the surface of the earth and the materials covering it. Remote Sensing has become a critical tool for assessing conditions in natural environments and quantifying change over time. One of the most prominent uses has been in mapping and monitoring of land cover and land use. Land cover refers to the physical material covering the surface of the earth. These are often collected into classes or categories such as grassland, forest, water, etc. Land use pertains to the use for which an area of land may be designated and typically refers to some anthropogenically modified environment such as agricultural practices, or developed or urbanized areas. Determining land cover and land use for broad

areas is most easily achieved using satellite imagery (Koeln et. al., 1999), though a precise understanding of land use often requires more detailed investigation of the region being assessed. Unique spectral signatures for different land cover types can be applied to imagery collected over an area to differentiate between the land covers that exist there. With MSI systems this translates to a set of observed or expected values measured in each band across the EMS. Improved spectral discrimination found in more advanced sensors such as the Landsat Thematic Mapper (Landsat TM or just TM) sensor operated by the U.S. Government not only allows for separating different cover types such as water from vegetation but actually separating out different types of vegetation.

Considerable research has gone into the use of remotely sensed data for vegetation analysis due to its promise for assessing commercially viable land cover such as forestry resources and land use in the form of agricultural activity. The Normalized Difference Vegetation Index (NDVI), derived by comparing recorded infrared and red light, is commonly used for surface characterization of vegetation. Sader et al., (1989) determined that NDVI values calculated from Landsat TM data were valuable for determining total biomass of forest stands. The NDVI has been put to considerable use in monitoring phenological changes in vegetation by utilizing time series imagery over a growing season (Belward and Loveland, 1995). Landsat TM spectral data along with biogeographical site

characteristics have been used in other similar studies estimating forest productivity (Lu, 2005). Above-ground biomass can be assessed using innovative processing techniques and monitoring over time. Using regression and classification techniques a high correlation was found between spectral and biogeographical variables of forest productivity proving that remotely sensed data provide a valid means of characterizing surface materials and land cover (Cook et al., 1989; Running et al., 1989).

The variety of land cover types that multispectral imagery has been applied to is extensive. In many instances these are focused on individual cover types or select groupings. Vegetation analysis with particular focus on forestry or agriculture has been pursued by Bauer et al. (1978), Fang (1980), Wall et al. (1984), Gilruth et al. (1990), Mladenoff et al. (1997), Jurgens (1997) and Stern et al. (2001). Guo et al. (2003) demonstrates the use of seasonal Landsat TM for discriminating between grassland types by differentiating species and management regimes, an example of the detail possible with remotely sensed data. Agricultural systems and productivity can be monitored particularly well when remotely sensed data collected over a growing season is available (Guerschman et al., 2003). Forestry and forest productivity is of increasing interest in light of increased atmospheric CO₂ concentrations and indications of global warming. Monitoring changes in potential carbon sinks may be

invaluable for planning mitigation efforts. Wu and Shao (2002), Chan et al. (2003), Tottrup (2004), and Lu et al. (2005), have engaged in research on techniques for improved assessment of forest resources especially in tropical ecosystems. As with agricultural analysis, data collected and analyzed as a time series proves most valuable for understanding current conditions and change over time.

Wetlands analysis has been equally robust due to the recognition of their important ecological and hydrological roles with Gilmer et al. (1980), Howman (1988), Lunetta and Balogh (1999), Kelly (2001), Proisy et al. (2002), and Grenier et al. (2007), providing excellent examples. Examples of analysis of urban or developed land has been accomplished by Jackson et al. (1980), Haack et al. (1987), Jensen and Cowen (1999), Lu and Weng (2005), Cao and Jin (2007), and Amarsaikhan et al. (2007), though this type of land use is often difficult to assess with moderate spatial resolution imagery due to the complexity and fragmented nature of the phenomenon. Texture has proven to be an important tool when investigating urban areas (Hsu, 1978; Dell'Acqua and Gamba, 2006).

Developing techniques for discriminating individual land cover and land use provides the basis for assessing land cover in a broader sense, spanning many cover types and broad regions quantitatively (Anderson et al., 1976; Hill and Kelly, 1987; Mladenoff et al., 1997; Vogelmann et al., 1998; Lloyd et al., 2004;

and Xu and Gong, 2007). As with forestry analysis, this process becomes increasingly relevant with regard to population growth, resource extraction, and other land cover changes and dynamics in the face of economic development and resulting global climate (Green et al., 1994; Foody et al., 1996; Baldocchi et al., 1996; Guerschman et al., 2003; Lloyd et al., 2004; Linke and Franklin, 2006; and Muñoz-Villers and Lopez-Blanco, 2007). The requirement for quantitative surface characterization data to feed global system models has led to the development of global land cover datasets at multiple scales (Belward and Loveland, 1995; Nemani and Running, 1996; DeFries et al., 1998; Koeln et al., 1999; Thomlinson et al., 1999; Hollister et. al., 2004; and Durieux et al., 2007). Such massive undertakings are extremely expensive and data and resource intensive. The prospect of maintaining such datasets is equally daunting. These requirements provide support for the development of new and systematic techniques that will take advantage of all available sources of data and provide rigorous and consistent land cover characterization and change analysis techniques. This research proposes that the integration of radar and multispectral imagery provides just such an opportunity.

2.3 RADAR (SAR) REMOTE SENSING CONCEPTS

Whereas the most common imaging sensors are passive and rely on reflected solar energy for measurement, there are some that include their own energy source. SAR utilizes an antenna to generate active energy to paint a portion of the earth's surface with microwave energy and then measure the level of returned energy. As with the visible and near visible wavelengths, microwaves interact with different materials in different ways. The returned energy, referred to as backscatter, can therefore be used to characterize the surface with which it came into contact (Ahern et al., 1993). SAR has some further unique attributes that extend its utility. Having its own energy source allows sensors of this type to image irrespective of the presence of daylight. Radar sensors can ignore weather conditions, an issue for most sensor types, since certain types of microwave energy are not inhibited by water vapor. Microwaves of different wavelengths have other unusual qualities such as the penetration of vegetation or hyper-arid soils (Smith et al., 1995; Wang et al., 1995). This allows for the characterization of surface and sub-surface physical conditions that may otherwise be obscured.

The microwave region of the EMS that SAR utilizes begins at wavelengths of 1000 μm (0.1 cm) and extends upward in wavelength to about 10 meters (Rany, 1998). Radar differs from other imaging systems in that the information

collected is less a function of chemical composition and more a result of physical interaction with the material imaged. Wavelength regions longer than the thermal infrared region yield little information about composition, but can yield much about physical characteristics such as temperature, surface roughness, or material particle size. This has led to investigation of the use of SAR in land surface characterization and more pointedly soil analysis.

A subset of the factors that need to be considered with radar are:

1. Wavelength
2. Incident angle
3. Look direction
4. Number of looks
5. Pixel spacing/spatial resolution
6. Polarization

(Lewis and Henderson, 1998)

These variables combine to provide added complexity to the use and application of microwave remote sensing or SAR.

2.3.1 SAR Wavelength

Wavelength is an extension of optical systems and is often referred to as a radar band; the following table defines the most common bands at which SAR imagery is collected.

Table 2.1: SAR Bands

Band	Frequency (GHz)	Wavelength (cm)
X	9.6	3.1
C	5.3	5.6
L	1.25	23.5
P	0.44	68

A particular SAR platform may have more than one band that it operates in. The current operational spaceborne systems typically have only one. Airborne platforms typically have between one and four. Intermittent Space Shuttle missions have carried SAR systems with up to three operational bands. Variations in wavelength are a function of differences in the energy of the signal and correspond to different degrees of utility. This makes different SAR bands useful for different applications and when combined provides utility that is similar to the bands and spectral signatures found with MSI systems (Saatchi and Rignot, 1997).

2.3.2 Incident Angle

The incident angle at which SAR imagery is collected refers to the angle of look of the sensor relative to the vertical with the ground (Figure 2.5). Imaging

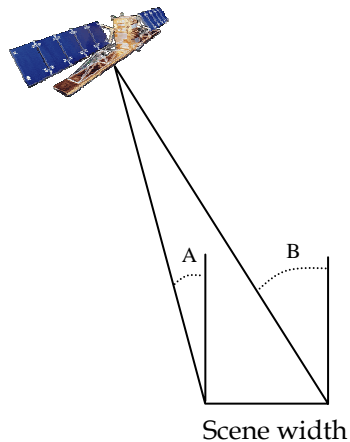


Figure 2.5: SAR Incident Angle (after Rany, 1998)

straight down or near nadir as is desired with most MSI platforms would result in all of the energy of the microwave pulses being returned to the sensor and very little variation with which to analyze surface features or conditions.

Looking off in an oblique fashion, or at an angle, provides for some energy being reflected back to the system while other energy is bounced away depending on the surface material illuminated. In this fashion, variations in surface features and objects may be differentiated. The angle of incidence can significantly affect the utility of data for specific applications (Cimino et al., 1986). In general, smaller angles result in greater vegetation penetration and more return from

surface materials. Larger angles result in a greater return from vegetation with less contribution from surface materials such as soil and surface geology. As depicted in Figure 2.5, the angle of incidence varies across any individual SAR scene. The portion of the image closest to the satellite track (A) is imaged at a slightly smaller angle than the portion of the surface farther from the satellite track (B). Any moderate resolution SAR image has an in-scene variation in incident angle of 5°-7°.

2.3.3 Look Direction

Look direction or azimuth has more to do with the surface being imaged than with the sensor itself. Due to the nature of SAR signals and wavelength the physical interaction with certain features will be affected by the orientation of the object relative to the path of the sensor. For example, an agricultural field that has been plowed with rows perpendicular to the imaging path of a SAR sensor will result in a different return than one that has been plowed parallel to the sensor track.

Aircraft-based SAR sensors provide greater control over look direction, it is determined by the aircraft flight path. This is not the case with spaceborne platforms. A satellite based SAR in a polar orbit will typically provide two

directions of imaging, one while the sensor is ascending in orbit from a southerly direction toward the north. The other while it is descending in orbit from north to south, these are typically referred to as ascending and descending mode. This translates to a change in look direction depending on the design of the system. For example, if a SAR system is designed to image to the east in ascending orbit, then it images to the west as it passes over the pole into its descending orbit. Fundamentally, SAR data collection in ascending or descending mode should have little impact on the data especially in natural land covers, however, if physical conditions on the ground change between an ascending collection and a descending collection one could expect differences in backscatter. Wood et al. (2002) investigated whether morning dew on vegetation would have a significant impact on the utility of data collected in ascending or descending orbit when assessing agricultural crops. They did not identify a clear correlation. While they did determine the image content was different between orbits this did not significantly affect the usability of the data for crop separation. This issue of image content differences between ascending and descending orbit collection warrants further investigation.

2.3.4 Number of Looks

SAR systems typically do not collect and process a single sample of returned microwave energy for each area of the ground imaged. Doing so would typically result in imagery that was very grainy or speckled due to the additive nature of microwave energy. One way to reduce this grainy appearance is to take multiple samples of energy from the same point on the ground and average them to establish a reasonable value for the area imaged.

These samples are essentially repeated pulses of microwave energy and are referred to as the number of looks. This multi-sampling procedure provides a better characterization for a given area (reducing speckle noise) and makes SAR imagery more useful (Rany, 1998). However, taking more looks of an area

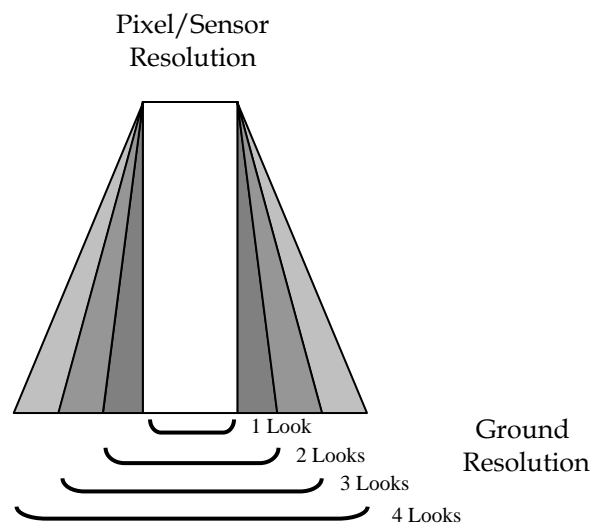


Figure 2.6: The Multi-look Effect

reduces the effective spatial resolution (Figure 2.6) of a SAR dataset as the individual samples are averaged.

2.3.5 Pixel Spacing and Resolution

Most users of MSI are familiar with the concept of spatial resolution or ground-sample-distance. The resolving power of an imaging system defines the ability of the system to distinguish between two objects that are close together. With a lower resolution two objects may not be resolved and may appear as a single object on the imagery. With higher resolution they may be distinguished separately. Typically the concept of spatial resolution is closely tied to the number and spacing of actual sensors on the sensor array of the imaging platform. This is not the case on a SAR imaging system. Pixel spacing refers to the distance between samples taken on the ground but will not correspond to the resolving power of the sensor. Samples on the ground may be spaced at 12.5 meters but may each include a surface area of 30m (each pixel sample containing data that overlaps with surrounding pixels), providing a 30m resolution. This issue is driven by the number-of-looks (Figure 2.6). There is a direct trade-off between image resolution and number-of-looks, as number-of-looks increases the nominal ground-sample-distance of the SAR sensor also increases, reducing resolving power of features (Rany, 1998).

The subject of pixel spacing and ground resolution is an important one that warrants further investigation. SAR imagery is typically delivered at system resolution (pixel spacing) and then processed into ground resolution. For example, SAR data from the Canadian RADARSAT-1 system is collected at a 12.5m pixel spacing but due to multi-look processing is deemed to provide a 25m ground sample distance. Therefore, the data are processed into a coarser resolution. Some research is going into processes that may be applied to single look data to maximize the value of data collected with a single look (resulting in higher speckle) without degrading the resolution as multi-look processing does in an effort to reduce speckle (Davidson et al., 2006).

2.3.6 Polarization

The final complicating factor when considering the utility of SAR imagery is the issue of polarization. The orientation of the transmitted microwaves and those collected as a return can be controlled and measured. This may provide a number of potential bands of data collected for each SAR band. The combinations are HH, VV, HV, and VH, in either a vertical (V) or horizontal (H) orientation and corresponding to send and receive mode for each pair. Depending on the surface material illuminated, the orientation of the microwaves will be altered to differing degrees and this change in polarization

may be used to help characterize the surface. Only a selected number of imaging platforms, primarily aircraft-based, record SAR imagery with varying polarization combinations. Two recent systems, ALOS-PALSAR and RADARSAT-2, are collecting and more operational satellite systems are planned (Davidson et al., 2006).

Multipolarization SAR imagery has been used in many projects to evaluate and discriminate surface materials. It has proven valuable for land cover classification (Saatchi and Rignot, 1997), forest mapping (Dobson et al., 1995), wetlands delineation (Proisy et al., 2002), agricultural applications (Karjalainen et al., 2008), and coastal mapping (Baghdadi et al., 2007). Planned SAR systems are incorporating multipolarization capabilities to expand the utility of SAR data collected.

2.4 VEGETATION ANALYSIS WITH RADAR

SAR has proven to be very effective as a compliment to MSI remote-sensing techniques in land cover mapping and terrestrial ecosystem assessment. The fact that SAR is independent of solar irradiance and unaffected by cloud cover is one significant reason why it is effective for use in land cover classification. This has proven especially true in northern latitude boreal forest and tropical rainforest

where the acquisition of multispectral imagery data is often hindered by frequent cloud cover and smoke from fires. The sensitivity of the radar signal to moisture content is further complemented by its ability to discern the structural properties of vegetation and to assess stages of forest regrowth. This often allows for the separation of forest types, particularly when optical sensors are saturated over dense vegetation. A further value and differentiation from MSI systems is the fact that reflectance-based imagery only image the surface reflectance of materials while active microwaves in the form of SAR may penetrate the surface and interact with underlying structure.

Several studies, using a variety of classification approaches, have used SAR images for land cover classification in forested regions (Saatchi et al., 1996; Rignot et al., 1994; Ranson and Sun, 1994; Ranson et al., 1995; Cimino et al., 1986; Baltzera et al., 2003). The application of these data sources in process models is increasingly being explored. For example, Bonan (1993) has used a SAR-derived land cover map over the boreal forest of interior Alaska to improve the estimation of forest assimilation. Saatchi and Rignot (1997) developed land cover maps derived from multipolarization, multifrequency SAR systems and projected that they could become an important tool for terrestrial ecologists and process modelers. Proisy et al. (2002) further demonstrated the value of multipolarization and multifrequency SAR for the mapping of mangroves

swamp and canopy structure. They determined it was possible to differentiate species and to analyze the decline in mangrove density using time series data.

Collecting and integrating data over time proves to be particularly important for monitoring landscape change due to anthropogenic forces or climate change. Long-term stability in data sources and calibration of data between sources then becomes an issue. Shimada (2005) investigated the stability of L-band SAR from the Japanese JERS-1 system to determine the consistency of collection and stability of datasets collected for the Amazon rainforest over the life of that system. It was determined that the data collected were consistent as was vegetation (of undisturbed regions) such that the area could be used for calibration of other systems. A similar, 19-year study using L-band data from multiple SAR systems confirmed consistency across platforms (Balztera et al., 2003).

Dobson et al. (1995) presents a three-step process for estimation of forest biophysical properties from orbital SIR-C (Shuttle Imagine Radar-C) polarimetric SAR data. Direct estimation of total above-ground biomass based strictly upon land cover derivation was shown to be unreliable unless the specific effects of forest structure were explicitly taken into account. Their process first involved classification using SAR data to identify terrain on the basis of structural categories. Polarimetric SAR data at L- and C-bands were then used to estimate

basal area, height, and dry crown biomass for forested areas. The estimation algorithms were empirically determined and were specific to each structural class. The last step used a simple biophysical model to combine the estimates of basal area and height with ancillary information on trunk taper factor and wood density to estimate trunk biomass. Total biomass was then estimated as the sum of crown and trunk biomass. The results show that for the forest communities examined (sub Boreal) biophysical attributes can be estimated with relatively small RMS-errors (root mean square-errors). The addition of X-SAR (multipolarization) data to SIR-C was found to yield substantial further improvement in estimates of crown biomass in particular.

The prospect of discriminating forest structure with SAR has been further explored with regard to understanding how animal species diversity and population density are affected by edge effects, habitat heterogeneity, and landscape composition. Imhoff et al. (1997) have investigated the ability of SAR to provide useful information on vegetation structure for the purpose of mapping bird habitats. The approach exploits the apparent ability of SAR sensors to respond to vegetation structure. In boreal and coniferous temperate forests, tree stand parameters such as height, stand density, and sometimes leaf area can be inferred using polarimetric radar and classification algorithms employed to map stands (Dobson et al., 1993; Ransom et al., 1995).

SAR sensor data have also been used to monitor gross vegetation habitat parameters for conservation purposes (Lawrence et al., 1995). Using SAR data, it may be possible to distinguish among several different vegetation structures in predictable ways, based on wavelength and the degree of consolidation of living plant tissue. Past research has shown that SAR backscatter is linked to vegetation structure, and that the ratio of vegetation surface area to volume may be a useful measure of structural consolidation (Imhoff, 1995a). If SAR can discriminate among vegetation structural types, and this information is layered onto floristic data acquired from aerial photography, Landsat TM, and other sensors, the potential for high spatial resolution mapping of animal habitats, over large areas, is immense.

Biomass mapping using SAR has also met with substantial success although the application and saturation level varies depending upon the forest type. Research with temperate forest biomass derivation has been accomplished by Dobson et al. (1992, 1995), Kasichke (1992), LeToan et al. (1992), Israelsson et al. (1994), Proisy (2002), Kuplich (2005), and Rauste (2005), . Hoeckman et al. (1995), Pope et al. (1994) and Imhoff (1995b) have been successful with tropical forests and comparisons to temperate coniferous stands. Monitoring biomass in tropical forests is deemed to be of considerable importance especially with the assessment of them as carbon sinks (Kuplich et al., 2005). Ahern et al. (1993),

Kasischke et al. (1994), Beaudoin et al. (1994), and Wang et al., (1995) have compared a variety of forest biomes. These collected works have shown that low-frequency (0.4-5 GHz) SAR measurements are very sensitive to forest biomass. Kasischke et al. (1995) evaluated the correlation between above-ground biomass and coefficient of backscatter with SAR. Using airborne SAR data they determined that SAR at different polarizations in the C-band were highly correlated with various components of biomass (e.g. bole biomass, stem biomass, and needle biomass) within stands of loblolly pines.

Wigneron et al. (1997) investigated the response of P-band (~0.44 GHz) and L-band (~1.4 GHz) finding that the penetration depth of the measurements exceeded the crown layer. The scattering processes that contribute to backscattering involve the crown layer (mostly branches), tree trunk, and the ground surface. Since the trunk and branch components represent more than 90 percent of the total above-ground biomass of mature forest canopy, a good correlation was found between backscattering and the total biomass. Conversely, for higher frequency measurements [C-band (~5 GHz) and X-band (~10 GHz)], the penetration depths did not exceed the crown layer thickness in most cases. The scattering effects which contribute to backscattering occur mainly in the upper layer of the canopy; foliage (needles) and small branches are the dominant scatterers. As a consequence, the sensitivity of C-band

backscattering to the total above-ground biomass diminishes significantly when biomass exceeds about 6-10 kg/m² (60-100 tons/ha). Therefore, C-band backscattering was found to be useful for providing discrimination between low-biomass canopies (Dobson et al., 1992) and for monitoring biomass changes during early successional stages in temperate coniferous forests (Kasischke et al., 1994). Also C- and X-band backscattering data can be used in combination with P- and L-band data for retrieving forest characteristics (Dobson et al., 1995; Kasischke et al., 1995). In particular, this addition was found to yield substantial improvements in estimates of crown biomass.

Successful biomass mapping based on SAR classified vegetation has been effectively used in analysis of vegetation successional processes and prediction of future biomass accumulation (Williams et al., 1994). Their study predicted successional stage, established existing measurements of biomass ranges within successional stages, and incorporated knowledge of the rates and processes influencing vegetation succession. This model, used in conjunction with stage-specific rates of successional change, displays both present and projected patterns of biomass on the landscape. The resulting biomass projections demonstrate the importance of present-day distribution of vegetation types, and not just biomass distribution, for predictions of future distributions of biomass on the boreal landscape.

However, SAR has clear limits to its application. As mentioned previously there are situations where canopy complexity and volume of biomass are such that backscatter saturation becomes a problem. Imhoff et al. (1995a) have concentrated recent research efforts on evaluating the effects of saturation limits on making global biomass inventories with SAR sensors. Applicability was assessed by comparing biomass saturation limits to a global vegetation type and biomass database. C-band can be used to measure biomass in biomes covering 25 percent of the world's total ice-free vegetated surface area (which accounts for 4 percent of the Earth's store of terrestrial biomass). L- and P- band can be used to measure biomass in biomes covering 37 percent and 62 percent of the total vegetated surface (accounting for 8 percent and 19 percent of total biomass). Tropical biomes occupying approximately 38 percent of Earth's vegetated surface contain 81 percent of the estimated total terrestrial biomass and unfortunately have biomass densities above the saturation limit of current SAR systems. Since P-band radar systems cannot currently operate effectively from orbital platforms, scientists are limited to the L-band threshold. Emphasis should be shifted toward using SAR to characterize forest regeneration and development up to the saturation limits shown by Williams et al. (1994), rather than attempting to measure biomass directly in heavy forests. The development of new and innovative technologies for measuring biomass in high-density vegetation was encouraged as a result of this study.

Wetlands mapping is another area of considerable interest due to the ability of SAR data to discriminate inundated land below a closed vegetation canopy. Considerable work has been done on this issue in the Amazon basin as well as other forested wetland regions of the world (Townsend, 2002; Parmuchi et al., 2002). Agricultural monitoring and analysis is also receiving a great amount of attention since SAR imagery is not beholden to local weather conditions and the timing of data collection can be very important when considering crop phenology (Wood et al., 2002; Karjalainen et al., 2008).

The extensive body of research that exists with regards to SAR provides definitive evidence that SAR data are extremely valuable though difficult to understand and interpret. SAR imaging assesses different qualities of surface materials than those measured by MSI systems and allows for more robust characterization of surface conditions and especially those associated with vegetation land cover types. The complementary nature of SAR data to MSI data and analysis leads directly to the premise that the integration or fusion of these two unique datasets, as is the focus of this research, should provide for even more robust analysis of surface conditions and processes.

2.5 SPECKLE REDUCTION

One of the most significant issues with the use of SAR data for land cover classification is the presence of speckle noise. The speckle phenomenon is a direct result of the coherent nature of the radiation emitted by radar imaging systems. Point scatterers within each sensor footprint impart either additive or subtractive strength to the signal measured by the sensor. The effect of speckle is to provide erroneous digital number (DN) values that are of either greater or lesser magnitude than the “true” value expected. The result of this is a dataset with a statistical distribution containing a large standard deviation over relatively small areas. In effect, an area on the ground that is ostensibly homogenous will exhibit a granular or speckled appearance and will result in recorded values that are greater or lesser than warranted by the properties of the area imaged. One way of considering a SAR image is as a composite of two fields of data. One field of data comprises the pure radar return without the contribution of point scatterers, the second field of data consists of the additive and subtractive signal generated by point scatterers and is the source of the speckle phenomenon (Mejail et al., 2003).

SAR images that are to be used for quantitative land cover assessment should be processed to remove or reduce the presence of speckle. Ideally, removing the “speckle field” would provide a data layer consisting of pure SAR

return and the best source of information for characterizing surfaces.

Unfortunately it is impossible to determine the precise impact of speckle on a pixel-by-pixel basis. As a result, the multi-look process was developed on the system side, and a number of filters have been developed on the data processing side in an effort to mitigate the impact of speckle on specific applications of SAR data. Under most circumstances, speckle suppression should occur before other filters or processes are performed on SAR data or SAR data are integrated with other data sources (Hong et al., 2005).

Two primary categories of filters have been used or developed for speckle suppression (Durand et al., 1987). One group of filters relies on the assumption of a definable speckle model while a second and, more simplistic group, makes no assumptions concerning the nature of speckle. All of these rely on the use of a moving window concept of convolution, or spatial filtering. Mathematical calculations are performed on a collection of pixels in a moving window (Figure 2.7) of a user defined size (typically with an odd number of pixels on a side such as 3×3 , 5×5 , ... $N \times N$) that constitute a neighborhood for any specific pixel and that systematically scan an image dataset (Jensen, 1996). The pixel (p_c) falling at the center of the window is the pixel of interest. Based upon the

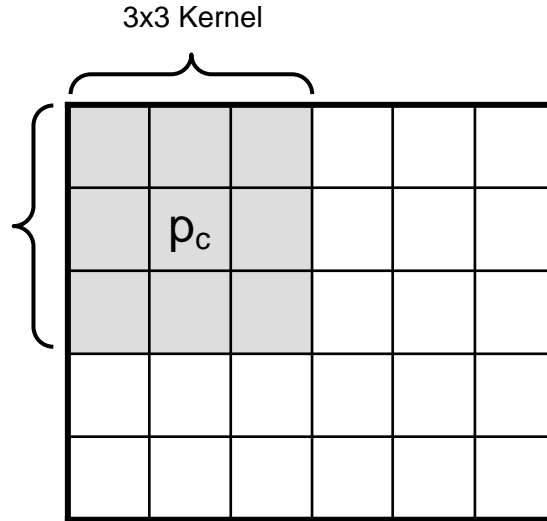


Figure 2.7: The Neighborhood Filter Process

characteristics of the sample of pixels contained by the moving window the value of p_c may be replaced by a value that is deemed to be more appropriate. An appropriate value is determined by defined statistical operation performed on the sample of pixels contained by the window.

Of those filters that make no prior assumption regarding the nature of speckle the most common are the Median and Mean filter. These replace p_c with either the calculated mean or the median pixel value of the sample set defined by the window size. Mean and median filters have proven to be effective at smoothing speckle noise and tend to make an image more visually pleasing but they cannot distinguish between useful information and speckle (Rany, 1998). Their application may have the consequence of further degrading the dataset by

incorporating speckle values into the calculation of replacement values for p_c . A number of variations on these basic filters have been developed to varying effect but fundamentally they are insensitive to the nature of speckle.

A more promising group of filters are those that take into consideration an assumptive model of speckle. These are typically referred to as adaptive filters in that they compare the statistical characteristics of speckle pixels with the window defined sample to determine if p_c is extraordinary and if so the magnitude of the value to replace it. Again, a number of these filters exist with new variations being developed.

The goal of filtering is to reduce the impact of speckle while maintaining useful information. This is a delicate process since one of the attributes of SAR imagery that has proven to be highly useful is that of texture. The variance of returns over an area can be assessed to determine relative surface texture and thereby differentiate between different surface types. As an example, still water is considered a perfect reflector of microwave energy bouncing it away from a SAR sensor. This results in a homogenous area of low DN values. Forest on the other hand is a complex surface that may result in a return that has a great deal of variance over the forested surface area. The difference in texture between these two surfaces may be assessed and used to differentiate between the two. Speckle suppression impacts the quantification of texture (Schistad and Jain,

1992). Processing for speckle with a small window can smooth speckle while preserving texture information in local areas. Adaptive filters have proven to be the most effective at distinguishing between useful information such as texture and speckle and are deemed to be most suitable for classification processes (Durand et al., 1987; Nyongui et al., 2002; Xiao et al., 2003).

A number of speckle suppression algorithms exist and have been evaluated for different applications (Durand et al., 1987). Most of the evaluation projects have compared different speckle algorithms to determine if they preserve edges and features. Two filters defined in the early 1980's and often applied in speckle suppression processes are the Lee-Sigma and Frost algorithms. These have been evaluated for their edge detection and preservation utility (Adair and Guindon, 1989). In this instance the Frost filter was found to be most effective. Smith (1996) proposed modifications to the standard Sigma filter that improves speckle suppression and preserves fine features. This effort also determined that speckle suppression filters might be run iteratively and in different combinations with varying windows sizes to increase feature recognition. The assumption is that as speckle is progressively reduced, the image approaches true feature representation. Theoretically, iterative filtering should arrive at a dataset that achieves stability with further iterations becoming unnecessary. Du et al. (2002) investigated this by applying the Lee filter

iteratively though they found that the dataset never did achieve a state of stability. Nevertheless, a speckle suppressed SAR dataset was found to be more valuable for land cover mapping in their study.

The Gamma-MAP (GM) filter has been one of the most successful with regard to classification results. Zaitsev and Zaitsev (1996) evaluated the GM filter with airborne data. Their analysis determined that the algorithm appeared to provide approximate microwave reflectance values and worked best as the number of looks increased for SAR data. Based upon these results they felt this was the most appropriate filter for fusion with optical data. Nezry et al. (1991) evaluated a number of filters including the GM and found it to be the most useful as it appeared to preserve texture and features in the SAR imagery. This was later contested (Collins et al., 1998) when the filter was used in a study to evaluate forest parameters relative to texture measures. In this study the GM filter was not found to preserve small-scale features. An interesting result of this research was the determination that texture should be processed at the pixel spacing scale rather than the ground resolution of the image. This implies that an appreciable amount of information is lost in the resampling step of the image fusion process. Most examples of texture processing in the literature do not calculate texture at the pixel spacing but rather at the ground sample distance scale. This is an area that warrants further investigation.

Alternative approaches to speckle reduction have been investigated with multifactor datasets. Multifrequency and multipolarization SAR data may be combined to evaluate the impact of speckle and combined to reduce its effect (Lee et al., 1991). New speckle suppression algorithms, as well as variations on existing ones, are being developed on an ongoing basis (Hagg and Sties, 1994; Wakabayashi and Arai, 1996; Lu et al., 1996; 1997; Dias et al., 1998; Nicholas et al., 2001; Belhadj and Jebara, 2002; Chunming et al., 2002; Xiao, 2003; and Vidal-Pantaleoni and Martí, 2004). The goal of most of these is to establish a feature preserving speckle suppression process. Since recent ones are relatively new to the discipline they cannot be easily evaluated or compared until they are incorporated into operational software platforms.

A variety of speckle suppression algorithms have been developed over the past three decades with none of them clearly distinguishing themselves as the ideal filter. In recognition of this fact a number of projects have focused on the development of metrics for comparing alternatives. In 1996, Sheng and Xia published a set of five metrics that were developed for evaluating the value of seven different radar filters. These were application-based tools for evaluation of suppression success. It was determined that some filters were better for certain applications than others. None perform well for all applications and there was clearly a trade-off between edge/feature detection and speckle suppression. A

set of statistical tools were published in 1999 (Xie et al.) to provided filter users an informative, and quantitative approach to choosing a suitable algorithm for specific applications. A demonstration of the metrics again determined that the most suitable filter depended on the application at hand. With regard to the specific preservation of texture in SAR images, Dong et al. (2000) evaluated a number of speckle filters using a defined set of criteria. These included 1) preservation of the mean, 2) reduction of the standard deviation, 3) preservation of edges, and 4) preservation of textural information. Among filters tested, a median filter was found to distort texture information the most and appeared not suitable for use with SAR data and texture analysis. The Lee and Frost filters performed fairly well.

Given the number of speckle suppression algorithms that exist and their apparent application specific value it is clear that no one filter is appropriate for all situations. Different evaluations have resulted in conflicting results given similar circumstances and processing models. It appears that the most appropriate means of assessing the value of individual filters is through an application specific empirical evaluation. The literature does support the contention that adaptive filters, such as the Frost or GM, are the most appropriate for land cover classification projects (Nyoungui et al., 2002). This research project applies a representative selection of speckle suppression

algorithms at a range of different window sizes in an empirical assessment to determine their value for improving the utility of SAR data for image fusion and land cover analysis.

2.6 ASSESSMENT OF TEXTURE IN RADAR IMAGERY

Texture is one of the two critical attributes of imagery that are leveraged for feature recognition and extraction; the second is tone (Haralick et al., 1973). As with tone, analysis of texture can be applied at virtually any scale from photomicrographs to broad area satellite imagery. The two are inextricably related and are always present in an image though one may dominate over the other for any given spatial extent. When a small sample of an image has little variation in DN values the dominant property of that area is tone. If a similar small area has a wider variation in DN values, the dominant property is texture. Pixel classifiers rely on tone to segment an image while contextual classifiers take texture into account. When using a pixel classifier such as Maximum Likelihood, texture must be incorporated through independent processing of and inclusion as an additional image layer. This is achieved by incorporating a texture measure dataset and essentially aids in turning a pixel classifier into a contextual one.

Two major categories of texture analysis exist (Haralick, 1979). A structural approach to texture characterization aims to identify and capitalize on basic primitive patterns that may be discernable and repeated throughout a dataset. This process can be very complicated especially when applied to an image dataset (Wang and He, 1990) and is not practical for land cover classification purposes. The second major approach to texture analysis is the statistical method. This attempts to capture and characterize the variation of gray tones across an image dataset.

As a key component of any individual image band, texture provides one of the elements that make objects or specific surface features recognizable. It is a valuable tool for image interpretation and specifically for land cover classification. With the advent of digital image processing, texture is now quantifiable with a variety of different algorithms and has been applied to a number of different problems. Texture has been assessed for lineament extraction and quantification of change in tropical forests using SPOT data by Riou and Seyler (1997), for the separation of orchards from surrounding forest (Gordon and Philipson, 1986), for cartographic feature extraction (Duggin et al., 1988), and it has proven valuable for including spatial context in standard land cover classification operations (Hsu, 1978; Lee and Philpot, 1991). The incorporation of texture information in the classification of high spatial resolution datasets has also

proven quite promising (Dikshit and Roy, 1996). Coburn and Roberts (2004) investigated the multiscale dimension of texture by applying texture measure filters using different kernel sizes (the statistical window over which texture may be assessed). Small kernels assess local texture and larger kernels assess broader texture patterns. Their research determined that multiscale texture analysis with MSI was more valuable than that collected at a single scale but no definitive combination was determined to be consistently superior.

Texture has developed into a particularly useful tool for the digital analysis of SAR imagery. The interaction of the microwaves with surface materials is dominated by reflection involving surface discontinuity in relation to the wavelength of the SAR band. In essence, smooth or rough surfaces are more quantifiable in SAR imagery than in MSI due to the nature of the interaction of SAR energy with the surface imaged.

This fact has been leveraged for a wide variety of applications. Land cover and terrain classification are prominent examples particularly in regions where MSI is not easily acquired due to weather conditions (Miranda et al., 1996; Luckman et al., 1997; Dobson et al., 1997; Pierce et al., 1998; Chan et al., 2003; and Lu, 2005). Texture analysis has also been applied for agriculture studies (Anys and He, 1995; and Treitz et al., 2000), geologic analysis (Stomberg and Farr, 1986), and flood delineation (Chenghu, 1998).

A variety of texture analysis algorithms exist and new variations are developed on an ongoing basis (Wang and He, 1990; Dobson et al. 1997; Pierce et al. 1998; Myint, 2003; and Xiao et al., 2003). Given the response of microwave energy to physical characteristics of the landscape, texture measures may provide the best means of integrating the texture element into the more traditional MSI land cover classification processes, which largely rely on tone. This project focuses on SAR texture and how to maximize its value while minimizing the impact of speckle.

2.7 ANALYSIS USING ANGLE OF INCIDENCE

The angle of incidence with which a SAR system images a given region of the earth has a significant impact on the return signal and the utility of the data collected. For some applications a given incident angle may be absolutely useless while for others it may be ideal. Most airborne platforms provide SAR data at varying incident angles while most operational spaceborne systems offer a single one. The Canadian RADARSAT platform offers a number of options in this regard allowing it to be used for more diverse applications. Fundamentally, the option to vary the angle of incident at which an area is imaged provides an opportunity to maximize the value of any individual dataset.

The value of different incident angles has been evaluated for a variety of applications. Typically, projects investigating vegetation dynamics such as land cover discrimination find smaller incident angles more appropriate (Cimino et al., 1986; Hussin and Hoffer, 1990), aiding in the determination of plant community structure, canopy closure, and surface material. The latter is particularly relevant for delineating forested wetlands. However, for specific studies such as the mapping of clearcuts in forested regions, larger incident angles prove more effective (Banner and Ahern, 1995). Ford and Casey (1988) found that while forested wetlands could be determined solely on the basis of variations in incident angle from SIR-B SAR data, three inland forest types could not be and they determined that cross-polarization data were necessary for such discrimination. Karjalainen et al. (2008) looked at polarimetric data at different incident angles for discriminating crop types in an agricultural system. While their research was successful, they determined that a time series of data collected at different incident angles can be problematic when trying to precisely discriminate detailed features such as crop type.

Larger incident angles are also most desirable for geologic applications (Kaup et al. 1982). Discrimination of surface structure is more easily achieved at greater angles. The presence of vegetation has an impact on the appropriate angle for geologic analysis however. More vegetation will require a lower

incident angle to gain more penetration of vegetation to resolve more surface features. Most spaceborne SAR systems do not collect data at angles that are considered most appropriate for geologic applications. The specific application and region of study will determine what is most appropriate. As a case in point, if one wants to identify and monitor oil lakes such as those created in Kuwait after the Iraqi defeat in the Persian Gulf War, it appears that an incident angle of approximately 37 degrees is most appropriate (Kwarteng et al., 1999). Moderate incident angle images are deemed most appropriate for urban feature analysis as well (Xia, 1996). Weydal (2002) investigated the use of data from different incident angles applied to urban areas and found that variations did exist but were not consistent across angles and therefore could not be definitively valuable or leveraged for specific applications.

As one of the controllable variables that increases the data dimension of SAR imagery, and presumably its value, incident angle is an important parameter to assess for improved analysis. Microwaves striking the surface at an angle approaching the vertical will result in greater vegetation penetration and increased interaction with and reflection from ground surface material. Microwaves striking the surface at a shallower angle will result in less penetration and more interaction with vegetative cover in the respective backscatter. Therefore, the type and density of vegetation will impact the

returned signal at any angle and some incident angles will provide better discrimination between specific vegetative surfaces. This phenomenon will be assessed in this research project. It is conceivable that SAR imagery from more than one incident angle may contribute significantly to a single classification operation. Combined with the potential for unique texture features developing due to changes in incident angle this could prove to be a particularly interesting aspect of this study.

2.8 TIME SERIES ANALYSIS

The advent of satellite-based remote sensing systems provides repeat coverage of most areas of the earth. This allows for temporal analysis of surface dynamics and more specifically change over time. Due to the collection parameters of most imaging systems, images are collected in a systematic process using a specified grid for image footprints. This provides significant opportunities to assess the value of combining imagery collected at different time periods for improved land cover mapping and surface characterization.

The analysis of time series images has proven to be very valuable. This is particularly the case for the analysis of vegetation where a series of images collected over time can be acquired in accordance with key phenological periods

of vegetation growth (Schriever and Congalton, 1995). Images may be timed to correspond with seasonal changes such as green up and senescence in deciduous vegetation or biomass changes as a result of dry season/wet season variations in subtropical and tropical plant communities. Time series analysis has also been successfully applied to wetlands mapping (Lunetta and Balogh, 1999). Two Landsat 5 scenes were acquired; one during leaf-on conditions the second during leaf-off, and successfully used to map wetlands at an 88% accuracy. The leaf-on image was used to map land cover and hydric soils that were identified with the leaf-off image.

For many temporal applications the chief concern is change in land cover (Hayes and Sader, 2001). A variety of techniques exist for analyzing temporal dynamics. Henebry and Rieck (1996) applied Principle Components Analysis (PCA) to 30 Advanced Very High Resolution Radiometer (AVHRR) Normalized Difference Vegetation Index (NDVI) 10-day composites. The project was aimed at evaluating different PCA outputs for their utility in classification. They found that Principal Components of less than six were valuable while higher components tended to degrade finer features. Texture measures have also been investigated for temporal analysis with Landsat data (Arai, 1991). In this case, texture measures were extracted for Landsat TM and Landsat Multi Spectral Scanner (MSS) data. A variety of processes were run to evaluate the possibility of

classifying Landsat imagery using texture values across multiple time periods. The inclusion of temporal texture data proved to be very useful. Munez-Villiers and Lopez-Blanco (2007) utilized Landsat and ETM+ data spanning 13 years to assess land cover conversion from forest to pasture and agriculture land with significant success.

Some research projects have focused on determining precisely how many time periods are necessary to maximize discrimination between land cover or vegetation classes. Price et al. (2002) used a three date Landsat 5 TM dataset to determine the optimal number of spectral bands from individual dates as well as in multi date combinations to discriminate grassland types in a prairie ecosystem. Their research determined that data from different time periods was very valuable but there is a point of diminishing return and even diminishing accuracy as the number of spectral bands expands beyond 10-12. These results would indicate that 2-3 MSI datasets are sufficient to accurately characterize similar plant communities. A similar approach was pursued using a 4 date TM dataset collected over a single growing season to determine the ideal number and spacing of imagery over an agricultural region of Argentina (Guerschman et al., 2003). Two dates were determined to be required for successful discrimination and if well spaced temporally provided the maximum amount of necessary information.

Due to the fact that many SAR systems provide single banded imagery, repeat coverage has become a critical tool for any analysis utilizing SAR. Multitemporal SAR has been successfully used in a number of cases for agricultural studies. The utility of SAR imagery collection tied to crop calendar has been specifically evaluated (Brisco and Ulaby, 1984). Crop discrimination was successfully performed at 83 percent accuracy, a 10 percent improvement over temporal SAR data not tied to the crop calendar. Ban and Howarth (1999) used a progressive classification and masking approach to classify a number of crop types over the course of a growing season. ERS-1 data covering the entire growing season (9 dates) were used in this case. Dates that were suitable for classifying specific crops were used and the areas classified were then masked for further discrimination of other crop types from other periods. An overall accuracy of 88.5 percent was achieved. Blaes et al. (2005) looked at the contribution of a multi date SAR dataset to compliment a single MSI dataset to determine the optimal number of SAR images required to monitor agriculture over a growing season. They determined that 3-5 SAR images were appropriate.

Forestry applications are another area that has received a great amount of SAR multitemporal analysis because many forests of interest are in areas that pose problems for MSI systems as a result of the predominance of cloud cover. Drieman et al. (1989) demonstrate this with multiple dates of C-band SAR data.

Individual scenes did not allow the discrimination of individual forest communities but combining the different dates into false color composites was successful. More complex combinations have used multifrequency, multipolarimetric, and multitemporal airborne SAR to demonstrate their utility in classifying hardwood species (Ranson and Sun, 1994). Multiple bands were reduced using PCA and the data were classified using the MLC. Hardwood and softwood stands could be differentiated, as could a number of other land cover classes, including clearings and regenerating forest. A post-classification 5x5 majority filter was used to achieve a hardwood classification accuracy of 95 percent.

As with MSI data from different dates, multitemporal SAR has proven particularly useful in wetlands classification. Multi date RADARSAT imagery has been used for monitoring wetlands changes in northern Australia (Milne et al., 2000). Images spaced throughout a year were registered to each other, smoothed using a median filter and differenced to create change images. These were used to identify inundated areas and to differentiate saturated soils from vegetation. A decision-based classifier applied to a multi date RADARSAT dataset achieved the highest accuracy when five dates of imagery were utilized in Parmuchi et al. (2002). Wang et al. (1998) investigated a series of images collected over nine months and determines that 4-5 images from different time

periods were required for successful classification, more were not necessary while less were not adequate. Compared to a single date of Landsat TM data, the SAR series provided higher classification results. A similar time series was used to analyze inundation patterns using RADARSAT scenes (Townsend, 2001; 2002). Seasonal flooding in forested wetlands of North Carolina was successfully mapped. Inundated areas could be discriminated despite leaf-on conditions though classification accuracy was somewhat lower (89.1 percent vs. 98 percent) than for leaf-off conditions. Overall accuracy was 93 percent. A Landsat derived mask was used to separate forest from non-forest land cover, and only forested regions were used in this analysis.

Land cover analysis has also seen a successful use of multi date SAR imagery. In one case combined ERS-1 and JERS-1 data were used to classify land cover (Kellndorfer et al., 1998). An accuracy of 80 percent was achieved though the most significant value was deemed to come from the two SAR frequencies used by these two sensors. Solaiman et al. (1999) have developed a fuzzy-based classifier to derive land cover from a multi-SAR dataset. The fuzzy concept attempts to capture not only pixel information but contextual information as well. This results in a classification that considers neighborhood values and incorporates the spatial domain when performing pixel categorization. Two dates were used and classification accuracy for each class was over 90 percent.

Verhoeve and De Wulf (1999) demonstrate a process for the multitemporal classification of land cover using four ERS dates. Extensive processing incorporating filtering, PCA transforms, pyramid generation for segmentation, texture filtering, and post-classification majority filtering resulted in a classification accuracy of 76 percent. In this project, texture was not found to be useful (it was performed on a PCA band) and post-classification majority filtering did not improve classification accuracy. Given the results of this project it is conceivable that there is a point at which additional processing and filtering produces negative results. Running successive algorithms for their own sake progressively remove the dataset from its representation of reality.

It is apparent that multi-date imagery provides another valuable dimension to analyzing land cover. The simple fact of phenological changes over a growing season and the utility of imagery for assessing vegetation means the two go hand-in-hand. One area of investigation that has not yet been assessed with regard to utilizing imagery from different time periods and particularly in conjunction with imagery from different systems is whether seasonality can be systematically leveraged for improved land cover assessment. Zhu and Tateishi (2006) looked at SAR and MSI multi date datasets to compare their value individually and in combination and found that temporal datasets are equally valuable but the time interval between images was also important to consider

and integrate into the analytical process. Incorporating a time span factor can allow for more change over longer spans between images and less change over shorter spans. This is particularly important for plant communities that exhibit seasonal variations.

This research investigates whether imagery collected during the dry season and the wet season in a subtropical landscape may be combined to improve land cover classification.

2.9 MSI AND SAR IMAGE FUSION

Datasets from different satellite and airborne-based systems have been integrated in a number of fashions for a variety of reasons. Probably the most common reason is for the purpose of integrating high spatial resolution panchromatic data with lower spatial resolution MSI data resulting in a higher spatial resolution color composite (also known as a pan-sharpened dataset). Fusing data from different sensor systems aims to leverage the unique value of each system to gain more than either could provide alone. A general definition of image fusion is given as 'Image fusion is the combination of two or more different images to form a new image by using a certain algorithm (van

Genderen and Pohl, 1994). Not all image fusion techniques involve complex algorithms.

Since SAR systems first began collecting data in the 1960's there has been interest in their value as a complementary data source to MSI systems. Prior to digital imaging systems and the advent of cheaper computer processing power most of this work was performed using visual interpretation techniques or the creation of color composites that integrated SAR data with optical data as a printed color image. MSI systems depend on the reflectivity of energy from the sun. By collecting information in different wavelengths one can reconstruct an image of the ground and through processing characterize ground cover. SAR systems provide information on surface roughness, geometry, and dielectric properties, also allowing some characterization of surface material. Both types of data are known to be independently valuable for land surface characterization. A respectable amount of research has gone into specifically comparing one data source to the other to assess their respective value (Aschbacher and Lichtenegger, 1990; Lawrence et al., 1998; Haack and Bechdol, 1999; Bin, 2003; Miles et al., 2003; Chust et al., 2004; UÇa et al., 2006; Shimabukuro et al., 2007). These comparisons are typically a precursor to assessing the value of utilizing these data in combination. Combining data from different imaging sources

proves to provide an expanded means for accurately characterizing the surface of interest.

Pohl and van Genderen (1998) provide a comprehensive review of image fusion literature and techniques. They define the common objectives of image fusion as:

- Image sharpening (Chavez et al., 1991)
- Improve geometric corrections (Strobl et al., 1990)
- Provide stereo-viewing capabilities for stereophotogrammetry (Bloom et al., 1988)
- Enhance certain features not visible in either of the single data alone (Leckie, 1990)
- Compliment data sets for improved classification (Schistad-Solberg et al., 1994)
- Detect changes using multitemporal data (Duguay et al., 1987)
- Substitute missing information (e.g., clouds-MSI, shadows-SAR) in one image with signals from another sensor image (Aschbacher and Lichtenegger, 1990)

- Replace defective data (Suits et al., 1988).

Image fusion is a tool to combine multisource imagery using advanced image processing techniques. It aims at the integration of disparate and complementary data to enhance the information apparent in the images as well as to increase the reliability of the interpretation. This leads to more accurate data (Keys et al., 1990) and increased utility (Rogers and Wood, 1990). Rogers and Wood (1990) also determined that fused data provides for robust operational performance, i.e., increased confidence, reduced ambiguity, improved reliability, and improved classification.

Fusion techniques may be applied to a variety of imagery types such as multi-scale MSI data. This process combines datasets of different spatial resolution to improve the ability to discern features or cover-types. The research performed in this project is primarily concerned with the fusion of MSI and SAR imagery. The classification accuracy of MSI is improved when more than one MSI dataset is used. This concept is well known from the use of multitemporal datasets for vegetation mapping or agricultural monitoring. Images from SAR sensors contribute in a different fashion. Working with MSI systems, interpreters typically develop a spectral signature for a feature of interest such as a particular agricultural crop. Unfortunately different crops can have very similar spectral signatures resulting in an inability to differentiate between them using MSI. SAR

data with their ability to provide an indication of the physical characteristics of a surface provides an added dimension for distinguishing between two cover types. SAR and MSI data provide information from different portions of the EMS and have been proven to be valuable when combined for analysis especially with regard to land cover classification (Haack et al., 1998).

A critical step in the fusion of remotely sensed imagery is the georectification process (Pohl and van Genderen, 1998). Most fusion operations involve processing of information between bands collected from different imaging platforms. Virtually all such procedures involve data of different spatial resolutions. Matching datasets to allow integration and to maintain the highest scientific rigor is critical to follow-on steps in the process. Ideally, registration should be pixel to pixel (for systems of equal spatial resolution) which is essentially impossible. Image to image registration is typically possible within a one pixel root-mean square error (RMS). Higher RMS's will result in fused datasets that have a nominal spatial resolution that is lower quality than either of the two input datasets.

A common process used for integrating SAR and MSI utilizes an Intensity-Hue-Saturation (IHS) transformation. This is typically performed with the goal of improving visual interpretation of the data. An IHS transformation takes a three-banded image from a Red-Green-Blue (RGB) color space and transforms it to IHS.

The goal of this process is to replace the intensity channel with a different data source such as a band of SAR data or SAR texture. Welch and Ehlers (1988) used an IHS transformation to combine Landsat TM and SIR-B data for feature extraction. The goal was to investigate this technique as a tool for visual extraction of features to update cartographic databases. The IHS transformed SAR and MSI dataset increased feature recognition by up to 25 percent. RADARSAT fine-beam data were also merged with Landsat TM using an IHS transform (Tanaka et al., 1999). The higher spatial resolution SAR data were well suited to enhancing cartographic features in Landsat TM to improve visual interpretation and allow for their extraction. A further evaluation regarded the use of high spatial resolution SAR for fine feature change detection also had promising results. Another example of the IHS transformation being used to fuse data sources for effective visible interpretation involved a number of different geophysical datasets (Rheault et al., 1991). This project evaluated the possibility and value of fusing image data with other data for geologic analysis. The fusion of SAR and MSI data was found to be very useful for the enhancement of structural geology and subsequent interpretation. The IHS process is common in geologic operations since it provides an output image that can be viewed in a standard RGB color space (Harris et al., 1990).

The same process has been used for land cover evaluation (Raghavawamy

et al., 1996). ERS SAR data were combined with IRS multispectral data to evaluate their usefulness for land cover interpretation. The SAR datasets were processed with a 5x5 median filter to reduce speckle. The combined datasets were processed in a number of ways including IHS transformation and PCA to create composite images for visual interpretation. Land cover was visually interpreted and compared to validation datasets for assessment purposes. The combined and processed images were deemed to be more valuable due to the ability to discern some features that were not directly observable in the individual datasets. Amarsaikhan and Douglas (2004) also utilized a PCA transformation and IHS fusion process to combine SPOT multispectral data and SAR. The combination proved to provide the highest classification accuracy in their study especially when an expert system classifier was applied to the data.

Dejhan et al. (2000) applied the process for flood delineation. In this case, two dates of SAR data collected by the JERS-1 platform with a third date of multispectral data also from the JERS-1 platform (OPS) were combined. The SAR data consisted of a pre-flood and during-flood image pair for a region of Thailand. A texture algorithm was run on the SAR scenes with the outputs differenced. The resulting dataset was then integrated with the OPS data through an IHS transformation where the differenced SAR texture dataset was substituted for intensity. This was then transformed back to an RGB color space and run through

a Neural Network classifier to determine land cover and inundation of land cover types during the flood event. This process resulted in classification accuracies ranging from 86-90 percent depending on the cover type. Miles et al. (2003) determined that wetlands could not be successfully discriminated in a boreal forest ecosystem without the inclusion of SAR data in their processing. They were also able to more effectively delineate the degradation of forest resources due to air pollution for the study area with the fused data. The value of a combined approach is further validated for wetlands mapping by Grenier et al. (2007) where SAR and Landsat 7 Enhanced Thematic Mapper + (ETM+) data were combined using a hierarchical multistage object-based classifier to delineate unique wetland classes.

Digital classification is a common goal of data fusion. The intent of such an operation is to gain more parameters for segmenting an image into classes of interest. An early example of efforts to integrate SAR and MSI data (Ulaby et al., 1982) used airborne SAR and Landsat MSS data in a classification process for crop identification. The goal was to evaluate SAR data as an additional band to determine if it provided useful information. Using a quadratic Bayes classifier each dataset was evaluated individually and then in combination. Classification accuracy was raised from 75 percent for Landsat MSS alone to 89.4 percent for the MSS dataset combined with two SAR dates.

Image fusion has also been applied for crop discrimination. Brisco et al. (1989) investigated the utility of integrating a single date of Landsat TM data with two dates of SIR-C HH data for the identification of agricultural crops. A subset of TM data, bands 3, 4, and 5, and two SAR dates were layer stacked into a single dataset against which a MLC was run. The combined dataset provided a classification accuracy of 77 percent, 30 percent points better than Landsat alone. Given the interest in agricultural crop identification, the authors concluded that an additional date of SAR imagery collected later in the growing season would have contributed significantly to discrimination between crop types that were otherwise confused.

This research was later expanded on (Brisco and Brown, 1995) by evaluating multi date, multispectral (TM), and SAR data again for crop classification. The authors determined that TM data were superior to SAR for direct classification but multi date SAR did bring classification accuracies up from 30 percent to 74 percent. Multi date TM data using Landsat channels 2-5 resulted in classification accuracies at 90 percent and the integration of SAR and TM resulted in a further improvement to 92 percent. Another useful aspect of this project was the investigation of SAR data as a replacement for cloud obscured TM data for the classification process. The synergism that exists between these sensors allows this replacement for small regions with a minimal

impact on classification accuracies. One notable conclusion of this research was that one date of multispectral data combined with multiple SAR dates provides suitable classification accuracies.

The Shuttle Imaging Radar (SIR-A/B/C) missions have provided a number of opportunities for additional studies. SIR-B data were combined effectively with MSI data from the French SPOT system to perform a classification of tropical vegetation (Nezry et al., 1993). This research gave close consideration to the nature of speckle and its impact on the usefulness of SAR imagery. A GM speckle suppression filter was used to reduce the effect of speckle in the SAR data. The data were then classified using a supervised classification method resulting in higher classification accuracies than the individual datasets alone. A further analysis was performed using wet season SAR data and SPOT data collected in the dry season (22 months apart) to determine if the two sources could be used for land cover change detection, also to positive effect.

Lozano-Garcia and Hoffer (1993) evaluated TM in combination with SIR-B SAR data at varying incident angles for land cover classification using a MLC and a contextual variation of the MLC. Three sensor combinations were evaluated, Landsat TM, SIR-B, and the two combined. All three combinations were deemed adequate for classification of general land cover type. However, the combined sensor dataset proved much better at classifying detailed cover types. The

combination of TM bands 2, 4, and 5 with SAR data at a 28 degree incident angle provided classification accuracies greater than 90 percent.

The integration of SIR-B data with Landsat TM data has also proved effective in situations where neither system performed adequately alone (Haack and Slonecker, 1994). The primary goal was to identify the location of villages in Sudan along with surrounding land cover. Due to the nature of materials used in building construction, the location of villages was difficult to separate from surrounding natural materials using multispectral data alone. SIR-B imagery was integrated as an additional band of data and signatures were evaluated for separability. Due to clearly defined histograms in specific TM bands for vegetation and between multispectral and SAR data for urban land cover, a Parallelepiped classifier was used resulting in an overall classification accuracy of 94.1 percent. When only the TM data were run through a MLC, the results were only 69 percent.

Merged data have also been investigated for forest type discrimination (Leckie, 1990). Nine bands of airborne collected multispectral data (MS) and two radar bands (X and C each with four polarizations) were assessed individually and in every combination to determine their value for forest stand identification and attribution. SAR data were included as panchromatic bands and the combined datasets were processed through a MLC. Three MS bands provided

the most value, near-infrared, green, and midwave IR, particularly for establishing feature boundaries. Combining the SAR and MS data provided the highest classification accuracy of 70 percent. One notable finding regarding the SAR datasets was that frequency (or band) provided significantly more value than variables introduced through cross polarization.

A number of projects have utilized innovative classification processes with multisensor data. Schistad-Solberg et al. (1994) investigated a new method of statistical classification utilizing a Bayesian based decision rule to integrate TM data with multi date ERS SAR data. One of the benefits of this method was the potential for inclusion of known changes in the region of coverage to aid in classification of imagery from multiple time periods. This model successfully demonstrated the utility of fused imagery despite a time difference by providing improved accuracy rates compared to single-source classifiers.

In another project a hybrid supervised/unsupervised classification process was used to combine ERS-1 and JERS-1 SAR data with SPOT multispectral data (Xie et al., 1998). Each dataset was processed separately and then in different combinations to determine which data were most complementary. The two SAR bands combined provided higher classification accuracy than the MSI data, 90.2 percent vs. 84.8 percent for level 1 classification. All data combined resulted in 94.8 percent accuracy. When level-II classification was sought, the combined SAR

with IR band from SPOT provided the highest accuracy at 83 percent, 7 percent higher than for SAR alone and 17 percent higher than for SPOT.

When it comes to more complex processing models a number of projects have investigated numerous options for fusion of datasets. Some of these have used more traditional approaches while others have investigated new fusion or classification techniques to find those that are more appropriate for given research questions or applications. An early example of sensor fusion investigated the complementarity of datasets to determine their value in classification of urban environs (Haack, 1984). Airborne SAR and airborne MSI data were integrated into a common dataset and evaluated in different combinations for their utility in land cover classification of urban or near-urban environments. Transformed divergence calculations were evaluated for inter-class variability and to determine the best channels for classification. The study concluded that one band from each major portion of the EMS, including microwave, would result in the best classification results.

Due to the ever-increasing interest in monitoring vegetation dynamics with satellite imagery there have been many innovative and more advanced approaches to system fusion and evaluation. Vegetation parameters such as biomass, leaf area index (LAI), and percent ground cover have been extracted from an integrating TM and SIR-B SAR dataset (Paris and Kwong, 1988). This project

concluded that the two datasets contribute valuable and unique information. TM data responds to green biomass while SAR data responds to woody components. Principal Component Analysis (PCA) and Canonical Correlation Analysis (CCA) have been performed on a similar dataset by Lee and Hoffer (1990) to determine if correlations can be drawn between the datasets and forest stand parameters such as biomass. Little correlation was found with individual PCA bands but a high correlation was found between the first band of CCA and forest stand biomass.

Fusion of multiple imagery sources, ERS-1, airborne SAR, and Landsat TM, has been applied to agricultural areas to assess soil conservation practices (Smith et al., 1995). A decision tree classifier utilized NDVI derived from TM and brightness values from SAR to assess presence of crops and bare fields or crop stubble to quantify post-cropping conservation in an agricultural area. The value of SAR for providing texture information was critical to the assessment of crop stubble. Finally, Zhu and Tateishi (2000) have developed two new fusion techniques to effectively integrate sensor data from multiple sources and multiple dates for successful agricultural monitoring and analysis. These models take into account the temporal dependence of images and the valuable traits of each data source. Classification accuracies were improved over a MLC especially when multiple sensors are integrated.

One of the more extensive fusion projects to date has looked at many of the

variables associated with integrating SAR data with MSI. L-Band and C-Band data from the third Shuttle Imaging Radar program (SIR-C) and Landsat TM data were evaluated for discrimination of land cover for a study area in Tanzania (Haack et al., 1998). A number of statistical operations were performed on the SAR data to evaluate their impact on fusion and land cover classification. Speckle suppression was performed using a 7x7 low-pass filter; a number of texture measures were evaluated at window sizes ranging from 3x3 to 17x17. A post-texture, pre-classification low-pass filter was evaluated to assess the value of smoothing texture values. Post-classification filtering was also performed using a 5x5 majority filter to evaluate the value of smoothing the classification results for the generation of thematic datasets.

Each of these processes resulted in incremental improvements in classification results using the MLC. A Variance texture measure at a 13x13 window size was deemed the most valuable for processing the SAR data. The low-pass filter for speckle suppression resulted in an increased classification accuracy of 4-6 percent. The post-texture low-pass filter resulted in a 4 percent improvement in classification with the Variance texture measure. Post-classification majority filtering resulted in improvements of 1-4 percent. Overall classification accuracies ranged from 79 percent for Landsat data alone to 85 percent for combined datasets. For discriminating between natural vegetation and

scattered agriculture the highest classification accuracy of 94 percent came from a combination of the SAR datasets with their texture processed data layers.

A further site was then investigated (Haack and Bechdol, 1999) with additional SAR data sources and similar processing. The dataset in this investigation added JERS-1 SAR data and Radarsat SAR to Landsat TM multispectral and SIR-C SAR, multipolarization data. In this instance speckle processing was not performed but was addressed to some degree with low-pass pre-classification filtering and post-classification majority filtering. Results at this site were again promising as it was determined that pre- and post-classification filtering of SAR data resulted in improved classification accuracies. Pre-classification filtering improved land cover classification with SAR data by approximately 15 percent, from 62 to 77 percent accuracy.

Another important result of the multisensor classification process was that a combination of two SAR data layers (SIR-C L-band and JERS-1, also an L-Band sensor) with their derived texture layers resulted in a classification of vegetation with 89.4 percent accuracy. This result was comparable to that of four Landsat TM bands, which resulted in 93 percent accuracy. This indicates that multisensor SAR datasets may be very valuable for land cover and vegetation characterization projects, and corroborates similar research (Xie et al., 1998), especially in areas with weather conditions not conducive to multispectral investigations.

This research was further expanded to investigate the effect of speckle suppression followed by texture extraction (Haack et al., 2000). A 5x5 median filter was applied to reduce speckle yet maintain local feature structure. The output was then processed with a Variance texture measure at a 21x21 window size. The combination of such differing window sizes reduced speckle locally while providing for the assessment of texture regionally. The resulting classification accuracy was 84 percent compared to 73 percent for Landsat TM alone. A similar multi-window filtering approach was used for land cover mapping around St. Louis, Missouri with improved results when SAR data were combined with MSI (Huang et al., 2007). The greatest value was achieved when multiple SAR statistical derivatives processed at different window sizes were combined.

2.10 DISCUSSION

The natures of MSI and SAR imagery lend themselves to complementary integration. The primary questions that remain are what are the best characteristics of each to leverage and what processing options provide the most accurate results when performing land cover classification. MSI has a long and well-documented history in this regard. However, there is a clear threshold in the area of 75-85 percent classification accuracy that is very difficult to exceed in

a systematic fashion. Almost every published fusion of SAR and MSI has resulted in improved accuracy levels though a number of different techniques have been used. Some of the most promising have involved the use of texture measures derived from SAR imagery. It is important to investigate how some SAR collection parameters and additional processing techniques may be leveraged to provide a further improvement of classification accuracy.

Parameters such as incident angle and the impact they have on the SAR data collected are fairly intuitive. Empirical assessments of land covers from different biomes could provide an index of appropriate assessment angles given specific goals and surface conditions. This project assesses two sets of SAR imagery from different seasons consisting of three different incident angles from two look directions. These should provide a fair appraisal of which incident angle provides the most value for dry season and wet season assessments of vegetation in a subtropical climate.

Processing options are clearly important considerations for making SAR imagery interpretable. Texture is a valuable dimension of data but the nature of SAR imagery lends an element of texture to a scene that is driven by the nature of the microwave sensing system rather than the nature of the surface imaged. Speckle suppression aims to alleviate this situation. However, the goal of speckle suppression is to minimize arbitrary texture while preserving

meaningful texture resulting from surface conditions. By empirically assessing different texture and speckle algorithms and window sizes, this project will provide a filter combination that provides the greatest value as measured by classification accuracy.

An aspect of this research that is truly unique is the intent to combine imagery from specific seasons. The general wisdom in the community, unless specific multi-temporal issues are being assessed, is that when image datasets from different systems are being fused one should endeavor to ensure that the datasets are collected as close together in time as possible. This will minimize change on the ground that could affect analysis results. Given the nature of SAR and MSI it is conceivable that co-temporal datasets do not provide the ideal combination of data for analysis. This project will assess datasets specifically collected in a dry and wet season to determine if one or the other, or a combination of data from both, provide an ideal dataset for increased land cover classification accuracy. The details of these datasets as well as the scientific methodology applied in the research are described in the next chapter (Chapter 3).

3.0 METHODOLOGY

3.1 RESEARCH OBJECTIVES

This research investigates different processing alternatives and SAR image parameters to assess the value of SAR independent of MSI and integrated with MSI for land cover characterization over a subtropical landscape. An empirical investigation of speckle suppression and texture measure algorithms is used in an effort to determine the most appropriate combination to apply when integrating MSI and SAR imagery. Furthermore, this research investigates SAR image collection parameters such as incident angle to determine if appreciable gains in classification accuracy can be achieved with specific tasking settings. Finally, the impact of seasonality on MSI and SAR integration has been assessed by fusing wet and dry season datasets in different combinations to determine if cross-season integration improves classification accuracy. The study site, dataset, and methodology are described in the following section.

3.2 STUDY SITE

Andros Island (Figure 3.1) is the largest island in the Bahamas Archipelago. It is located less than 150 km southeast of Miami, Florida and 50 km west of Nassau, Bahamas at approximately 80° west and 24.5° north. It is bounded to the east by the third longest barrier reef in the world and numerous

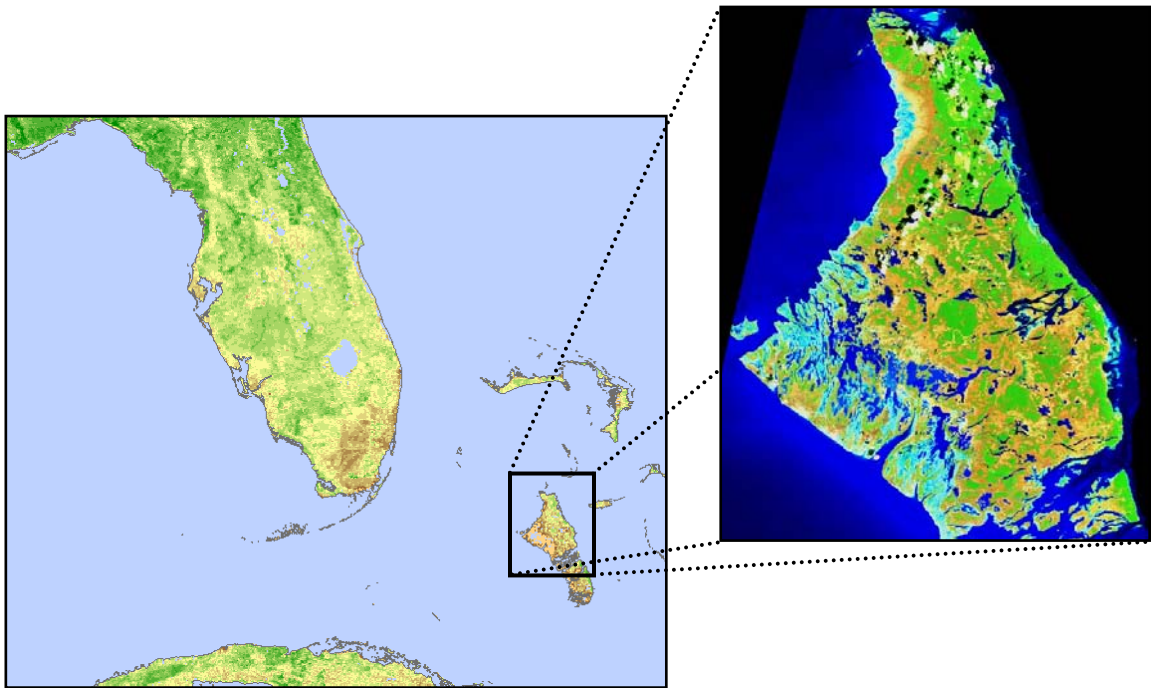


Figure 3.1: Andros Island, The Bahamas

patch reefs. A transect from the ocean to terrestrial landscapes includes seagrass beds, mangroves, mudflats, tidal creeks, intertidal areas, and rocky, silty, and sandy coastlines. Freshwater habitats are abundant, and range from creeks and

tidal rivers to ponds and the famous blueholes, or flooded sinkholes, which are similar to cenotes of Central America. Terrestrial habitats include endemic pine forests, several types of hardwood coppices, wetland savannas, and swashes (Josse et al., 2003). Most of these habitats are extremely diverse, readily accessible, and minimally disturbed.

There are very few human inhabitants on Andros and most of those are concentrated in small settlements along the east coast. Despite the small population size, much of the Island is easily accessible due to logging performed in the 1960's when stands of the endemic pine (*Pinus caribaea var. bahamensis*) were harvested. This process left behind a series of interconnecting roads throughout much of the island.

Andros Island includes over 60,000 hectares of undeveloped, largely unoccupied land. Almost all of this land is Crown Land, or government property. Aside from a few current, and a few failed, agricultural efforts, most of the Island remains wild. The government recently promoted the Island as having one of the largest tracts of still unexplored land in the Western Hemisphere. It is close to the United States, easily accessible, has a stable, democratic government and well-developed and reliable infrastructure, including roads, water, electric, and telephone services.

North Andros Island has been selected as the study site for this project due to its diversity of landscapes, easy accessibility, and limited ongoing human disturbance. The classic seasonality of precipitation makes it an ideal site for investigating the impacts of wet/dry season variations in satellite data with intact natural landscapes. Five land cover types have been selected for this study that are representative of the dominant terrestrial land covers found on Andros Island and have structural differences that make them ideal for investigation with SAR imagery.

3.2.1 Pineland

Extensive areas of Andros Island are covered with pine forests. The native Caribbean pine (*Pinus caribaea var. bahamensis*) dominates this community, but a variety of understory plants define the characteristics of any particular stand including bracken fern (*Pteridium aquilinum*), poisonwood (*Metopium toxiferum*), thatch palm (*Thrinax morrisii*), orchids (*Orchidaceae spp.*), and a variety of other species (Ford, 1997). The pinelands of Andros Island were harvested for lumber and pulpwood from the mid-1960's to the early 1970's. The current stands consist of seed plants that were left standing and secondary growth. As a result the pine forests are of approximately similar age, though there are intermittent stands that were left unharvested at the time and include trees of

greater age. The pinelands appear to be maintained by a fire regime that has a considerable impact on the understory (Bergh et al., 2003). The understory community consists of a variety of ferns and herbaceous plants in the early stages of fire recovery, and a mixture of woody shrubs in the later stages. The thatch palm (*Thrinax morrisii*), a palmetto, is common in many stands. Surface material is typified by very thin yet rich soil with exposed rough limestone common in many areas.



Figure 3.2: Pinelands Cover Type

3.2.2 Coppice

Also known as the Blackland communities, coppices include a number of broadleaf evergreen trees in pocket communities distributed throughout the pinelands (Bergh et al., 2003). The coppice cover type can be divided into two



Figure 3.3: Coppice Cover Type

categories, high coppice and low coppice reflecting the relative topography on which they are found. These communities are in a recovering state following the removal of valuable tree species during the prior era of logging activities.

Despite this they constitute the highest plant biodiversity communities on the

island (Correll and Correll, 1982). Broadleaf trees create a near closed canopy that provides a humid, shaded environment for a variety of herbaceous plants including a number of orchids, bromeliads, and ferns. The coppice communities have a more developed and deeper soil structure than the pineland though in many instances they develop over soil pockets in the limestone strata (Ford, 1997).

3.2.4 Rockland

The Rockland scrub community develops under some of the harshest conditions found on Andros Island. These areas are typically very dry and



Figure 3.4: Rockland Cover Type

exposed to the sun with limited soil and surface material consisting of exposed limestone. The availability of water is driven by the seasonality of Andros Island's climate. Most plants take hold in crevices and small pockets where soil may have accumulated and exhibit classic adaptation to extreme and arid environments. The plant community typically does not exceed two meters in height and includes a wide range of often dwarfed species common in the pineland and coppice communities (Ford, 1997).

3.2.5 Saw Grass Marsh

Andros Island has extensive freshwater marsh communities especially across its western regions though smaller examples are found around freshwater



Figure 3.5: Saw grass Cover Type

basins and blue holes across the island. These communities consist of a variety of freshwater plants dominated by Saw grass (*Cladium jamaicensis*) edged with Cattail (*Typha domingensis*) as well as sporadic Silvertop Palm (*Coccothrinax argentata*) and Pond Apple (*Annona glabra*) along the edges of deeper freshwater ponds. Saw grass marsh regions will often have terrestrial islands in their midst consisting of Pineland communities (Ford, 1997).

3.2.6 Mangrove

Mangrove communities are common in protected coves along the coast of Andros Island as well as across extended expanses of the western lowlands



Figure 3.6: Mangrove Cover Type

region of the island. There are four common mangrove species, each growing best in slightly different base material, elevation, and salinity conditions from the most prevalent Red Mangrove (*Rhizophora mangle*) along with less common Black Mangrove (*Avicennia germinans*) in shallow marine conditions, Buttonwood or silver mangrove (*Conocarpus erecta*) along the waters edge, to terrestrial White Mangrove (*Laguncularia racemosa*) (Sealey, 2003).

3.2.7 Differentiation of Cover Types

While all of these communities can be found in relative close proximity on Andros Island, the structural differences among them make them ideal for investigation using remote sensing techniques, especially those incorporating texture. The Pineland communities have a well-developed structure with the native pine creating an upper canopy, a clear and open midstory, and a low (typically herbaceous or one to two meter high shrub) understory. Coppices consist of a dense community with no clear canopy structure. The Rockland scrub has limited biomass and a very rough surface material that is expected to result in a significant texture response in the SAR imagery though tempered by standing water in the wet season. The Mangroves are relatively dense in biomass though of low to medium height and occupy a typically tidal inundated

surface condition. The smoothness and consistency of the Saw grass marshes are also expected to be a distinguishing characteristic in the SAR imagery.

3.3 DATASETS:

Three basic categories of data were assembled and used in this project. These consist of spaceborne remotely sensed data, ground truth information based upon field visits, and existing cartographic products and reports.

3.3.1 Remotely Sensed Data

One of the common difficulties of remote sensing research is the acquisition of data at appropriate temporal windows. This is further complicated when data from two different platforms are to be integrated. One of the stated goals of this project is to investigate the utility of integrating data from different seasons to actually improve land cover classification accuracy.

As a result, two multisensor datasets have been acquired for the study region, one during wet season conditions and a second during dry season conditions. The primary datasets consist of MSI from the U.S. Landsat 5 Thematic

Mapper (TM) sensor, and SAR imagery from the Canadian RADARSAT-1 platform.

3.3.2 Multispectral (MSI) Imagery

The Landsat 5 TM sensor is a multispectral scanner that collects imagery in visible and infrared wavelengths. Seven channels or bands are collected as follows:

1. 0.45-0.52 μm (visible blue)
2. 0.52-0.60 μm (visible green)
3. 0.63-0.69 μm (visible red)
4. 0.76-0.90 μm (near IR)
5. 1.55-1.75 μm (SWIR)
6. 10.4-12.5 μm (thermal IR)
7. 2.08-2.35 μm (SWIR)

(Morain and Budge, 1997)

Bands 1-5 and 7, the channels used in this study, have a nominal spatial resolution of 28.5 meters and a single image swath covers 185 km. The thermal band (band 6) was not utilized due to its coarser spatial resolution (approximately 120 meters). TM imagery (Path 13, Row 43) was collected on the 27th of Nov 1999 (wet season) and on March 3rd 2000 (dry season). Both dates of

Landsat imagery exhibit minimal cloud cover and cloud shadow, affecting less than 5 percent of the imaged area (see Fig. 3.7). Calibration and validation sites were selected to avoid these clouded areas.

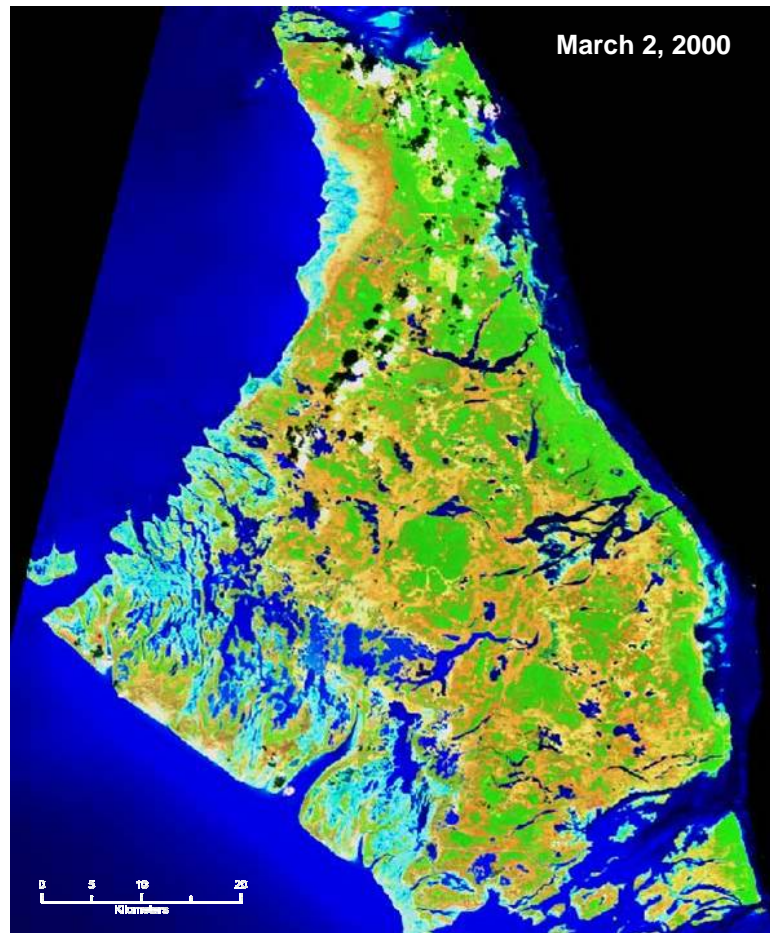


Figure 3.7: Landsat Thematic Mapper Imagery Bands 7,4,2

3.3.3 Synthetic Aperture Radar (SAR) Imagery

The Canadian RADARSAT system is a single band SAR sensor operating at a frequency of 5.3 GHz (C-band), with a wavelength of 5.6 cm and HH

polarization. A wide variety of sensor modes are available providing a number of different products based on changing incident angle and spatial resolution.

This sensor has proven useful for vegetation analysis. However, its active wavelength has resulted in mixed success particularly in tropical and temperate zones with dense vegetative communities resulting in backscatter saturation. This is not an anticipated problem in this application due to the relatively low biomass of Andros Island plant communities.

For the purposes of this project, RADARSAT Standard Beam (ST) data (see Fig. 3.8) were collected at three principle incident angles in both ascending and descending mode. ST modes 3, 5, and 7 were acquired for this project (a single ST2 dataset was also acquired and utilized in the analysis), the general parameters of which are defined in Table 3.1.

Eight images were collected during the 1999 wet season representing each Standard Beam incident angle in ascending and descending mode. An additional thirteen images were collected during the 2000 dry season representing each Standard Beam incident angle in ascending and descending mode.

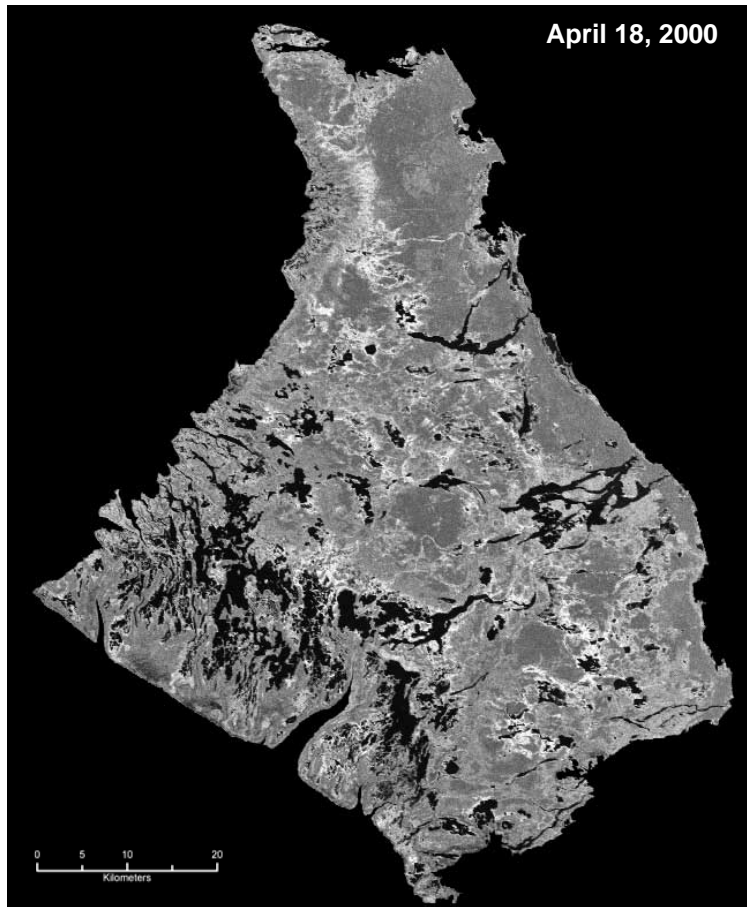


Figure 3.8: RADARSAT Standard Beam Mode 3 Descending

Table 3.1: Acquired RADARSAT Standard Beam Modes

Mode	Looks	Pixel Resolution (m)	Ground Resolution (m)	Incident Angle
ST2	4	12.5	17.85-22.56	24.23-31.25
ST3	4	12.5	22.99-27.25	30.47-36.94
ST5	4	12.5	20.56-23.21	36.54-42.23
ST7	4	12.5	18.19-19.58	44.87-49.42

3.3.4 GeoCover Ortho Imagery

A final imagery dataset to be utilized in this project is the Landsat TM derived GeoCover Ortho product of Earth Satellite Corporation. This dataset provides a consistent orthorectified image base for tying all related image datasets to and will provide a uniform analytical framework for the project (Koeln et al., 1999).

3.3.5 Ground Truth

An important aspect of this project is the identification of representative plant community and land cover sites for evaluating the success of land cover classification and proposed image integration processes. A dataset of calibration and validation sites was collected during fieldwork in November 1999 and May 2000 for this purpose that encompasses the five primary vegetation categories being assessed in this research. Available maps and georeferenced image maps were employed to locate and document sites in the field and precise geographic coordinates were obtained by use of a Trimble Global Positioning System (GPS) receiver. GPS coordinates were differentially corrected using base station data collected in Ft. Lauderdale, Florida. This processing resulted in ground truth geolocation well within the 25m RMS achieved during the coregistration process.

The field effort fully documented the location and characteristics of the selected sites for cover types of interest. Sites used for calibration were randomly selected from the collective study sites in each cover type and the remaining sites were reserved for accuracy assessments. One third of the sites were used in the calibration phase and the remaining two thirds were used in the accuracy assessment process. Table 3.2 lists the collected calibration and validation sites:

Table 3.2: Calibration and Validation Sites

Cover Type	Calibration	Validation	Site size (pixels)	Total Pixels
Pinelands	18	36	41 - 436	7157
Coppice	10	20	16 - 344	3360
Rockland Scrub	4	8	36 - 324	1302
Mangrove	8	16	30 - 114	1930
Saw grass	8	16	46 - 218	2330

3.3.6 Cartographic Datasets

Existing topographic maps of Andros Island provided by the Bahamas' Environmental Research Center (BERC) were scanned into digital files and georeferenced to a common projection and coordinate system (UTM Zone 18 N, WGS 84). They were used for fieldwork and to aid in the identification of appropriate calibration and validation sites for the image classification process.

These maps are the result of a British aerial photography and topographic survey operation in the late 1960's and early 1970's to accurately map the entire island. Due to the small population on the island there has been little change in the past three decades as corroborated by field visits. The map series consists of 24 topographic reference maps at a scale of 1:25,000 and provide a very suitable base of surface information for use with the spatial resolution of imagery in this research project.

3.4 ANALYSIS PROCESS

The procedures used for this research entailed a digital classification using standard processing techniques applied to spatially coregistered sets of MSI and SAR spaceborne data, all resampled to the same pixel size. Spectral signatures were extracted for the various land cover types using supervised calibration sites established during field visits. After signature extraction, a MLC was employed to classify the dataset and a contingency table compiled for accuracy assessment. The contingency tables were created from a separate set of validation sites also derived from the field efforts.

The results from this study compare the accuracy assessments from various classifications for individual land cover types and for all types combined

for overall classification accuracy. Multiple data combinations and statistical manipulations of the data were examined. The specific processes implemented depended on the data source (SAR or TM) and include comparisons of the original sensor data independently and in combination. The fundamental variables investigated by this research are:

- SAR processing options for improved sensor fusion
- SAR incident angle impact on fusion classification results
- The value of cross-season datasets for improved land cover classification.

3.4.1 TM Image Processing

The TM imagery includes the two seasonal dates. A preliminary classification process was performed to determine which bands are most valuable for the purposes of this project. Prior research efforts have determined that selecting only a subset of Landsat TM bands may improve the results of classification (Crist and Cicone, 1984; Haack, 1984). In fact, Price et al. (2002) determined that a single band (near-infrared TM band-4) of TM data was sufficient for discriminating six grassland types. A vegetation index derived from a two or more band ratio was moderately more valuable. As discussed in the following

results section of this research, all MSI bands are used in most of the classification processes. When testing specific SAR-MSI combinations the number of MSI bands are occasionally reduced and in those cases the selected bands are duly noted. Limiting the number of multispectral bands increases the weighting or value of individual SAR bands added to the process. Furthermore, the thermal band (Band 6) for Landsat TM has been set aside for the purposes of this analysis.

3.4.2 SAR Image Processing

The SAR datasets include the selected 21 dates (13 dry and 8 wet season) and incident angle datasets. Two primary operations were performed on the SAR datasets to evaluate their impact on classification accuracy. Speckle suppression was performed using varying window sizes. The literature review has indicated that window sizes for speckle suppression should be relatively small to maintain local area features (Schistad and Jain, 1992). Initially the speckle suppression algorithms were therefore run with windows ranging from 3x3 to 11x11. This was expanded to 13x13 and 15x15 due to early results in the processing phase which indicated a trend of improving classification accuracies as the window size approached the original upper limit of 11x11.

Texture measures of varying window sizes were performed on original and

speckle-suppressed datasets to evaluate their combined impact. Prior research has determined that the Variance texture measure contributes the most to successful land cover classification (Anys and He, 1995; Pierce et al., 1998; Haack et al., 1998; 2000; Haack and Bechdol, 1999) and as a result is the sole texture measure applied in this research. Window sizes ranging from 3x3 to 27x27 are evaluated.

3.4.3 SAR Speckle Suppression Algorithms

Five speckle suppression algorithms are evaluated in this analysis; two statistical and three adaptive. Durand et al. (1987) determined that adaptive filters are the most appropriate for image classification processes. Despite this finding, many subsequent research efforts continued to perform speckle suppression using median filtering (Pierce et al., 1998) even though it degrades texture information (Dong et al., 2000) and impedes feature separation (Sheng and Xia, 1996). The following speckle suppression algorithms are assessed in this study:

Median Filter: The median filter replaces the pixel at the center (p_c) of the sample window with the median value of the surrounding pixels. Though this filter is deemed not suitable for image classification purposes it continues to be used in SAR processing efforts and is being included for comparison purposes.

Local Region Filter: This algorithm divides the sample window into eight sub-

windows for which a variance value is calculated. The region with the lowest variance is then averaged and this value replaces the value at p_c . This adaptive filter preserves texture over larger areas while ensuring uniform areas are maintained.

Lee-Sigma Filter: A variation of the Lee filter (Lee, 1983), the Lee-Sigma assumes a Gaussian distribution of speckle noise and uses the range of DN values within the sample window to estimate what the value of p_c should be.

Frost Filter: The Frost filter is similar to the original Lee filter and uses local statistics to assign a value for p_c . The calculation of p_c involves a convolution of sampled values to establish a likely reflectance value, making it a filter that adapts to the contents of the neighborhood being evaluated.

Gamma-MAP Filter: The MAP filter is an adaptive speckle filter based upon a Gaussian distribution that assumes the value of p_c lies between the degraded (speckled) DN value and the local average. The filter uses posteriori probabilities to calculate the new value.

These filters are evaluated in an empirical fashion to determine their respective value as part of a standard land cover classification procedures. Based upon the analytical process in Figure 3.9, including texture and speckle suppression filtering, there are four possible paths for each SAR dataset. Each TM

dataset is processed independently and then combined with each of the possible SAR processes. Finally, based upon the results of the earlier processing stages different combinations of SAR and TM are processed and tested to evaluate the value of different combinations.

3.4.4 SAR Processing Paths

SAR Path 1: SAR datasets in the first path receive:

1. Image resampling and image registration to the common dataset
2. Image classification and accuracy assessment.

This results in the SAR images being included in the classification process with no sensor specific processing to evaluate their value for direct classification synonymous with an additional channel of information in a multispectral system.

SAR Path 2: SAR datasets in the second path receive:

1. Speckle suppression using the five described filters and range of window sizes
2. Image resampling and image registration to the common dataset
3. Image classification and accuracy assessment.

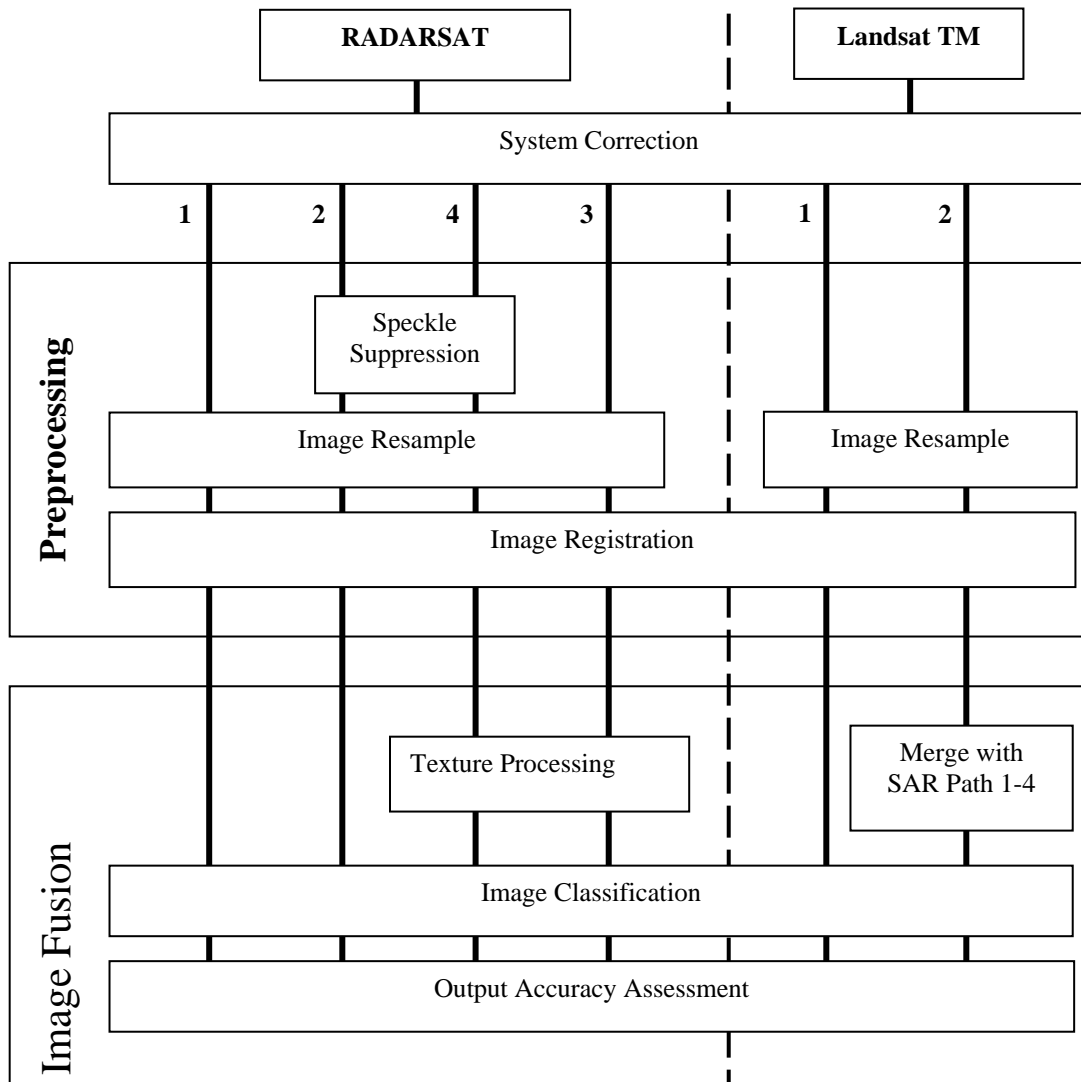


Figure 3.9: Image Processing Paths

SAR Path 3: SAR datasets in the third path receive:

1. Image resampling and image registration to the common dataset
2. Texture processing using a Variance filter and a range of window sizes

3. Image classification and accuracy assessment.

SAR Path 4: SAR datasets in the fourth path receive:

1. Speckle suppression using the five described filters and range of window sizes
2. Image resampling and image registration to the common dataset
3. Texture processing using a Variance filter and a range of window sizes
4. Image classification and accuracy assessment.

3.4.5 TM Processing Paths

TM Path 1: TM datasets in the first path receive the following processing:

1. Image resampling and image registration to the common dataset
2. Image classification and accuracy assessment.

The independent processing of the TM datasets provides a baseline for comparison of all of the other processing alternatives and combinations.

TM Path 2: TM datasets in the second path are processed as follows:

1. Image resampling and image registration to the common dataset

2. Merge with SAR data from SAR Paths 1-4
3. Image classification and accuracy assessment.

Following the independent processing of TM data, the TM datasets are combined with the SAR datasets from SAR Paths 1-4 to assess processing alternatives and seasonal combinations. The merge process involves combining the data (previously coregistered) from independent processing paths (SAR or TM) into a single multilayer image dataset upon which the classification and accuracy assessment processing is performed.

Once the systematic processing and comparison of SAR and TM data and different processing alternatives are complete, a number of different combinations of SAR, processed SAR datasets, TM, and selected TM bands are tested in various combinations to determine if unique combinations of data provide valuable results. Combinations of SAR processed layers, such as texture processed on raw SAR combined with a speckle suppressed layer, and with limited TM bands or multiseason TM combinations, may provide some interesting and valuable results.

For all attempts at characterization of the land cover types, an accuracy assessment is performed. This assessment utilizes the validation sites reserved from the field work. A standard confusion matrix is generated for each classification process that provides results as percentage of correctly classified

pixels as well as a tally of misclassified pixels and the classes in which those fall (Foody, 1992; Congalton and Green, 1999). For the purposes of this study and comparing processing alternatives, total classification accuracy and producer's accuracies are calculated and presented. Since the goal of this research is not the production of a finished land cover dataset for Andros Island (which a user may utilize for land management purposes), but to compare processing alternatives, a user's accuracy is not calculated or discussed in the results section.

The fusion of imagery from different sources often proves to be a very valuable means of assembling more robust datasets and, by extension, knowledge of physical landscapes and processes. Determining the most suitable system parameters and fusion techniques in an empirical fashion provides a practical and application based assessment of the compatibility of different imaging systems for land cover characterization. The spectral responses of multispectral satellite systems, which are chemically based, combined with the reflected microwaves of SAR systems, which are physically based, provide a more rigorous means for assessing plant communities. In essence multispectral data provides a means for assessing the quality and health of vegetation while SAR imagery provides an assessment of complexity or structure. A systematic and consistent method of processing and fusing them into a useable dataset may

provide a valuable tool for assessing land cover and plant communities worldwide.

4.0 RESULTS

4.1 PROCESSING OF LANDSAT TM

The seasonal Landsat Thematic Mapper (TM) datasets were processed in a standard supervised classification (Maximum Likelihood Classifier) approach using the same combination of calibration and validation sites (hereafter referred to as study sites) used in all of the analysis paths presented in Figure 3.9. The results of the exclusively TM processing provides a foundation from which to discuss the results for exclusively RADARSAT (SAR), Landsat TM data fused with SAR data, and various combinations of SAR and TM datasets. For discussion purposes the March 2000 Landsat 5 TM dataset will be referred to as Dry TM due to its correspondence with the dry season on Andros Island. The November 1999 Landsat 5 TM dataset will be referred to as Wet TM. Furthermore, all classification values discussed are in the context of producers' accuracy rather than user's accuracy since this research is comparing relative classification accuracy of processing techniques and is not intended to produce a finished land dataset for the study area.

Individually, the TM scenes provided reasonable classification results with a total classification accuracy of 80.6% for Dry TM and a total classification accuracy of 80.7% for Wet TM. The fact that these results are virtually identical is surprising considering the seasonality of the datasets. However the similarity of the overall classification results obscures the fact that there are some notable seasonal differences when individual vegetation classes are considered.

Looking in more detail at the results involves considering the classification accuracy of individual classes and comparing those. Table 4.1 presents the classification results for each dataset and provides the results for each land cover category considered.

Table 4.1: Classification Results of Landsat TM

TM Dataset	Total Accuracy	Producers' Accuracy				
		Coppice	Pinelands	Rockland	Saw grass	Mangrove
Dry TM	80.6%	89.2%	81.8%	70.5%	77.9%	70.7%
Wet TM	80.7%	93.1%	84.5%	57.8%	77.9%	62.7%

As can be seen, there are some seasonal differences exhibited by classification accuracies among vegetation classes. The percentage of Coppice accurately classified was slightly higher with Wet TM than Dry TM, a difference of 3.9%. The Pinelands class saw a similar difference with Wet TM exhibiting a slight improvement over the Dry TM dataset. There was no difference in the

classification of Saw grass between the two time periods with each resulting in a 77.9% classification accuracy.

The major change in classification is found in the Rockland and Mangrove classes. The classification accuracy for the Rockland class dropped 12.7% from the dry season to the wet season. While the decline in accuracy in Mangrove is of a smaller magnitude at 8.0%, the result is still significant. Reviewing the contingency table for the Wet TM (Table 4.2) dataset one finds that there is

Table 4.2: Contingency Table for Wet TM Classification Results

	Coppice	Pinelands	Rockland	Saw grass	Mangrove	
Coppice	1213	265	2	0	0	1480
Pinelands	83	2093	44	0	29	2249
Rockland	6	69	283	35	130	523
Saw grass	1	3	161	584	99	848
Mangrove	0	47	0	131	433	611
	1303	2477	490	750	691	5711
Producer's Accuracy	93.1%	84.5%	57.8%	77.9%	62.7%	Total 80.7%

increased confusion between the Rockland and Saw grass classes. This may be due to an increase in chlorophyll activity in this community as well as increased standing surface water during the wet season. For the Mangrove class, similar confusion is found with 14.3% and 48.8% of pixels being misclassified as Saw grass and Rockland respectively. A similar dynamic may be at play here with

differing levels of chlorophyll activity and changes in the surface matrix due to standing water and changes in the degree of exposed limestone.

The collection of datasets from two different seasons provides the opportunity to assess the value of multitemporal datasets for effective land cover classification. While each seasonal dataset provided virtually identical total classification accuracies, some differences were manifest in individual vegetation classes. A combination of the two datasets captures some of the seasonal variability and presents the opportunity for an improved characterization of vegetation classes.

Table 4.3 presents the results of a supervised classification of Dry TM and Wet TM in combination. Including data from both time periods increased the

Table 4.3: Contingency Table for Combined Dry TM and Wet TM

	Coppice	Pinelands	Rockland	Saw grass	Mangrove	
Coppice	1207	169	0	0	0	1376
Pinelands	64	2179	22	0	2	2267
Rockland	28	126	524	48	86	812
Saw grass	0	2	22	633	92	749
Mangrove	4	1	0	69	511	585
	1303	2477	568	750	691	5789
Producers Accuracy	92.6%	88.0%	92.3%	84.4%	74.0%	Total 87.3%

total classification accuracy to 87.3%, a greater than 6% improvement over the individual seasonal dates with significant improvements in four of the five vegetation classes.

Notably, there is no significant improvement in the classification of the Coppice class which was already in the area of 90%. The Pinelands classification of the combined datasets is an improvement of 3.5% over Wet TM and 7.2% over Dry TM. The improvement in the Saw grass category is 6.5% over the individual season datasets. The combined season classification of Mangrove exhibits a nominal improvement of 3.3% over the Dry TM dataset and a more significant 11.3% improvement over the Wet TM dataset. It was in this latter dataset that there was greater confusion between the Rockland, Saw grass, and Mangrove classes. A look at the contingency table (Table 4.3) indicates that there is still some confusion with the Saw grass and Rockland classes though it is significantly reduced.

The class with the greatest improvement in the combined season dataset is the Rockland class. This exhibits a 21.8% increase in classification accuracy over the Dry TM and a 34.5% improvement in classification over the Wet TM dataset. Reviewing the contingency table (Table 4.3) reveals that in this class there is no longer any confusion with the Mangrove class and a nominal confusion with Saw grass and the Pinelands class.

The results of the TM processing are promising in a number of areas. The overall classification accuracy is respectable at approximately 80% for each seasonal dataset. Structural differences between the Coppice and Pinelands classes easily differentiate them from the other classes which are characterized by low canopies, lower biomass volumes, and a greater similarity in surface matrix including a greater likelihood of being inundated during the wet season. Combining the seasonal datasets apparently captures this variability and provided the opportunity to further differentiate the classes resulting in improved classification accuracy.

4.2 PROCESSING OF UNFILTERED SAR

Each SAR dataset was processed with the standard supervised classification procedure used in this research effort to assess their individual value for discriminating land cover. Each dataset represents a single instance of SAR data collected from the RADARSAT system on 21 different dates spanning the range of variables assessed in the study. Table 4.4 presents the classification results of the individual datasets while Table 4.5 contains statistics on the collective results. Note that five datasets did not adequately cover study sites for two categories (Coppice and Rockland) to utilize them in assessing their value

for those cover types. They are shaded in the table and are excluded from the summary statistics for those classes.

Table 4.4: Unfiltered SAR Classification Accuracy Results

Dataset	Producers Accuracy					
	Tot. Accuracy	Coppice	Pinelands	Rockland	Saw grass	Mangrove
0330	33.3%	18.6%	43.3%	30.8%	22.0%	38.8%
0401	33.6%	9.9%	50.7%	46.2%	0.0%	47.6%
0415	26.6%	11.0%	35.7%	50.3%	19.5%	25.4%
0416	34.1%	14.3%	58.1%	15.9%	23.6%	11.3%
0418	40.7%	20.6%	66.3%	20.4%	26.0%	4.7%
0430	26.9%	35.5%	20.3%	28.6%	27.6%	32.9%
0509	37.3%	39.4%	46.8%	37.2%	0.0%	20.3%
0510	32.4%	0.0%	54.5%	32.0%	19.1%	28.8%
0512	43.7%	NA	62.2%	NA	15.5%	48.1%
0517	34.3%	0.0%	61.4%	37.9%	24.9%	9.4%
0602	35.8%	18.8%	59.8%	35.4%	30.7%	11.1%
0603	36.2%	12.3%	53.7%	29.2%	36.4%	23.4%
0612	32.7%	10.1%	45.5%	74.1%	11.1%	24.3%
0923	36.3%	NA	52.4%	NA	18.8%	11.5%
1017	44.7%	NA	54.3%	NA	53.1%	24.8%
1201	42.0%	0.0%	76.1%	33.5%	28.9%	19.4%
1203	35.4%	40.1%	37.5%	24.4%	27.1%	35.2%
1204	35.6%	NA	50.9%	NA	27.5%	52.8%
1217	32.1%	0.0%	53.4%	72.9%	7.3%	26.0%
1218	32.9%	25.0%	42.4%	32.8%	23.1%	24.5%
1220	46.2%	NA	71.9%	NA	17.2%	28.9%

Datasets containing a single band of data commonly provide substantial variation in classification results. This is clearly evident in the range of values in Table 4.4. Total classification accuracy for all 21 datasets span values ranging from 26.6% to 46.2%.

In a number of instances classes are clearly not distinct enough to permit clear differentiation using a single radar band. Of substantial note and concern is the number of cases (6) where zero pixels were assigned to a class. This occurred with six different SAR images and was confined to the Coppice and Saw grass classes. After thoroughly evaluating these instances and reprocessing the datasets these results were repeated. It was concluded that on those dates the similarities between the Coppice and Pinelands classes, and the Saw grass and Rockland classes, were such that the later classes received a full assignment of pixels in the classification process. An example of this is found with the SAR 0510 and SAR 0517 datasets. When perusing the contingency table (Table 4.5 and Table 4.6) of each of these it is clear that the Coppice class is not distinct from the Pinelands class. The classification accuracy for Coppice is 0.0% for both while

Table 4.5: Contingency Table SAR 0510

	Coppice	Pinelands	Rockland	Saw grass	Mangrove	
Coppice	0	0	0	0	0	0
Pinelands	676	1351	154	277	166	2624
Rockland	299	520	147	165	130	1261
Saw grass	126	154	159	143	196	778
Mangrove	202	452	0	165	199	1018
	1303	2477	460	750	691	5681
Producers Accuracy	0.0%	54.5%	32.0%	19.1%	28.8%	Total 32.4%

the pixels misclassified as Pinelands are 51.9% (676/1303) and 62.1% (809/1303) respectively. There are also two instances in Table 4.4 where the Saw grass class could not be discriminated (SAR 0401, SAR 0509) and a similar degree of

Table 4.6: Contingency Table SAR 0517

	Coppice	Pinelands	Rockland	Saw grass	Mangrove	
Coppice	0	0	0	0	0	0
Pinelands	809	1520	204	245	145	2923
Rockland	299	569	212	274	210	1564
Saw grass	49	87	143	187	271	737
Mangrove	146	301	0	44	65	556
	1303	2477	559	750	691	5780
Producer's Accuracy	0.0%	61.4%	37.9%	24.9%	9.4%	Total
						34.3%

confusion is found with other classes. In later stages of processing once speckle suppression or texture measure filters were applied to the data these events no longer occurred.

These contingency tables are typical of the individual SAR datasets in that there is consistently a high degree of confusion between individual classes with substantial variation within each table and a great degree of variability across datasets.

While discussion of individual datasets may not be valuable at this point, some interesting observations can be made regarding their overall accuracies and

collective statistics. Figure 4.1 depicts the total accuracy of the classification results for each dataset, in this case ordered by date. It is notable that a linear trend line applied to the data indicates a general increase in classification accuracy as the date increases, in this case moving from the Dry Season and through the Wet Season. This trend is apparent even if the five datasets highlighted in Table 4.4 Unfiltered SAR Classification Accuracy Results (which resulted in higher total accuracy values but when only three classes were considered) are excluded from the chart. This improvement spanning the time period of SAR collection may indicate that SAR data covering these vegetation classes provides improved discrimination under wetter conditions found during the wet season. This possibility is investigated and discussed further in Section 4.4 when seasonal variables are evaluated.

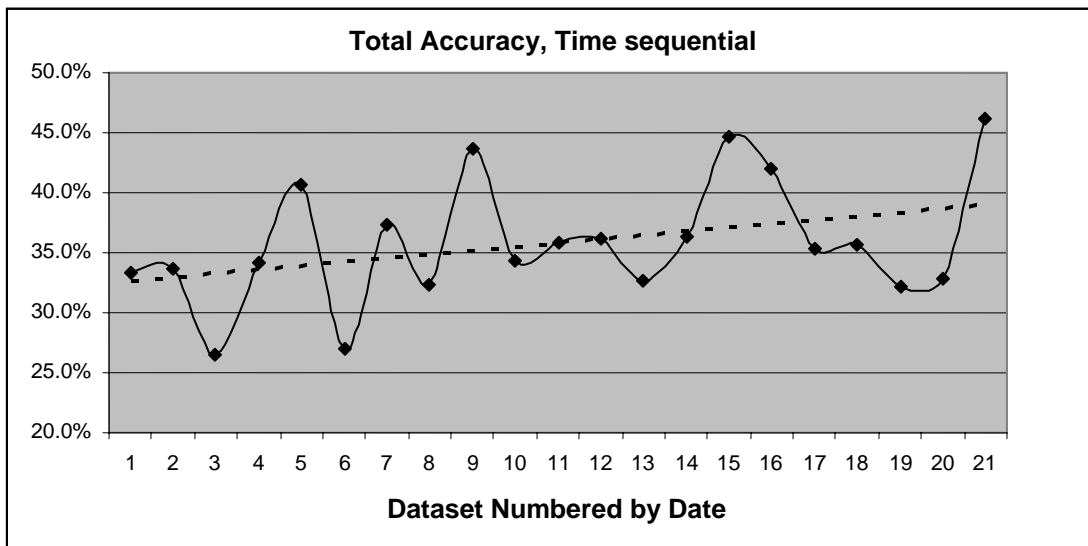


Figure 4.1: Total Classification Accuracy for Unfiltered SAR

Table 4.7 presents the summary statistics for the classification accuracies for all 21 SAR datasets. Considering these values provides some interesting context. First, the average total accuracy of 35.8% is a respectable result for an individual spectral band of data and is not in itself discouraging. The average accuracies of individual bands are also noteworthy. As a point of reference, consider that with five land cover classes, a random assignment of “accurate” pixels to individual classes would result in a classification accuracy of 20% per class. Instances where the value is higher are a clear improvement on random assignment, instances where the result is close to or less than 20% the effort is no better than random assignment.

Table 4.7: Summary Statistics for 21 SAR datasets

	Producers Accuracy					
	Tot. Accuracy	Coppice	Pinelands	Rockland	Saw grass	Mangrove
Average	35.8%	16.0%	52.2%	37.6%	21.9%	26.2%
Max	46.2%	40.1%	76.1%	74.1%	53.1%	52.8%
Min	26.6%	0.0%	20.3%	15.9%	0.0%	4.7%
St. Dev	5.2%	13.6%	12.7%	16.4%	11.8%	13.1%
Variance	0.269	1.842	1.603	2.685	1.403	1.726

Given that fact, the results in Table 4.7 indicate that the SAR datasets may not individually provide value in discriminating Coppice or Saw grass from the other vegetation classes evaluated. SAR data does successfully discriminate the

Pinelands category and to a lesser degree the Rockland category. The Mangrove class has an average accuracy that is nominally higher than 20% but no clear conclusions can be drawn here.

Attempting to classify vegetation categories using individual raw (unfiltered) SAR scenes will consistently result in a great deal of variability in results. The presence of speckle in SAR scenes results in a significant variance in DN values across relatively small areas, including areas comparable in size to the study sites used in this analysis. This fact alone can explain the classification accuracies achieved in this stage of this project. The classification accuracy results of individual SAR scenes that have been processed to reduce speckle or assess texture are discussed in Sections 4.6 and 4.7.

4.3 COLLECTION MODES

Having processed the individual SAR datasets for their classification results presents the first opportunity to evaluate some of the SAR collection variables assessed in this study. The angle of incidence should have a significant impact on classification accuracy due to the structural differences of the vegetation classes. As discussed in Chapter 2, greater incident angles typically result in greater backscatter (signal returns) from vegetation while lesser incident

angles are expected to more readily penetrate vegetation and result in returns from the surface matrix.

Table 4.8 compiles classification accuracy's by RADARSAT ST mode (3, 5, and 7). ST3 collects at lesser angles of incidence while ST7 collects at greater angles. The average total classification accuracy result for these modes provides no clear indication of value or improvement in vegetation differentiation as incident angle increases. If any trend is present it appears to indicate that the overall results are exactly the reverse of what was expected. However, it should be noted that the classification accuracy for the ST3 Pinelands class is very high relative to its companion classes. In fact, the other four values are lower than or equal to the values collected in mode ST5 and ST7. This single value accounts for the higher total accuracy value for ST3.

Table 4.8: Classification Accuracy by Incident Angle

RADARSAT Mode (# of scenes)	Total Accuracy	Producers Accuracy				
		Coppice	Pinelands	Rockland	Saw grass	Mangrove
ST3 (6)	40.0%	9.8%	63.5%	30.7%	22.4%	24.9%
ST5 (7)	33.9%	16.0%	48.9%	36.4%	20.0%	27.9%
ST7 (7)	35.5%	17.3%	50.5%	48.9%	22.4%	24.6%

It is unclear why the ST3 Pinelands class has such a high classification accuracy. The vegetation of the Pinelands class does contain a more complex

structure than the other categories assessed. This result may indicate greater penetration of the upper canopy and interaction with the understory and surface matrix.

The Coppice and Rockland classes do indicate some positive progression in classification accuracy as incident angle increases. This is most pronounced with the Rockland class and less so with the Coppice class. However, the Saw grass and Mangrove classes demonstrate no comparable progression.

RADARSAT collection in ascending and descending orbit dictate the direction of look for SAR datasets. While there are some known conditions under which look direction may be important, most specifically when imaging row crops, in assessing natural vegetation no significant difference in results would be expected from datasets collected in ascending or descending mode.

Table 4.9 contains the average accuracy of the classified SAR datasets combined by look direction as defined by ascending or descending mode. The numbers of scenes collected in ascending mode or descending mode (11 and 10 respectively) are equal as are the incident angles of the scenes within each collection (with 3 or 4 scenes falling in each satellite mode for ascending or descending orbit). The results in this table support the expectation that look direction provides no significant value when assessing natural vegetation over relatively flat terrain. The accuracy results in each cover class are comparable

between collection orbit with the exception of the Rockland and Saw grass classes. The differences in these classes cannot be explained by seasonal differences or incident angle as there are equal contributions of either factor in each category. Surface topography can impact backscatter and may dictate preferable look directions depending on the slope or aspect of particular study sites (linear features or surface textures oriented in a specific direction relative to the satellite track) especially when considered in combination with incident angle. There is no such systematic variation in these study sites, natural vegetation over flat surface topography, and the reason for these variations is unknown at this point. It is notable that the classification accuracy of Saw grass and Rockland swap in magnitude. There is a 15% increase in Rockland accuracy and a 12.3% drop in Saw grass from ascending to descending orbit collections. With the exception of these classes, orbit of collection does not appear to provide any value for land cover differentiation.

Table 4.9: Classification Accuracy by Look Direction

Orbit (# of scenes)	Total Accuracy	Producers Accuracy				
		Coppice	Pinelands	Rockland	Saw grass	Mangrove
Ascending (11)	35.3%	13.2%	51.6%	30.1%	27.7%	25.2%
Descending (10)	36.4%	18.7%	53.0%	45.1%	15.4%	27.2%

4.4 SEASONALITY

One of the principle goals of this research is to determine whether the season of collection provides value when combining SAR datasets with multispectral (MSI) datasets. When evaluating the results of individual unfiltered SAR datasets in Section 4.2 there was an indication that classification accuracies tended to be higher for wet season dataset when compared to dry season datasets. In Table 4.10 the individual SAR classification accuracy results are combined by season to determine if any significant difference exists in classification accuracy.

Table 4.10: Average Accuracy by Season

Season (# of scenes)	Total Accuracy	Producers Accuracy				
		Coppice	Pinelands	Rockland	Saw grass	Mangrove
Dry (13)	34.4%	15.9%	50.6%	36.5%	19.7%	25.1%
Wet (8)	38.1%	16.3%	54.9%	40.9%	25.4%	27.9%

The results in Table 4.10 are promising in that the average overall accuracy of wet season SAR datasets is 3.7% above that of the dry season datasets. The advantage is present in every land cover category though to differing degrees, with the result in the Coppice class providing a nominal and perhaps insignificant improvement. Whether this advantage can be leveraged when SAR and TM datasets are combined is evaluated and discussed in Section

4.9. When looking at the best scene from each season (Table 4.11), the possible value gained from wet season SAR is readily apparent. Again, with the exception of the Coppice class a clear advantage is found in each of the other classes. As was seen in Section 4.2, the Coppice class is not consistently separable from the Pinelands class when individual dates of SAR are utilized.

Table 4.11: Best Scene Accuracy for each Season

Season (scene)	Total Accuracy	Producers Accuracy				
		Coppice	Pinelands	Rockland	Saw grass	Mangrove
Dry (0418)	40.7%	20.6%	66.3%	20.4%	26.0%	4.7%
Wet (1201)	42.0%	0.0%	76.1%	33.5%	28.9%	19.4%

4.5 SEASONAL AND MULTITEMPORAL COMBINATIONS

RADARSAT-1 only collects SAR data in a single microwave channel. This approximates a panchromatic visible imaging system in that a single instance of data is collected at a given point in time. One method of analysis used for such single band data is to combine datasets from different time periods to create a multi-band dataset for evaluating surface conditions. The principle of change detection relies on evaluating differences over time. With multitemporal datasets differences across time are captured rather than differences across spectral regions (as with a multispectral dataset).

The 21 SAR datasets were combined into a single multitemporal dataset to assess the value of combining SAR from different instances in time for characterizing surface conditions. To further assess the value of seasonality, the datasets were also divided by season. The classification accuracy results of the multitemporal SAR datasets are presented in Table 4.12.

Table 4.12: Multitemporal Dataset Classification Accuracy

Multitemporal Dataset (#)	Total accuracy	Producers Accuracy				
		Coppice	Pinelands	Rockland	Saw grass	Mangrove
Dry (13)	50.5%	39.1%	62.1%	54.2%	34.8%	44.9%
Wet (8)	55.4%	45.9%	67.0%	43.9%	22.3%	75.7%
All (21)	65.8%	65.4%	73.6%	67.6%	41.3%	63.8%

The value of combining multiple instances of SAR data into a single multitemporal dataset for the purpose of characterizing land cover is clearly evident in the total accuracy results of this table. A total accuracy of 65.8% is 30% better than the average accuracy of 35.8% experienced with individual SAR scenes as presented in Table 4.7 Summary Statistics for 21 SAR datasets. The classification accuracy for each category of land cover exhibits significant improvement with the most notable being the accuracy of the Coppice classification which was four-times better (65.4% vs. 16.0%). Note that the Coppice class was the most difficult to discriminate with individual SAR scenes. The combined SAR overcomes this difficulty. The classification accuracy for

Rockland, Saw grass, and Mangrove effectively doubled while the Pinelands class improved 21.4% from an average accuracy of 52.2% to a classification accuracy for the combined datasets of 73.6%.

Running a classification on the SAR dataset combined by season also provides interesting results. The multitemporal datasets improved classification accuracy over the average of individual SAR datasets with a difference of greater than 15% in each season.

Note that the value of wet season SAR data over dry season SAR is again borne out when the datasets are combined. This is despite the fact that the number of SAR datasets differs for each season with 13 datasets being present for the Dry season dataset and 8 included in the Wet season dataset. A greater number of wet season instances would likely improve classification accuracy further.

The contingency tables for the multitemporal SAR datasets provide an opportunity to investigate in more detail the differences in classification between the two seasons as well as their relation to the combined dataset. Table 4.13 provides the results for the dry season dataset. The most notable observation here is that during the dry season there is significant confusion between the Coppice and Pinelands class such that a greater number of pixels have been assigned to the latter under the Coppice category. A similar confusion exists in

the Saw grass category where a majority (though slim) of pixels have been assigned to the Mangrove class.

Table 4.13: Multitemporal Dry Season Contingency Table

	Coppice	Pinelands	Rockland	Saw grass	Mangrove	
Coppice	509	334	72	24	28	967
Pinelands	719	1538	172	37	50	2516
Rockland	38	222	301	161	161	883
Saw grass	9	40	10	261	142	462
Mangrove	28	343	0	267	310	948
	1303	2477	555	750	691	5776
Producers Accuracy	39.1%	62.1%	54.2%	34.8%	44.9%	Total
						50.5%

During the wet season (Table 4.14) the classification of Coppice has improved yet a significant confusion with the Pinelands class still exists. The confusion of Saw grass with Mangrove is more severe but the classification of

Table 4.14: Multitemporal Wet Season Contingency Table

	Coppice	Pinelands	Rockland	Saw grass	Mangrove	
Coppice	598	345	117	73	42	1175
Pinelands	445	1659	33	193	45	2375
Rockland	88	46	198	45	12	389
Saw grass	61	180	103	167	69	580
Mangrove	111	247	0	272	523	1153
	1303	2477	451	750	691	5672
Producers Accuracy	45.9%	67.0%	43.9%	22.3%	75.7%	Total
						55.4%

Mangrove has improved by 30.8%. Note that the classification accuracy of the Rockland and Saw grass categories both declined in the wet season dataset relative to the dry season dataset. In addition the mixture of cover types confused with Rocklands has also changed. For example, in the dry season dataset the Rockland category was most significantly confused with the Pinelands class. The same class in the wet season dataset was confused equally with the Coppice and Saw grass classes.

With all of the data combined into a single multitemporal dataset, overall classification has improved significantly. Table 4.15 provides the contingency

Table 4.15: Multitemporal Combined SAR Contingency Table

	Coppice	Pinelands	Rockland	Saw grass	Mangrove	
Coppice	852	278	79	91	70	1370
Pinelands	277	1822	29	77	19	2224
Rockland	102	74	321	11	8	516
Saw grass	9	31	46	310	153	549
Mangrove	63	272	0	261	441	1037
	1303	2477	475	750	691	5696
Producers Accuracy	65.4%	73.6%	67.6%	41.3%	63.8%	Total 65.8%

table for the classification results. Confusion in the Coppice class has been largely mitigated with a classification accuracy of 65.4% though 21.3% of pixels are still being misclassified as Pinelands. The class with the least improvement is

the Saw grass category where a still significant proportion of pixels are being misclassified as Mangrove.

The results of the multitemporal SAR classification demonstrate that multiple SAR datasets collected at different points in time can be used successfully to characterize surface materials with respectable accuracy. Further investigation in this area could determine a minimum number of time periods required for reasonable results. Selecting a sample with a good time distribution that best captures differences in surface conditions across time could provide comparable results with a limited number of datasets.

4.6 SAR SPECKLE SUPPRESSION

Speckle suppression attempts to reduce the impact of speckle noise by statistically normalizing a pixel value based upon the value of surrounding pixels. Changing the kernel size varies the size of the neighborhood that is used for normalizing the central pixel. In this analysis, five speckle suppression algorithms were used to assess the relative value of each of them and at seven different kernel sizes. Initially five kernel sizes were planned but due to the increasing accuracies achieved as the kernel expanded to 11x11 further processing was initiated to determine if the trend continued as the kernel

expanded to 13x13 and 15x15. The results of this process are presented as data values in Table 4.16 and graphically in Figure 4.2.

Given the average classification accuracy for unprocessed single scene SAR of 35.8% the application of a speckle suppression filter has a clear and immediate positive impact on classification results. Each of the five speckle filters results in significant improvements in classification accuracy. Note that the values in Table 4.16 and Figure 4.2 are the average classification accuracy for the 21 SAR datasets each having been individually filtered for speckle and then processed using the standard supervised classification process performed in this study.

Table 4.16: Average Total Classification Accuracy by Speckle Suppression Filter

Filter	Kernel Size						
	3	5	7	9	11	13	15
Frost	39.9%	46.0%	48.9%	50.6%	50.9%	52.5%	52.6%
Gamma-MAP	44.7%	48.7%	50.5%	51.3%	52.2%	52.3%	50.3%
Local Region	39.2%	44.8%	46.5%	48.4%	50.4%	48.7%	49.9%
Lee-Sigma	43.4%	47.2%	49.3%	49.9%	49.9%	50.2%	50.3%
Median	43.3%	46.1%	48.1%	49.4%	50.5%	51.4%	49.7%

The Frost filter and the Local Region filter provided comparable benefit with a 3x3 kernel providing an average accuracy of 39.9% and 39.2% respectively; an approximately 4% improvement over the unfiltered SAR results.

The Lee-Sigma and Median filters also provided comparable results at a 3x3 kernel with 43.4% and 43.3% accuracy results respectively. The Gamma-MAP (GM) filter resulted in a 44.7% average accuracy which amounts to an increase in accuracy of 8.9% over unfiltered SAR.

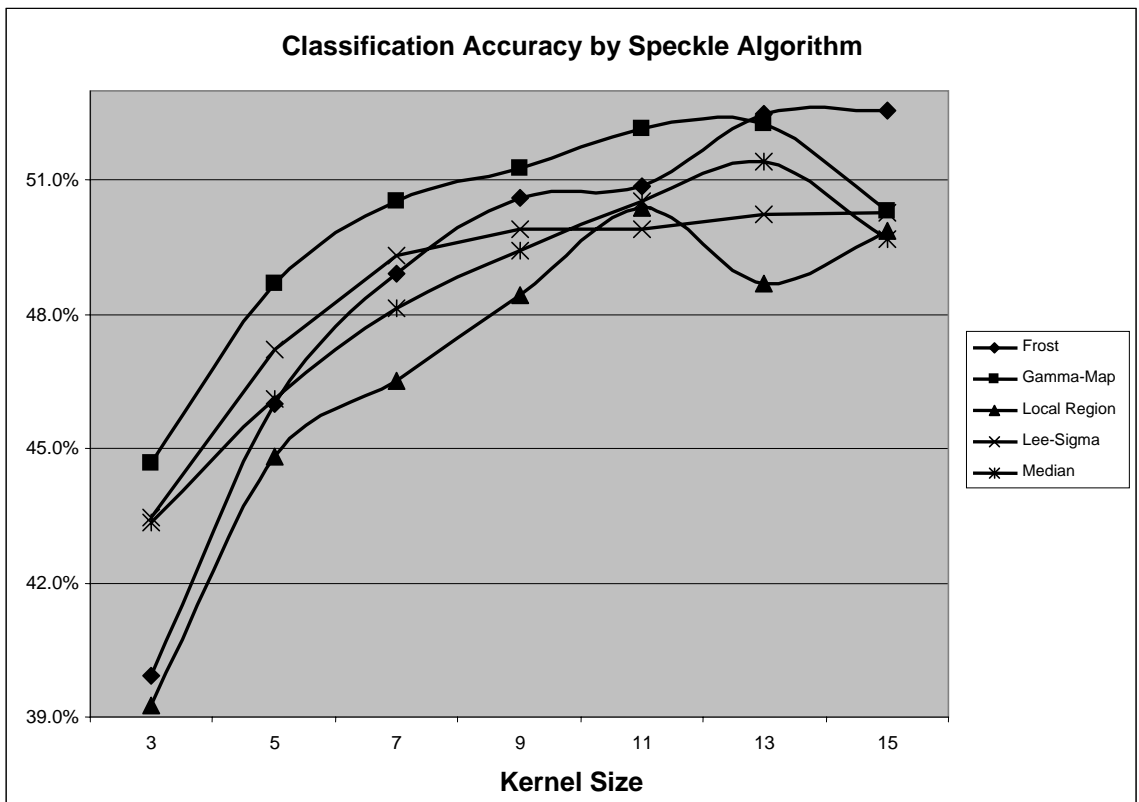


Figure 4.2: Average Classification Accuracy for Speckle Suppressed SAR

Looking across Table 4.16 one sees a steady increase in classification accuracy as the kernel size expands. This trend is most readily apparent in

Figure 4.2 where classification accuracies are seen to improve dramatically as the kernel increases from 3x3 to 9x9 and then depending on the filter leveling off or in several cases declining.

The GM filter appears to provide the best overall classification results in the early and middle kernel values but the Frost (FR) filter surpasses GM in the larger kernel windows. With the exception of the FR filter, the general trend in classification values appears to reach a maximum and then taper off between the 11x11 and 13x13 kernel sizes, but expanding the kernel values beyond 15 would be required to determine if this apparent decline continues. The results presented in Table 4.16 and Figure 4.2 indicates that speckle suppression using any filter is beneficial while the GM filter appears to be most beneficial. Furthermore, kernels of between 9x9 and 13x13 appear to provide the greatest value.

To further assess the value of speckle suppression filtering, the classification results of filtered datasets were compared to the results achieved with unfiltered datasets. This permits the evaluation of the effect of speckle filtering on individual land cover classes. Table 4.17 and Table 4.18 are contingency tables that present the results of a representative dataset, in this case SAR 0418.

Table 4.17: SAR 0418 Dataset Unfiltered

	Coppice	Pinelands	Rockland	Saw grass	Mangrove	
Coppice	201	336	90	123	64	814
Pinelands	518	1643	188	234	129	2712
Rockland	146	168	116	144	113	687
Saw grass	81	98	174	195	264	812
Mangrove	28	232	0	54	28	342
	974	2477	568	750	598	5367
Producers Accuracy	20.6%	66.3%	20.4%	26.0%	4.7%	Total 40.7%

Table 4.17 provides a fairly typical example of the results experienced with the unfiltered SAR datasets. The Total accuracy of 40.7% is somewhat higher than the average for the unfiltered SAR datasets. The Coppice class

Table 4.18: SAR 0418 Dataset Filtered with GM at 11x11 kernel

	Coppice	Pinelands	Rockland	Saw grass	Mangrove	
Coppice	400	374	78	80	12	944
Pinelands	8	1789	0	62	44	1903
Rockland	563	313	177	253	141	1447
Saw grass	3	1	211	321	317	853
Mangrove	0	0	0	34	84	118
	974	2477	466	750	598	5265
Producers Accuracy	41.1%	72.2%	38.0%	42.8%	14.0%	Total 52.6%

exhibits significant confusion with the Pinelands class as well as the Rockland class. Its resulting accuracy of 20.6% reflects this confusion. The result achieved

in the Pinelands class is high and fairly typical of the collective datasets. The Rockland class demonstrates significant confusion across the Coppice, Pinelands, and Saw grass classes and the Mangrove class was effectively indecipherable from other cover types.

Once the speckle suppression filter is applied, much of the confusion is reduced resulting in significant improvements in the classification results of all of the cover types. The Coppice class accuracy has improved by 19.5%. There is no longer confusion with the Pinelands class though there is now significant confusion with the Rockland category. A similar situation is found in the Pinelands class where an overall improvement has occurred. The Rockland accuracy has nearly doubled to 38.0% with the most prevalent confusion being with the Saw grass marsh. The Saw grass class has improved by over 16% with the greatest confusion experienced with the Rockland class. The accuracy of the Rockland class has seen the greatest relative improvement but is still a low value. The pattern of confusion across other classes is similar to that found in the unfiltered data.

It should be noted that while the average results presented in Figure 4.2 show consistent improvement with expanding windows, this consistency, and the presentation of results as averages, masks a great deal of variability in the underlying data. One would expect that SAR data collected with similar

parameters would exhibit similar results in evaluating classes of land cover though this is not necessarily the case. Table 4.19 and Table 4.20 are the results of the 0416 dataset and the 0510 dataset with the Frost filter and a 9x9 kernel size. They each were collected with identical system parameters and in the dry season with 24 days separating them.

Table 4.19: SAR 0416 Frost 9x9

	Coppice	Pinelands	Rockland	Saw grass	Mangrove	
Coppice	630	1262	36	90	48	2066
Pinelands	498	1016	78	119	74	1785
Rockland	175	188	359	316	157	1195
Saw grass	0	0	53	154	294	501
Mangrove	0	11	0	71	118	200
	1303	2477	526	750	691	5747
Producers Accuracy	48.3%	41.0%	68.3%	20.5%	17.1%	Total 39.6%

Dataset SAR 0416 FR9 was relatively valuable for discerning the Coppice class and relatively poor for the Pinelands with significant confusion between it and the Coppice class. The Rockland class achieved a high classification accuracy at a 68.3% and with no prominent confusion with any other individual class. Saw grass was confused with Rockland and to a lesser extent Pinelands. Mangrove was confused with Saw grass and Rockland.

The 0510 dataset (Table 4.20) with similar system parameters and the same processing filters presents some notable differences that are not readily

Table 4.20: SAR 0510 Frost 9x9

	Coppice	Pinelands	Rockland	Saw grass	Mangrove	
Coppice	299	330	20	78	18	745
Pinelands	592	1589	91	205	159	2636
Rockland	401	462	249	319	218	1649
Saw grass	0	0	209	69	156	434
Mangrove	11	96	0	79	140	326
	1303	2477	569	750	691	5790
Producers Accuracy	22.9%	64.2%	43.8%	9.2%	20.3%	Total 40.5%

explained. The Coppice class exhibits a much lower accuracy value of 22.9% yet similar patterns of confusion with Pinelands and Rockland. The Pinelands class is much more typical as is the Rockland class. Saw grass was not discernable and the results of the Mangrove class are comparable though a slight swap in the degree of confusion between Saw grass and Rockland is present in the later. The classification accuracy results for individual scenes demonstrate a great deal of variability as is typical when classification processes are applied to singular SAR data.

When compared to the results for individual SAR data, it is clear that speckle suppression is a valuable filtering option for improving the value of SAR data for surface feature characterization. To assess the value of speckle suppression when processing multiple datasets the multitemporal SAR dataset consisting of all of the SAR datasets was processed using the five speckle

suppression filter with each of the kernel sizes applied to them. The results of this process are presented in Table 4.21 and Figure 4.3.

Table 4.21: Average Classification Results for Speckle Suppressed Multitemporal SAR (21 scenes)

Filter	Kernel Size						
	3	5	7	9	11	13	15
Frost	66.3%	72.6%	75.5%	73.3%	69.6%	64.6%	60.7%
Gamma-MAP	72.6%	76.5%	80.7%	83.9%	82.3%	80.4%	75.6%
Local Region	67.7%	73.3%	74.9%	75.2%	73.6%	71.5%	72.7%
Lee-Sigma	73.0%	78.5%	79.4%	80.5%	80.9%	81.4%	82.3%
Median	69.9%	75.1%	80.1%	81.6%	83.7%	83.6%	83.8%

Once again, the classification accuracy achieved following the application of a speckle suppression filter demonstrates significant improvement over the accuracy achieved with unfiltered SAR data. The multitemporal SAR dataset discussed in Section 4.5 achieved a classification accuracy of 65.8%. The same dataset with speckle suppression filters applied achieved classification accuracies between 60.7% and 83.9%. As with the averaged results, the general trend seen in Table 4.21, and graphically presented in Figure 4.3, is of improving accuracies as the kernel size expands until a peak is achieved in the middle kernel range of 7x7 to 11x11 windows with a tapering off of accuracy values. The two values (64.6% and 60.7%) that fell below the total classification accuracy (65.8%) of the

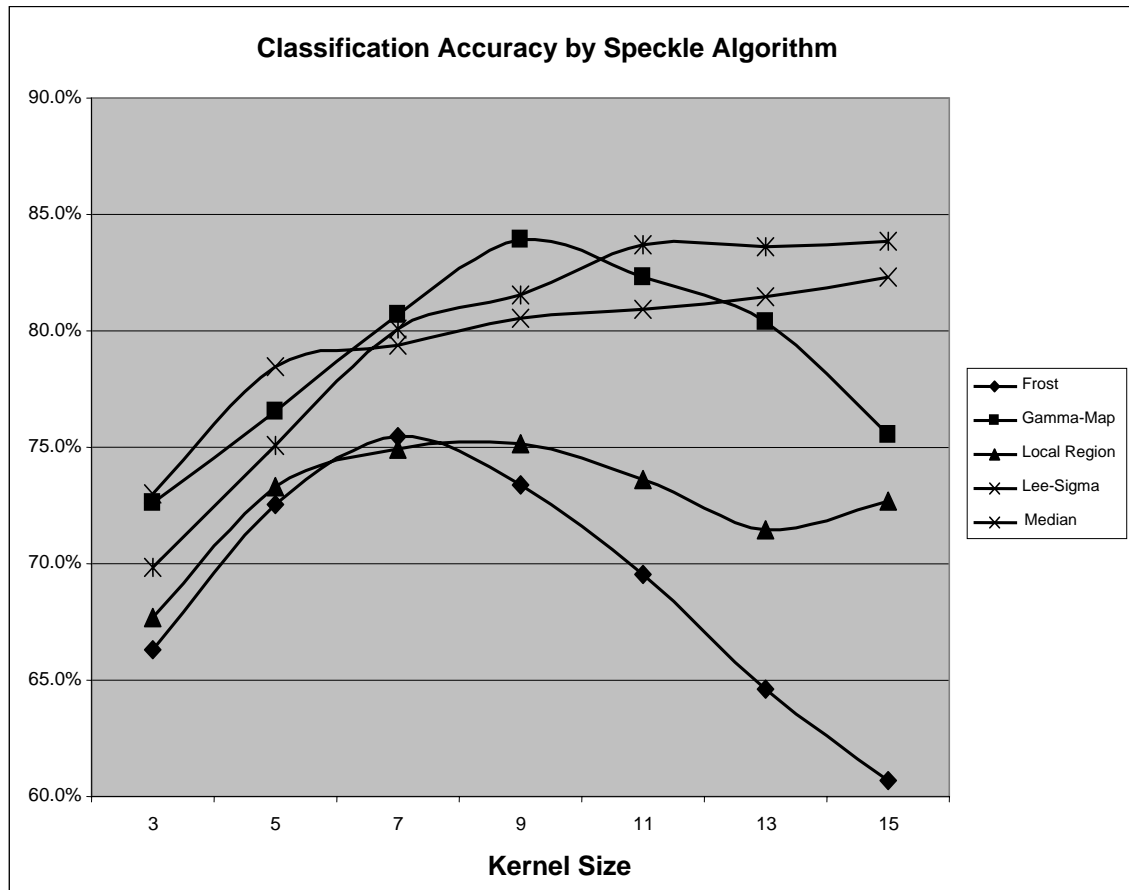


Figure 4.3: Average Classification Results for Speckle Suppressed Multitemporal SAR (21 scenes)

unfiltered multitemporal SAR dataset were from the Frost filter at its largest kernels (13x13 and 15x15); all other values surpassed that of the unfiltered multitemporal SAR. It is notable that the Lee-Sigma and Median filters do not taper off as the others do and expanding the kernels on those filters would be required to determine at what point a maximum accuracy with those filters is achieved.

The combined filtered SAR datasets result in classification accuracies that are comparable to that achieved with multispectral imagery such as the Landsat TM data used in this study. This is a significant result. In Section 4.12 this issue is pursued further to determine the minimum number of datasets required to achieve such results by starting with a single date, adding progressive dates, and assessing classification accuracy for each combination.

4.7 SAR TEXTURE

SAR texture processing seeks to characterize differences in surfaces by quantifying the texture of DN values in an image. These differences in texture can be used to differentiate or classify an image into categories of land cover. To assess the value of texture for land cover classification, each SAR dataset was processed using the Variance texture measure with kernels ranging from 3x3 to 27x27. The larger the kernel the broader the area used to assess texture.

The first set of results presented in Table 4.22 provides the average classification accuracy for individual SAR datasets with the Variance texture measure at each of the investigated kernel sizes. The results of this process

Table 4.22: Average Classification Accuracy of Variance Texture Measure

Variance Kernel Size												
3	5	7	9	11	13	15	17	19	21	23	25	27
36.1	38.8	43.5	46.3	49.2	50.9	51.9	50.5	50.9	50.1	49.8	49.7	50.3

indicate that on average the value of texture increases as the kernel size increases until it reaches the 15x15 window size. Texture assessed beyond that size appears to provide no further value. This trend is further apparent in Figure 4.4.

As was the case with speckle suppression processing, these results indicate that there is inherent value in using measures of texture in SAR for land cover classification. The average classification accuracy achieved with unfiltered

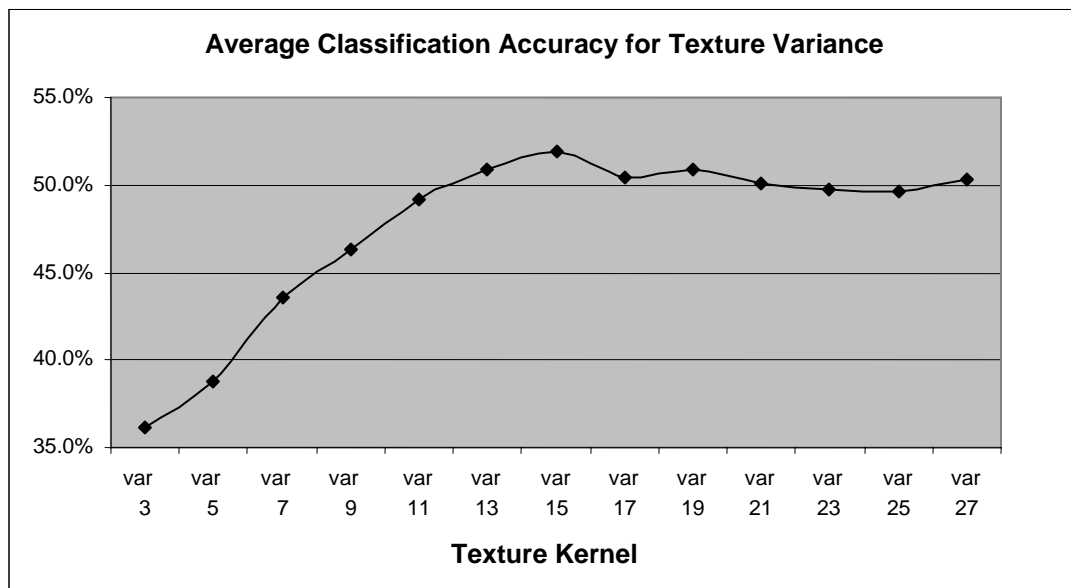


Figure 4.4: Average Classification Accuracy of Variance Texture Measure

SAR data was 35.8%. The Variance texture measure improved on this only nominally at the 3x3 kernel size but as the kernel expands the classification accuracy does as well until a maximum improvement of 16.1% is achieved with the 15x15 kernel. With the spatial resolution of these data this amounts to the assessment of texture for surface areas up to 400m x 400m in this study site. This may indicate that texture at this scale and below is meaningful for land cover characterization. The value then evens out beyond the 15x15 kernel. Texture beyond the 400m scale may not be meaningful for land cover purposes.

As was the case with processing unfiltered SAR imagery and the speckle suppression datasets, averaging the classification accuracy values masks a significant amount of variability in the results achieved from any individual scene or process. Figure 4.5 includes the classification accuracy of texture datasets at a 15x15 kernel ordered by date. The accuracy values range between 45.4% and 60.5% with a standard deviation of 5.1. An interesting point to note regarding this chart is the trend in higher accuracy values toward the wet season SAR datasets. This trend is present in the majority of Variance kernel datasets and parallels that seen in the unfiltered SAR processing results, indicating that the same phenomenon affecting SAR signal return by season is present in the texture of the returned data as well.

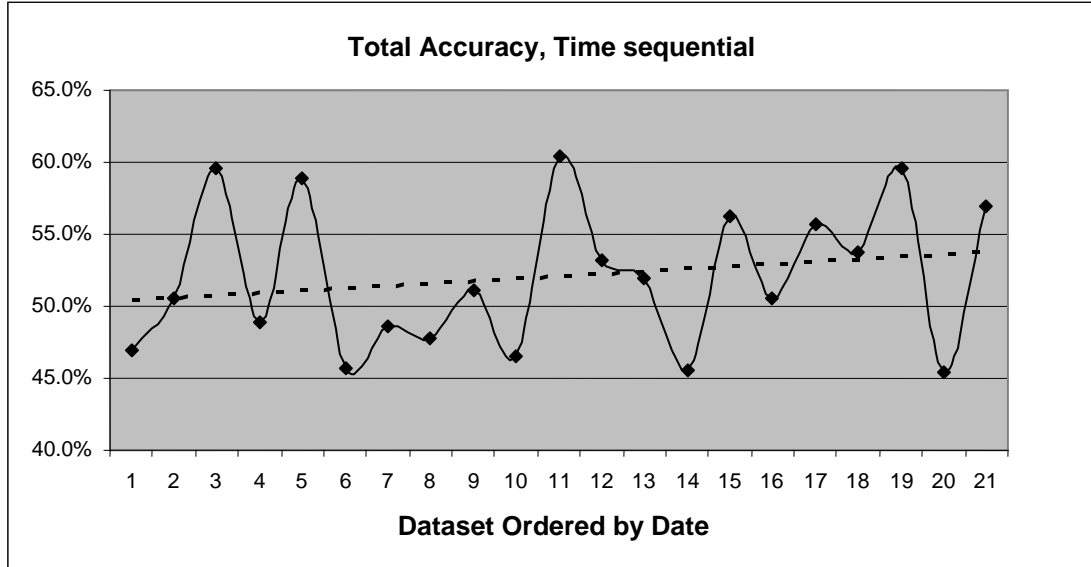


Figure 4.5: SAR Classification Accuracy for Variance with a 15x15 Kernel

Due to the variation in results for each dataset, it is not particularly valuable to discuss them individually. However, looking at some of the variables discussed in Section 4.3, results from datasets collected with different processing parameters, does provide some very intriguing observations.

No difference was apparent in classification accuracies achieved with unfiltered radar datasets when collection mode (ascending and descending) was considered (in Section 4.3). Once a texture measure is applied to the dataset, a clear differentiation appears with the average classification accuracy for data collected in descending mode resulting in an improvement in accuracy of as much as 12.9% over those for ascending mode data (achieved with a 15x15

kernel). Figure 4.6 graphs the average classification accuracy of datasets collected in each system mode for each Variance kernel. There is only a nominal difference in accuracy as the kernel expands from 3x3 to 7x7 but beyond that point, data collected in descending mode appears to provide a higher classification accuracy of approximately 5%. This trend continues though declining in magnitude until at the 27x27 kernel, it is no longer present.

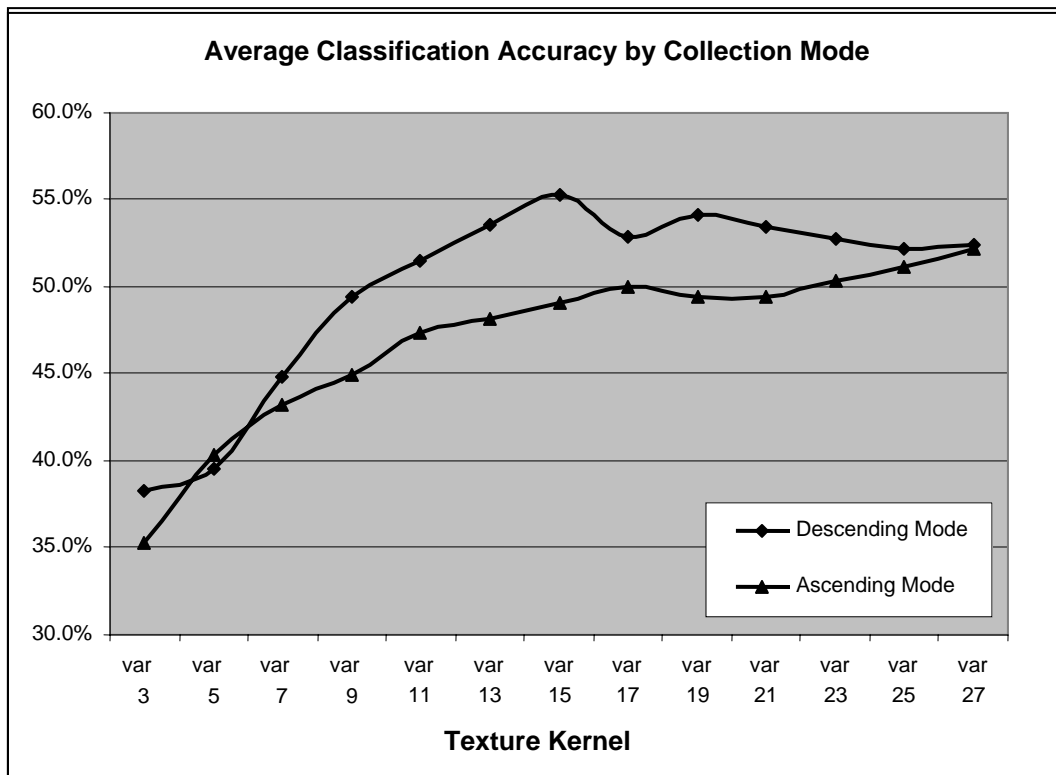


Figure 4.6: Comparative Average Texture Classification Accuracy by System Mode and Kernel Size

Ascending and descending mode determine the look direction of the sensor and the time of collection. The differences exhibited in Figure 4.6 may be due to either of these factors. With natural vegetation and limited topographic variation it is unlikely that look direction is resulting in a significant difference in return. Ascending mode data are collected at approximately 6pm local time while descending mode data are collected at approximately 6am local time. It is possible that these time differences may provide an explanation for the difference in return and resulting classification accuracy. It could be presumed that vegetation in the early morning hours has a higher moisture content than vegetation in the evening following a period of extended exposure to the sun.

A similar differentiation exists when comparing the datasets according to angle of incidence (see Figure 4.7). The differentiation is apparent throughout the series though becomes most pronounced when the kernel expands to 15x15 and beyond. As Figure 4.7 indicates, the difference between mode 3 and 5 for incidence angle is only nominal but beginning with a 5x5 kernel, mode 7 consistently achieves a higher classification accuracy with a peak improvement of 7.2% at the 27x27 kernel. Based upon these results, it would appear that the angle of incidence does impact the texture of an image. With our understanding of the SAR signal returned from different angles of incidence this result is not surprising. Vegetation is known to be a significant factor in SAR texture and

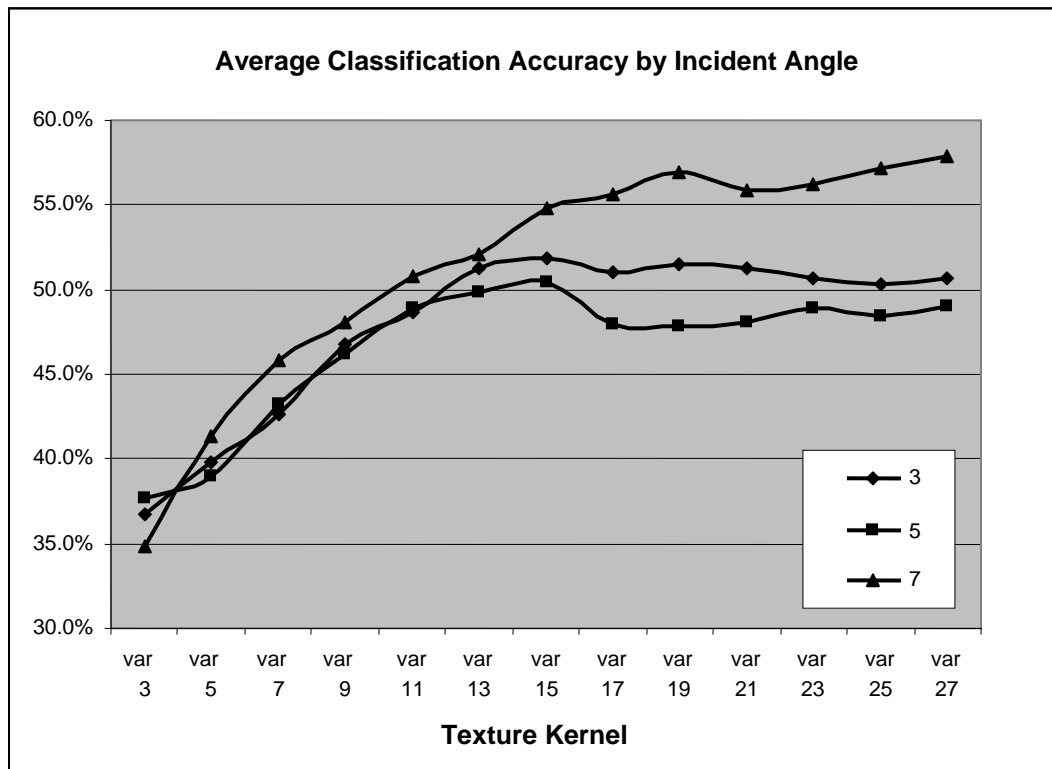


Figure 4.7: Comparative Average Texture Classification Accuracy by Angle of Incidence and Kernel Size

mode 7 is expected to have a greater return from vegetation. Whether this is a variable that can be consistently captured to accurately characterize land cover is the question. These results indicate that it may be possible but only at greater texture window sizes.

As with the speckle suppression processing of SAR data, all of the Variance texture measure SAR datasets were collected into a single multitemporal dataset and processed to determine what value texture measure

has when applied. The results of this processing are presented in Table 4.23 and Figure 4.8. The classification accuracies achieved with the multitemporal dataset

Table 4.23: Multitemporal SAR Classification Accuracy (%) Variance (21 scenes)

Variance Kernel Size												
3	5	7	9	11	13	15	17	19	21	23	25	27
52.5	60.7	62.1	65.5	67.7	64.4	64.1	64.4	62.4	62.1	64.9	62.7	68.1

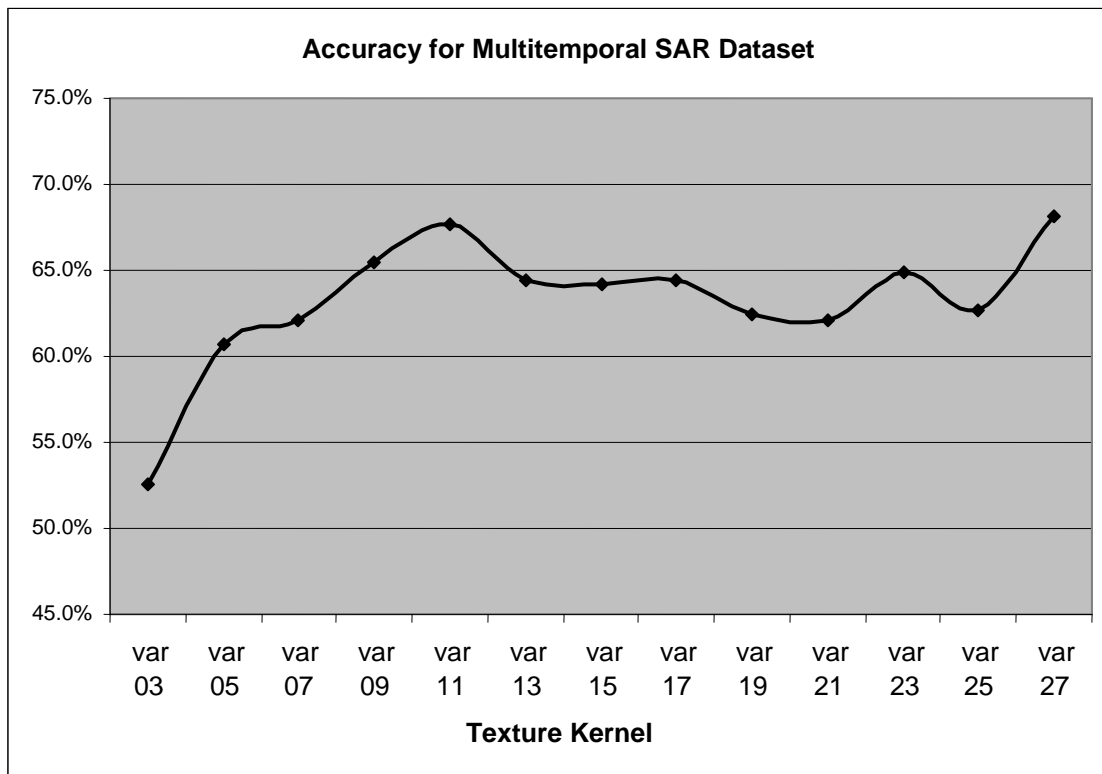


Figure 4.8: Accuracy Results of Texture Measure for Multitemporal SAR (21 scenes)

are an improvement over the average values of individual datasets. However, given the classification accuracy of 65.8% achieved with the unfiltered multitemporal SAR dataset presented in Section 4.4, there does not appear to be a significant value achieved from multitemporal texture datasets. The overall accuracy of multitemporal SAR dataset processed for texture results in a lower classification accuracy of 52.2% at a 3x3 kernel and improves as the kernel expands but only surpasses the unfiltered multitemporal SAR results when the kernel is 11x11 and 27x27 and not to a substantial degree. The results of the speckle suppression processing provided a significant improvement by comparison.

Perhaps more interesting is the variation in differentiation between cover types as the texture kernel expands (Figure 4.9). When the individual land cover classes are compared, as opposed to total accuracy, an interesting pattern appears. At the 3x3 kernel, all of the classes start with a classification accuracy ranging between 25.2% (Coppice) and 71.8% (Pinelands). As the kernel expands, with the exception of the Mangrove class, all of the classes converge at the 9x9 kernel with a range from 64.4% to 75.4%. As the kernel window expands beyond 9x9, the classification accuracy for the Coppice and Rockland classes improves to the upper 80's and low 90's while the Pinelands and Saw grass classes range

between 50% and 70%. The classification accuracy of the Mangrove class declines from the 5x5 kernel and settles into a range between 20% and 40%.

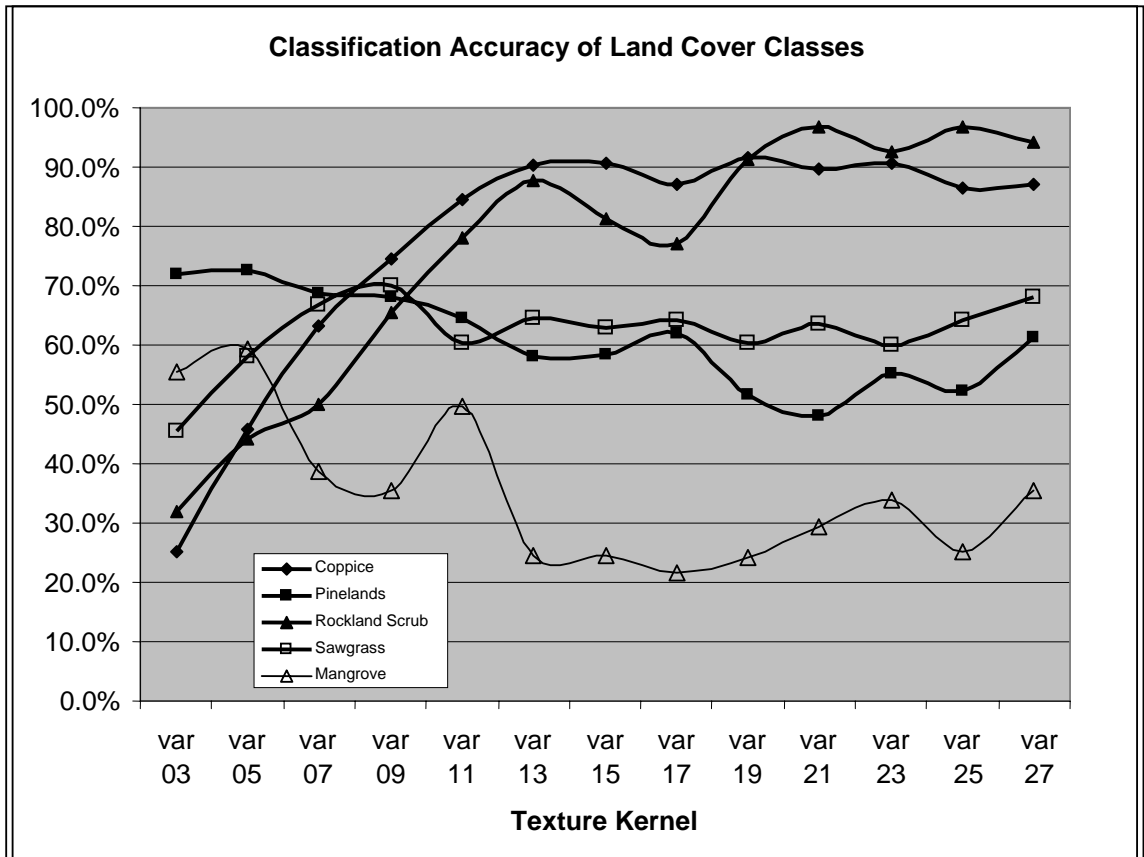


Figure 4.9: Classification Accuracy of Land Cover Classes for Multitemporal SAR by Texture Kernel (21 scenes)

While this clustering of results is not specifically valuable for directly classifying land cover relying solely on texture measures, they may provide a means for segmenting imagery into broad categories that then may be further divided using some other technique or imagery source.

Based upon the results in this portion of the study, it is clear that texture measures provide a means of extracting meaningful information from SAR data beyond that which can be achieved directly from unfiltered SAR. However, in this study, texture measures do not provide as valuable a dataset for land cover discrimination as speckle suppression does.

4.8 SAR TEXTURE IN SPECKLE SUPPRESSED DATASETS

SAR data were then processed to determine the value of measuring texture on datasets that have been processed to suppress speckle. A single dataset (SAR 0418) was selected for this operation. The GM speckle suppression algorithm was applied at each kernel size (3x3 – 15x15) resulting in seven datasets. Each was then processed for texture using the Variance texture measure at each texture kernel (3x3 – 27x27) resulting in a total of 91 datasets. Classification accuracy was then assessed and contingency tables compiled. For comparative purposes the results achieved with SAR 0418 in each of the prior sections are included here.

Table 4.24 presents the contingency table for supervised classification results of SAR 0418 as an unfiltered dataset. The total classification accuracy of 40.7% is nominally greater than the average achieved for individual unfiltered

Table 4.24: SAR 0418 Unfiltered

	Coppice	Pinelands	Rockland	Saw grass	Mangrove	
Coppice	201	336	90	123	64	814
Pinelands	518	1643	188	234	129	2712
Rockland	146	168	116	144	113	687
Saw grass	81	98	174	195	264	812
Mangrove	28	232	0	54	28	342
	974	2477	568	750	598	5367
Producers Accuracy	20.6%	66.3%	20.4%	26.0%	4.7%	Total
						40.7%

SAR datasets. The producers accuracy achieved in individual classes are representative with considerable confusion across classes but a relatively high accuracy achieved for the Pinelands class. The Mangrove class resulted in very poor results with the majority of pixels being misclassified as Saw grass.

The classification results for SAR 0418 with the GM speckle suppression filter applied at each kernel size are contained in Table 4.25. As was the case for all of the SAR datasets, the GM filter significantly improved the value of SAR 0418 for discrimination of land cover categories.

Table 4.25: Classification Accuracy for SAR 0418, Speckle Suppressed

Gamma-MAP Kernel Size						
3	5	7	9	11	13	15
55.9%	53.2%	55.2%	52.7%	52.6%	55.2%	52.5%

The contingency table for SAR 0418 with a GM 7x7 kernel (Table 4.26) demonstrates considerable improvement in each land cover category except the Pinelands class which experienced a slight decline. Confusion in the Mangrove class still exists with the Saw grass but confusion with other categories have been reduced resulting in a significant improvement in classification results.

Table 4.26: SAR 0418 Speckle Suppressed Gamma-MAP 7x7

	Coppice	Pinelands	Rockland	Saw grass	Mangrove	
Coppice	627	795	90	93	19	1624
Pinelands	9	1566	3	57	45	1680
Rockland	323	105	172	205	92	897
Saw grass	15	1	150	311	242	719
Mangrove	0	10	0	84	200	294
	974	2477	415	750	598	5214
Producers Accuracy	64.4%	63.2%	41.4%	41.5%	33.4%	Total
						55.2%

Table 4.27 provides the SAR 0418 texture measure results. This individual dataset reflects the general results found with all of the SAR datasets as

Table 4.27: Classification Accuracy (%) for SAR 0418, Texture Measure

Variance Kernel Size												
3	5	7	9	11	13	15	17	19	21	23	25	27
27.4	47.3	57.5	59.3	62.1	57.3	58.9	59.0	59.3	60.5	53.1	51.6	49.2

discussed in Section 4.2. The texture measure for SAR 0418 indicates improved classification accuracy at the 5x5 kernel and beyond, with a leveling off in the 9x9 to 21x21 range and then declining as the kernel expands to 27x27.

Results for SAR 0418 with a 9x9 Variance texture measure are presented in Table 4.28. At this texture kernel, the total classification accuracy is respectable for a single dataset at 59.3%. However, at this kernel size the texture values result in the Rockland class being confused with Coppice and Saw grass. The Saw grass class is greatly confused with the Mangrove class.

Table 4.28: SAR 0418 Variance Texture Measure with 9x9 kernel

	Coppice	Pinelands	Rockland	Saw grass	Mangrove	
Coppice	605	534	139	74	28	1380
Pinelands	266	1868	3	19	49	2205
Rockland	20	23	3	2	2	50
Saw grass	66	30	160	210	178	644
Mangrove	17	22	0	445	341	825
	974	2477	305	750	598	5104
Producers Accuracy	62.1%	75.4%	1.0%	28.0%	57.0%	Total 59.3%

While it may be expected that measuring texture in SAR data corrected for speckle would provide a more accurate assessment of the texture of surface materials, the results of this study do not support this conclusion. The classification accuracy results for every combination of SAR 0418 filtered to suppress speckle and then processed for texture are presented in Table 4.29. In

general, classification accuracies achieved are significantly lower than those achieved with either speckle suppression or texture measure alone. In many instances the accuracy results are lower than that achieved with the unfiltered SAR 0418 datasets.

Table 4.29: SAR 0418, Speckle Suppression followed by Variance Texture

GM	Variance Kernel Size												
	3	5	7	9	11	13	15	17	19	21	23	25	27
3	36.9%	42.5%	44.8%	39.8%	35.9%	37.5%	30.4%	35.6%	47.8%	42.2%	47.5%	50.7%	53.1%
5	42.6%	40.6%	38.6%	33.5%	33.6%	30.2%	30.0%	36.0%	40.5%	42.7%	43.5%	41.7%	45.9%
7	31.8%	30.5%	30.6%	36.9%	35.1%	31.8%	37.4%	39.1%	41.3%	44.7%	42.6%	39.7%	46.1%
9	29.7%	48.0%	34.1%	35.5%	40.7%	42.4%	36.7%	46.0%	45.1%	43.2%	50.0%	44.0%	43.2%
11	25.2%	41.5%	34.1%	36.9%	31.3%	33.8%	34.1%	37.0%	38.2%	50.4%	37.3%	52.6%	57.1%
13	23.9%	12.6%	51.0%	51.0%	45.1%	35.2%	36.2%	32.3%	44.8%	46.5%	48.5%	48.5%	47.7%
15	41.9%	22.9%	48.7%	31.3%	30.8%	33.0%	49.0%	51.3%	38.8%	28.1%	33.9%	45.8%	47.1%

Graphing these results (Figure 4.10) reveals an interesting trend, the classification accuracy tends to improve as the texture kernel expands. This parallels the results found with the datasets exclusively processed for texture in Section 4.7 and is the opposite of the results experienced once SAR texture measure data are fused with MSI data as discussed in Section 4.11. The reason for this trend is unknown though it is possibly a function of study site size and is discussed more fully in Chapter 5. The results presented in Figure 4.10 provide no indication of an optimum sequence of filtering operations that provides value in land cover classification processes.

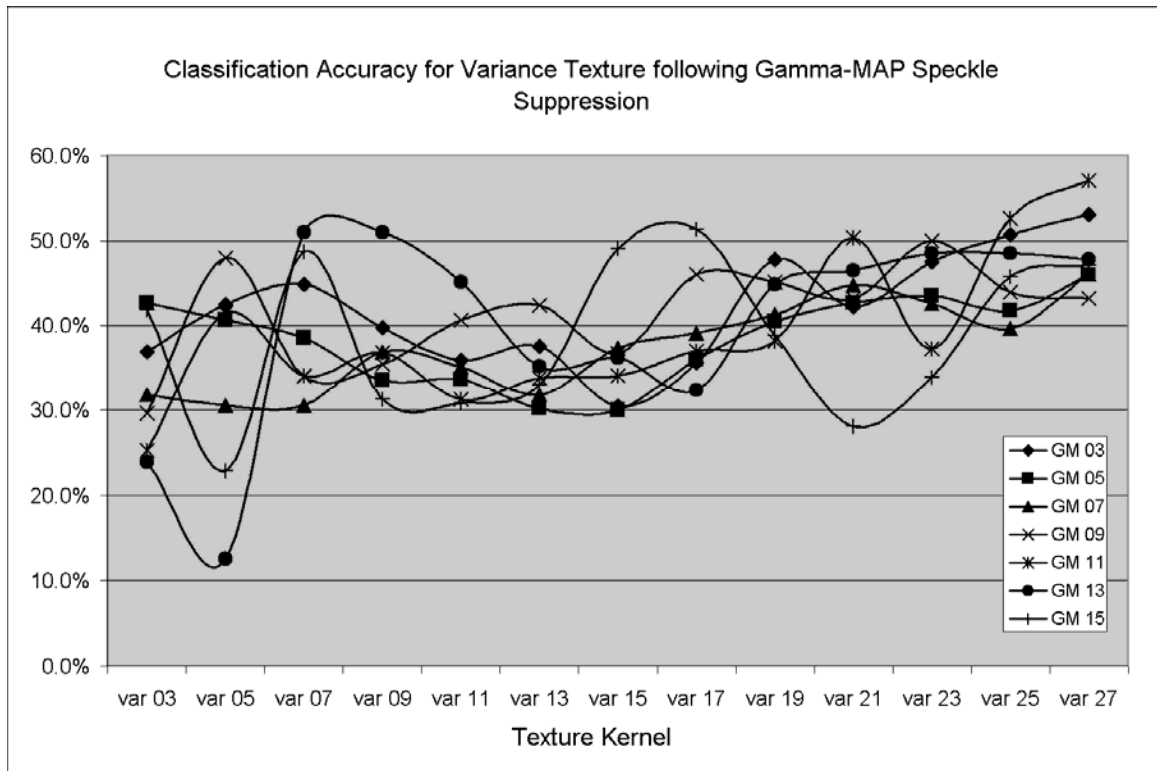


Figure 4.10: SAR 0418 Speckle Suppressed followed by Variance Texture Measure

For the purpose of comparison, the contingency table for SAR 0418 processed to suppress speckle with a GM 7x7 filter, and then measured for texture using the a Variance 9x9 filter is included (Table 4.30). Compared to the results presented in Table 4.24, Table 4.26, and Table 4.28, the results of a sequential processing operation are significantly lower. The data in the sequentially processed version of SAR 0418 have been degraded to such a degree that it is less valuable than the original unfiltered SAR dataset.

Table 4.30: SAR 0418 GM 7x7 followed by Variance Texture Measure at 9x9

	Coppice	Pinelands	Rockland	Saw grass	Mangrove	
Coppice	320	777	123	101	82	1403
Pinelands	407	1144	37	47	13	1648
Rockland	204	482	165	234	150	1235
Saw grass	29	51	180	153	177	590
Mangrove	14	23	0	215	176	428
	974	2477	505	750	598	5304
Producers Accuracy	32.9%	46.2%	32.7%	20.4%	29.4%	Total 36.9%

When visually reviewing the image dataset resulting from the Variance texture measure following speckle suppression, it is clear that the Variance texture measure may not be an appropriate tool for assessing texture in speckle suppressed data. While the GM filter suppresses speckle across broad regions of an image, variability is preserved in edges with significant change, such as land-water boundaries. In these areas speckle is not suppressed. When the Variance texture measure is applied to a GM suppressed dataset, edges retain high variability (speckle) while core areas are homogenized. As a result, edges produce a higher variance value while core areas elicit no variance or minimal variance. The Variance texture measure following a GM speckle suppression filter produces a dataset similar in appearance to that produced by a high-pass filter. It is possible that the Variance texture measure is an inappropriate filter to apply to speckle suppressed data as none of the speckle filters investigated in

this study provided worthwhile results when followed by a Variance texture process.

4.9 LANDSAT TM FUSED WITH UNFILTERED SAR

The first investigation of the efficacy of combining SAR data with multispectral data was performed using raw unfiltered SAR data with the Landsat TM dry season and wet season datasets. Each SAR dataset was combined first with Dry TM then with Wet TM, the standard supervised classification processing was performed and an accuracy assessment determined. Given the number of datasets involved (21 SAR combined with each of 2 Landsat TM datasets for a total of 42) the results are presented here in aggregate and compared with the results of the exclusively TM or SAR datasets.

Combining individual SAR datasets with each TM dataset resulted in a nominal improvement over the results of each TM dataset alone. The values for the TM_SAR dataset presented in Table 4.31 constitute the average values for the 42 combinations of SAR and TM data, the values for SAR are the average results for 21 SAR datasets while the results for Dry_TM and Wet_TM are for the individual scenes. Adding TM data to SAR data significantly improves the

classification results while adding SAR data to TM only nominally improves results.

Table 4.31: TM and Unfiltered SAR Classification Results

Dataset	Total Accuracy	Producers Accuracy				
		Coppice	Pinelands	Rockland	Saw grass	Mangrove
TM_SAR	82.9%	89.2%	84.1%	65.6%	77.1%	77.1%
Dry_TM	80.6%	89.2%	81.8%	70.5%	77.9%	70.7%
Wet_TM	80.7%	93.1%	84.5%	57.8%	77.9%	62.7%
SAR	35.8%	16.0%	52.2%	37.6%	21.9%	26.2%

By dividing the 42 combinations by season it is possible to discern any advantage from cross season data integration. In Table 4.32 the results from the 42 combined datasets are grouped according to data type and season, providing

Table 4.32: Average Classification Accuracy by Season Combination

Dataset	Total Accuracy	Producers Accuracy				
		Coppice	Pinelands	Rockland	Saw grass	Mangrove
Dry_TM Dry_SAR	83.0%	91.8%	86.2%	83.2%	68.9%	73.0%
Dry_TM Wet_SAR	84.0%	91.7%	86.6%	84.3%	69.0%	74.6%
Wet_TM Dry_SAR	82.8%	93.3%	81.4%	82.4%	82.3%	77.4%
Wet_TM Wet_SAR	82.2%	87.2%	83.0%	67.8%	85.5%	78.6%

each seasonal combination as a set of averages for the corresponding datasets.

The total accuracy for each combination is in line with the overall TM_SAR

accuracy in Table 4.31. However, it is worthwhile noting that the combination of Dry_TM and Wet_SAR did result in a nominally higher classification accuracy. This is notable given the fact that the wet season SAR datasets when processed individually tended to result in higher classification accuracies than those collected in the dry season. Also notable is the fact that the SAR data when combined with Wet_TM provided a better means of discerning the Saw grass class than the SAR data combined with Dry_TM.

While the results of combining unfiltered SAR with TM data provide only nominal improvement over the TM datasets exclusively, the speckle suppression and texture filtering of SAR data may improve on this. The combination of Dry_TM and Wet_SAR resulting in a slightly higher classification accuracy may indicate that there is an advantage to cross-season integration. Collecting MSI data when conditions are optimal (in the dry season) and SAR data when conditions are not optimal for MSI and combining the datasets may result in improved classification and improved discrimination of certain cover types over single date MSI data alone.

4.10 LANDSAT TM FUSED WITH SPECKLE SUPPRESSED SAR

Speckle suppression processing of SAR data significantly improved its utility for land cover classification. One of the principal goals of this project was to determine if this advantage can be leveraged in combination with MSI to improve on standard land cover results achieved with MSI.

In Table 4.33, the classification results of combined speckle suppressed SAR data and the MSI data are presented. As with the speckle suppressed SAR

Table 4.33: Fused TM and Speckle Suppressed SAR Average Accuracy Results

Filter	Kernel Size						
	3	5	7	9	11	13	15
Frost	84.7%	84.8%	85.0%	85.1%	85.2%	85.1%	85.2%
Gamma-MAP	84.9%	85.2%	85.4%	85.5%	85.5%	85.3%	85.2%
Local Region	84.8%	84.8%	85.0%	85.2%	85.2%	85.4%	85.3%
Lee-Sigma	84.9%	84.9%	85.1%	85.2%	85.4%	85.4%	85.4%
Median	84.9%	85.2%	85.2%	85.5%	85.5%	85.5%	85.2%

results presented in Section 4.6, these results are averages of total classification accuracy results for all SAR date and TM date combinations by speckle suppression filter and kernel size.

The most notable observation regarding these results is the marginal improvement in classification accuracy achieved when the Landsat TM and speckle suppressed SAR are processed as a fused dataset. As presented in Table

4.1 in Section 4.1, processing of the Landsat scenes resulted in classification accuracy of at best 80.7%. Landsat TM combined with unfiltered SAR provided an average classification accuracy of 82.9%. Table 4.33 shows that in this study, speckle suppressed SAR combined with Landsat TM only improved on the unfiltered SAR by 2-3 percentage points. As the kernel window expands from 3x3 to 15x15 there is marginal improvement.

There appears to be some minor though consistent differences between speckle suppression filters. These become more apparent when presented in graph form (Figure 4.11). The GM and Median filter provide the largest improvement in average classification accuracy in the smaller kernel window sizes before tapering off after the 11x11 and 13x13 kernel sizes. The other three filters also provide improved classification accuracy as the kernel expands but level off at a lower accuracy and then decline at the largest windows.

For comparative purposes, one of the datasets with the higher classification results was selected to assess how it differed from the purely SAR and purely TM results. The fused dataset that contained Dry TM and SAR 1203 (wet season) provided a total classification accuracy of 88.6%. The results of all of the combinations of processing applied to this data combination are contained

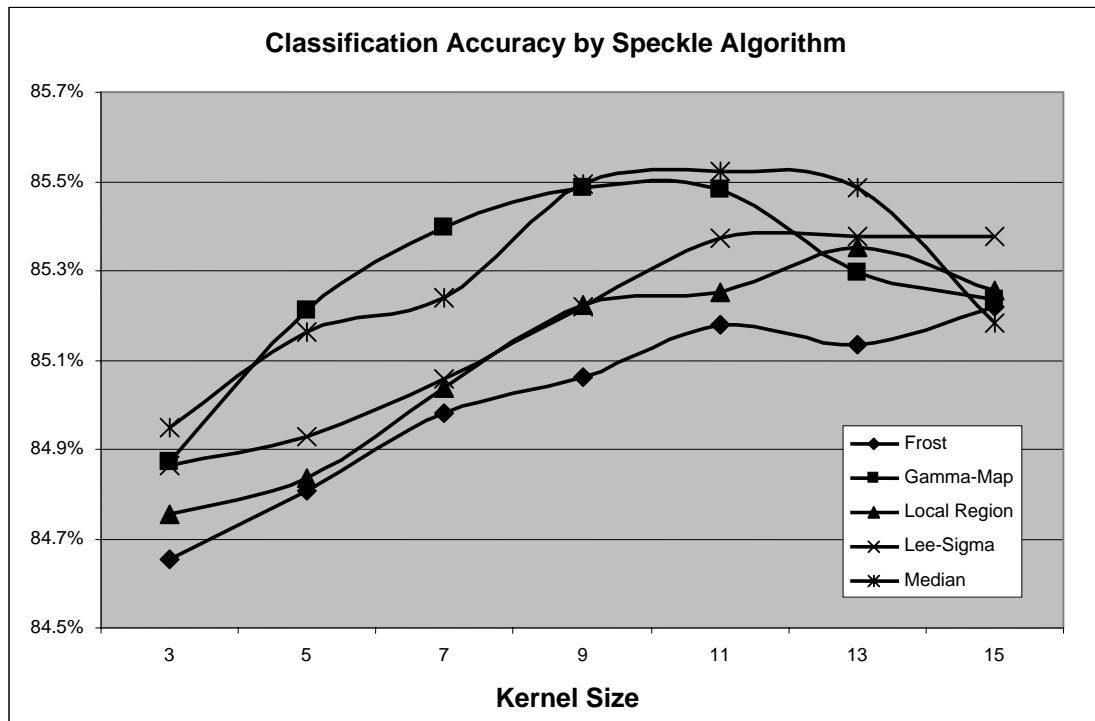


Figure 4.11: Fused TM and Speckle Suppressed SAR, Average Accuracy Results

in Table 4.34 though only one of the 35 speckle suppression processes is included (Gamma-MAP, 9x9 (GM09)).

Table 4.34: Classification Results for Dry TM and SAR 1203

Dataset	Total Accuracy	Producers Accuracy				
		Coppice	Pinelands	Rockland	Saw grass	Mangrove
SAR 1203	35.8%	16.0%	52.2%	37.6%	21.9%	26.2%
1203-GM09	56.2%	69.1%	60.7%	63.3%	46.7%	22.7%
Dry_TM	80.6%	89.2%	81.8%	70.5%	77.9%	70.7%
TM/SAR	85.2%	90.0%	87.7%	83.5%	79.3%	74.5%
TM/SAR-GM09	88.6%	93.2%	88.9%	84.6%	88.8%	81.2%

With each stage of processing classification results improve. SAR filtered to suppress speckle improves on unfiltered SAR, SAR combined with TM improves on TM alone, speckle suppressed SAR combined with TM provides the best results. A notable point regarding the TM/SAR-GM09 results concerns the accuracy results of the Saw grass and Mangrove classes. For the most part, the speckle suppressed SAR dataset does not provide significant improvement over the unfiltered SAR combined with TM (Table 4.31) with the exception of the Saw grass and Mangrove classes. In these two categories the filtered SAR combined with TM provide an improved discrimination of 9.5% for the Saw grass class and 6.7% for Mangrove when compared to the unfiltered SAR dataset combined with TM. Note that this value is only achieved when the SAR and TM are combined, the results for 1203-GM09 for those two classes were not particularly noteworthy in and of themselves.

4.11 LANDSAT TM FUSED WITH SAR TEXTURE

The averaged results of the TM datasets combined with SAR Variance texture measure datasets are presented in Table 4.35, and graphically in Figure 4.12. At small window sizes the SAR texture data provides a moderate improvement in classification accuracy when combined with Landsat TM. The

Table 4.35: Fused TM and SAR Texture Measure Average Accuracy (%) Results

Variance Kernel Size												
3	5	7	9	11	13	15	17	19	21	23	25	27
84.2	82.5	80.6	79.4	77.2	74.9	72.4	70.5	68.7	67.8	66.3	65.7	65.1

improvement is comparable to that achieved with unfiltered SAR data.

However, contrary to expectation, the value of a SAR texture measure dataset declines as the kernel expands. At a 7x7 kernel the classification results are comparable to TM data with no accompanying SAR dataset and steadily declines through the 27x27 kernel. This trend is the opposite of what was experienced

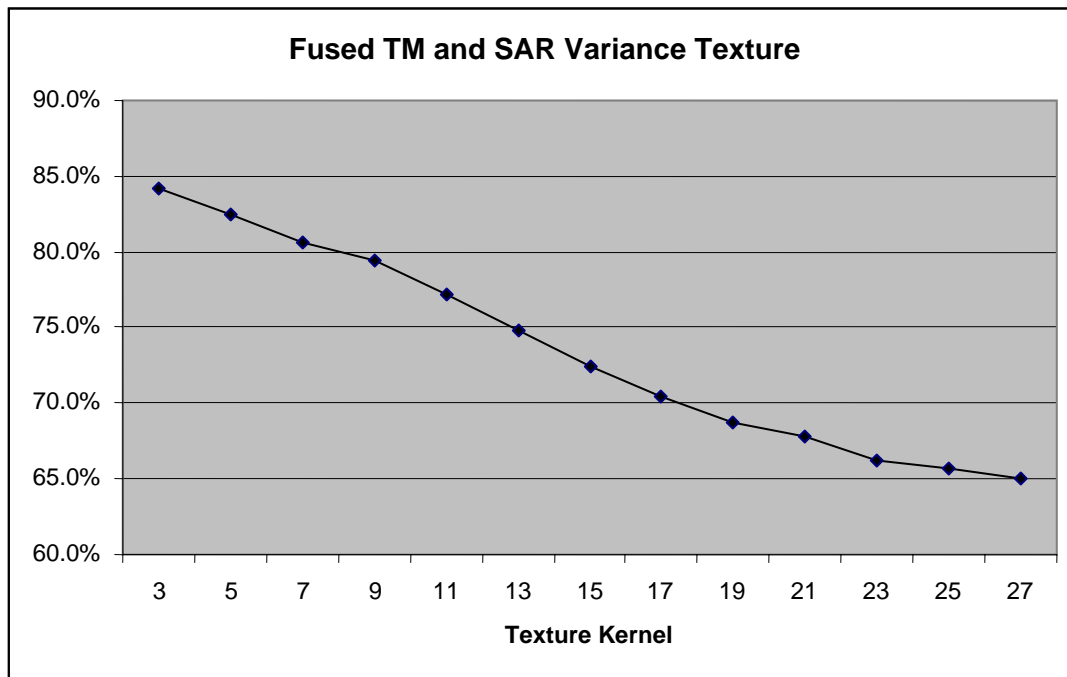


Figure 4.12: Fused TM and SAR Texture Measure Average Accuracy Results

with the exclusively SAR texture data discussed in Section 4.5. Rather than improving and then leveling off as the kernel expands, based on these results the SAR texture data actually impairs the ability of the Landsat TM data to discriminate land cover. While these data in Figure 4.12 are averaged results, this downward trend is present regardless of the other variable investigated with no apparent difference in Collection Mode, Incident Angle, or Seasonality.

When comparing the classifications results divided into ascending and descending collection mode, the same divergence that was apparent with the TM

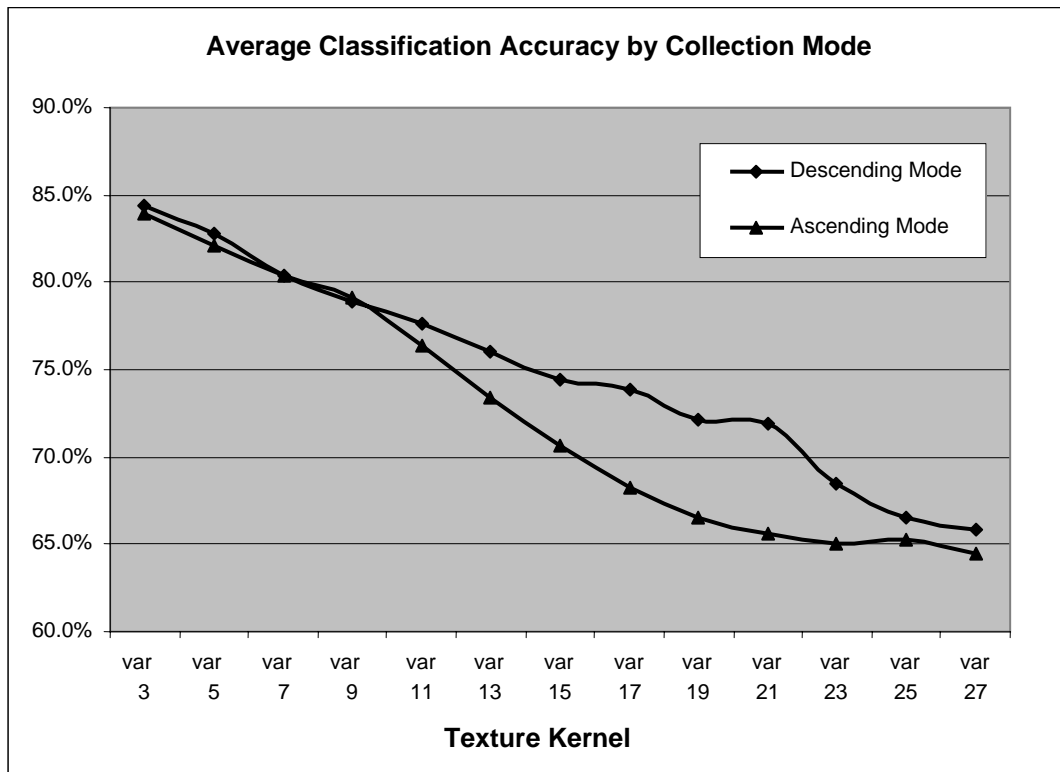


Figure 4.13: Fused TM and SAR Texture Measure by Collection Mode

and unfiltered SAR results presented in Figure 4.13 is manifest in these results. There is limited difference in results until the kernel expands to 9x9 at which point the results for ascending mode data declines more rapidly than the results for descending mode data. In Figure 4.6 where exclusively SAR data were processed, the descending mode data also exhibited higher results, though in an improving fashion as the kernel expanded.

One set of results that are confounding regarding the comparative classification accuracy of TM and SAR texture measure are those divided by

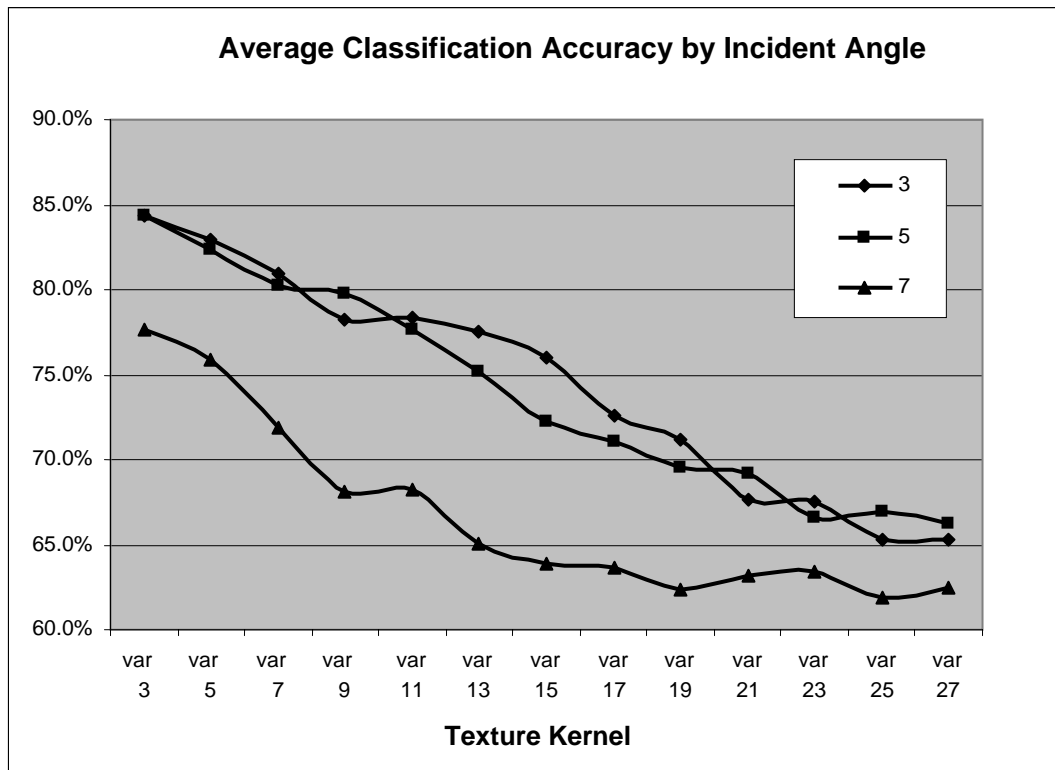


Figure 4.14: Fused TM and SAR Texture Measure by Incident Angle

incident angle. The results of individual SAR texture measure datasets indicated only a nominal difference between mode 3 and 5 while mode 7 diverged notably and in a positive sense beyond the 13x13 kernel (Figure 4.7). With the fused TM and SAR data (Figure 4.14) mode 3 and 5 again provide comparable results but mode 7 diverge for the worse, and across the range of kernels.

One area where an earlier trend is apparent that does perhaps prove meaningful is regarding the combination of data by season. Though the overall classification results are declining as the kernel expands, the combination of dry season TM

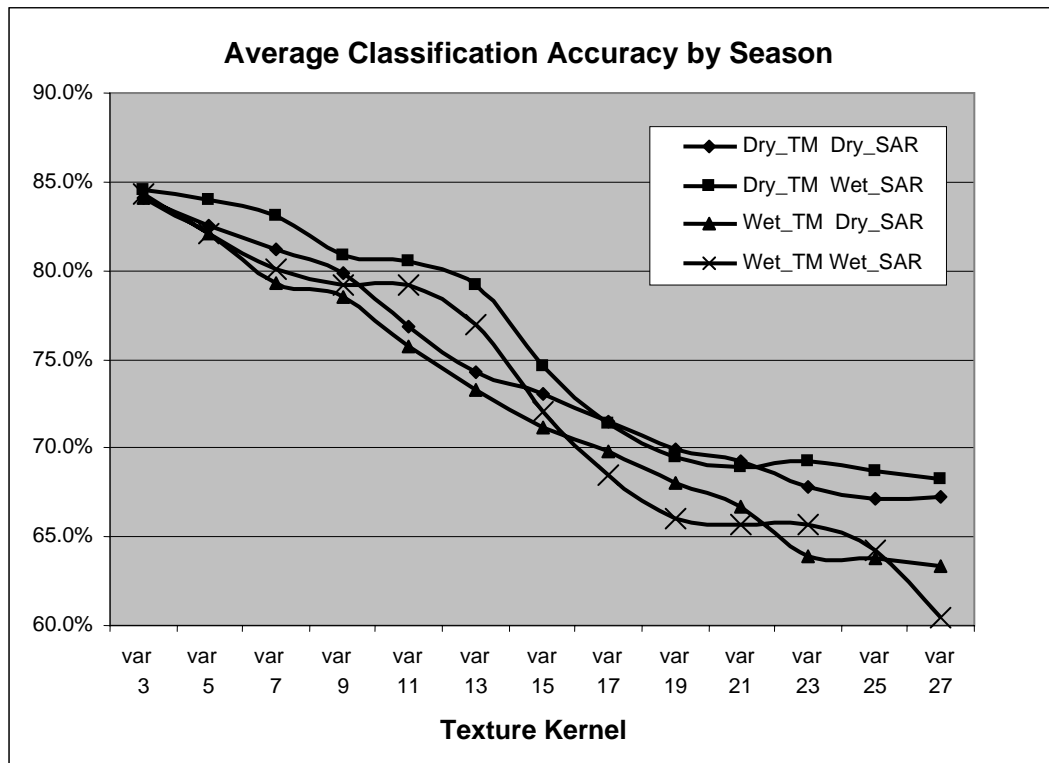


Figure 4.15: Comparative Average Classification of TM/SAR Texture

data with wet season SAR texture measure (Figure 4.15) continues to provide the highest classification accuracy. This again indicates that there may be value in combining SAR and TM data from different seasons to maximize their value.

4.12: VARIOUS COMBINATIONS

MSI and SAR data were fused in different combinations to determine what value could be gained from integrating datasets. The first set of processes performed was on SAR data to determine the efficacy of processing a single layer into multiple datasets, combining them, and using them to perform a classification of land cover. In this case one dry season (SAR 0418) and one wet season (SAR 1203) dataset were selected. Each was processed for every combination of speckle suppression and Variance (VAR) texture measure, combined into a single dataset, and classifications were run on combinations of the unfiltered dataset with different filters and kernel size. Figure 4.16 presents the results of SAR 0418.

As presented in Table 4.4, unfiltered SAR 0418 resulted in a classification accuracy of 40.7%. When this dataset is combined with a version of itself that has been processed for speckle suppression with a GM filter, the results improve approximately 14%. When SAR 0418 is combined with a texture measure filter,

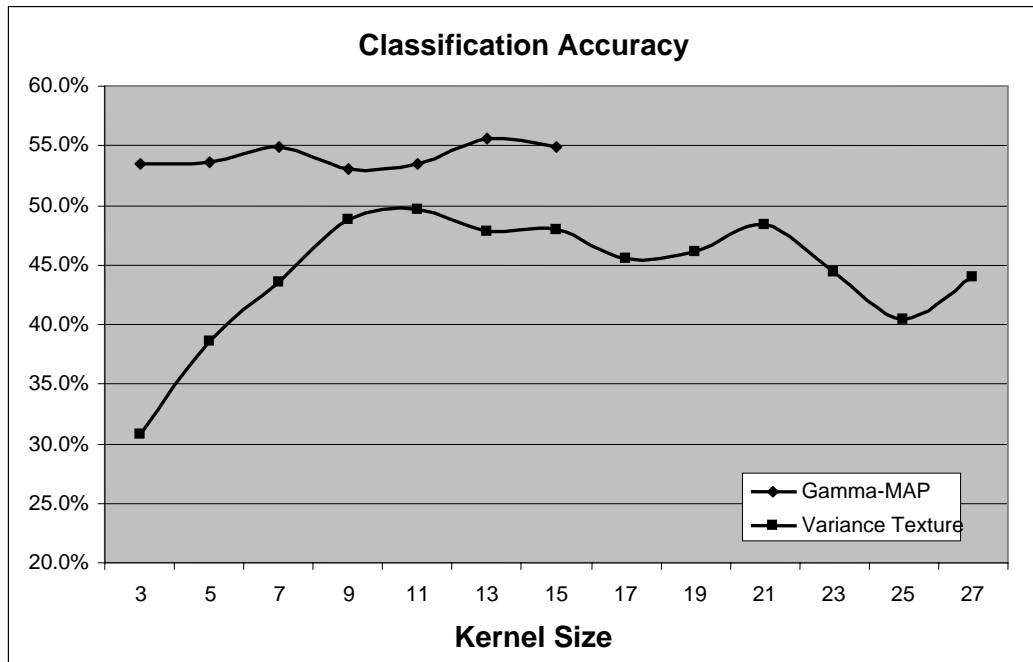


Figure 4.16: Unfiltered SAR 0418 and Filtered SAR 0418 Datasets

the results improve as the kernel expands from 3x3 - 11x11 to a peak improvement of nearly 10% above the original data and then slowly decline as the kernel expands to 27x27.

These results indicate that improved land cover classifications can be achieved by combining filtered versions of a dataset with its unfiltered version. To test this further, the SAR 0418 dataset was then combined with a single GM instance and a single texture instance to determine if the three collectively could further improve results.

Table 4.36 is the contingency table for SAR 0418 combined with GM 7x7 and VAR 11x11. The combination of three datasets generated from this single date has resulted in a total classification accuracy of 64.2%. This is a 23.5% improvement over the unfiltered version of SAR 0418.

Table 4.36: SAR 0418 as Three-banded Image (Unfiltered, GM7, VAR11)

	Coppice	Pinelands	Rockland	Saw grass	Mangrove	
Coppice	852	453	79	63	13	1460
Pinelands	277	1782	29	24	4	2116
Rockland	102	60	321	38	5	526
Saw grass	9	163	46	564	500	1282
Mangrove	63	19	0	61	76	219
	1303	2477	475	750	598	5603
Producers Accuracy	65.4%	71.9%	67.6%	75.2%	12.7%	Total 64.2%

Note that the selection of the Variance kernel size has a significant impact on the results of this combined dataset. When the same process was performed with SAR 0418 combined with GM 7x7 and VAR 5x5, the total classification accuracy dropped to 49.0%. The Variance filter in this case subtracted from the value of the unfiltered and GM combination.

SAR 0418 filtered combinations were then fused with Dry TM to determine the value of combining multiple filtered instances of SAR data with TM data. The results of these as well as the SAR combinations are contained in Table 4.37. The combinations of datasets are as follows:

- A) 3-band dataset (Unfiltered SAR, GM7, VAR11)
- B) 3-band dataset (Unfiltered SAR, GM7, VAR5)
- C) 9-band dataset (DryTM, Unfiltered SAR, GM7, VAR11)
- D) 8-band dataset (DryTM, GM7, VAR11)
- E) 8-band dataset (DryTM, Unfiltered SAR, GM7).

Table 4.37: SAR 0418 Process Combinations with Dry TM

Dataset	Producers Accuracy					
	Tot. Accuracy	Coppice	Pinelands	Rockland	Saw grass	Mangrove
A	64.2%	65.4%	71.9%	67.6%	75.2%	12.7%
B	46.2%	40.1%	65.2%	12.2%	38.1%	33.6%
C	80.6%	95.6%	91.8%	42.3%	81.7%	42.7%
D	81.2%	95.5%	91.9%	47.5%	80.1%	44.7%
E	87.1%	95.6%	91.0%	82.3%	75.5%	73.1%

When combined with Dry TM, the SAR 0418 combination provides a total classification accuracy of 80.6%. This is no better than the TM dataset when processed alone. However, when the Variance texture measure dataset is dropped from the fused dataset, the classification improves to 87.1%. Clearly, the Variance dataset is contributing confusion to the classification process, especially in the Rockland and Mangrove classes where the most significant gain is achieved by its exclusion. The accuracy result with dataset E is comparable to

the results achieved from the combination of DryTM and WetTM as presented in Section 4.1, Table 4.3. Essentially, a single TM date combined with a single SAR date (in unfiltered form coupled with a GM07 speckle suppressed form) provides a classification accuracy comparable to two TM datasets from different dates.

To further investigate and validate these results, wet season SAR 1203 was processed in similar combinations as SAR 0418 just discussed. Figure 4.17

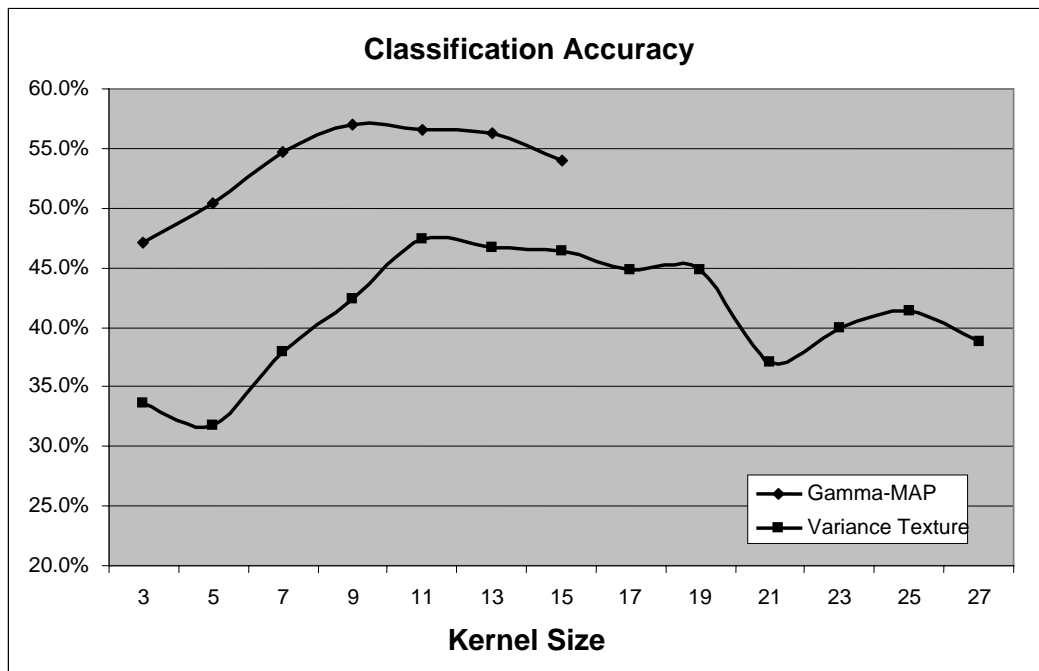


Figure 4.17: Unfiltered SAR 1203 Coupled with Filtered SAR 1203 Datasets

presents the results of unfiltered SAR 1203 coupled with each instance of SAR 1203 processed to suppress speckle and processed to measure texture.

The results are closely in line with those experienced with SAR 0418 (Figure 4.16). Unfiltered SAR coupled with a GM speckle suppression version of itself improves classification accuracy and the results improve as the kernel expands to a peak at the 9x9 filter with a nominal decline out to the 15x15 kernel. When coupled with a Variance texture measure of itself, the classification results improve to the 11x11 kernel window and then steadily decline as the kernel expands to 27x27. When processed as a single unfiltered SAR dataset, SAR 1203 resulted in a classification accuracy of 35.4% (see Table 4.4). When coupled with a speckle suppressed version of itself the accuracy of classification improves to 47.1% at GM 3x3 and 57.0% at GM 9x9. When coupled with Variance texture measure instances of itself, classification accuracy results actually decline at 3x3 and 5x5 kernels before improving to 37.9% at a 7x7 kernel and peaking at 47.4% at an 11x11 kernel.

SAR 1203 combined with GM 7x7 and VAR 11x11 instances of itself result in a classification accuracy of 59.2% (Table 4.38) providing an improvement of 23.8% over SAR 1203 unfiltered, a 4.6% improvement over SAR 1203 coupled with its GM 7x7 instance and an 11.8% improvement over SAR 1203 coupled with VAR 11x11. As was demonstrated with the SAR 0418 dataset, combining an unfiltered SAR dataset with filtered version of itself appears to maximize the information content of the SAR dataset.

Table 4.38: SAR 1203 as Three-banded Image (Unfiltered, GM7, VAR11)

	Coppice	Pinelands	Rockland	Saw grass	Mangrove	
Coppice	852	370	79	59	16	1376
Pinelands	277	1739	29	5	0	2050
Rockland	102	172	321	200	108	903
Saw grass	9	24	46	341	447	867
Mangrove	63	172	0	145	120	500
	1303	2477	475	750	691	5696
Producers Accuracy	65.4%	70.2%	67.6%	45.5%	17.4%	Total 59.2%

When different instances of SAR 1203 are combined with Dry TM the results are again consistent with those experienced with SAR 0418 (Table 4.37). Dry TM combined with the 3-banded version of SAR 1203 or when combined with GM7 and VAR11 provides results no better than Dry TM alone (Table 4.1), but when the Variance texture dataset is dropped, Dry TM coupled with an unfiltered instance of SAR 1203 and its GM7 instance provides a classification accuracy of 87.8% comparable to two Landsat TM scenes combined. These results again indicate that a single TM scene combined with a single SAR dataset can be used to generate results comparable to two TM scenes.

One of the goals of this study is to assess the value of cross-season SAR and MSI combinations. SAR 0418 was collected during the dry season and as such Table 4.36 provides an example of Dry TM combined with dry season SAR data. SAR 1203 was collected during the wet season providing an example of

Dry TM combined with a wet season SAR dataset (Table 4.39). Both combinations prove to be valuable in this case.

Table 4.39: SAR 1203 Process Combinations with Dry TM

	Producers Accuracy					
	Tot. Accuracy	Coppice	Pinelands	Rockland	Saw grass	Mangrove
Unfiltered+ GM7+VAR11	59.2%	65.4%	70.2%	67.6%	45.5%	17.4%
Unfiltered+ GM7+VAR5	48.1%	47.9%	55.3%	68.6%	40.3%	14.6%
DryTM+ Unfiltered+ GM7+VAR11	80.6%	92.4%	89.1%	30.6%	78.7%	68.2%
DryTM+ GM7+VAR11	80.8%	92.6%	89.1%	32.1%	77.9%	69.6%
DryTM+ Unfiltered+ GM7	87.8%	93.0%	88.7%	83.2%	86.7%	79.0%

The processing of multitemporal SAR classification results discussed in Section 4.3 and 4.4 demonstrated that SAR data collected from multiple instances in time can provide land cover classification results comparable to that achieved with multispectral MSI data, especially when a speckle suppression filter is applied to raw SAR data (Table 4.20). One question that arises from this determination is how many SAR datasets are required to achieve results comparable to a single 6-banded MSI dataset.

The multitemporal SAR dataset processed with a GM filter at a 9x9 kernel was used to determine at what point multitemporal SAR provides results

comparable to a single Landsat TM scene used in this study (classification accuracy of ~80%). Two methods were used to select SAR dates to assess in this process. Randomly selected SAR GM09 dates were accumulated and a classification process run against them in an effort to determine a value based on no control over contributing datasets. Also, a separability process (Transformed Divergence) was applied to the entire SAR collection to determine the best datasets to use as a 1-date, 2-date, 3-date, 12-date, combination.

As Figure 4.18 demonstrates, adding SAR dates as additional bands improves the accuracy of a land cover classification process. In this case, the

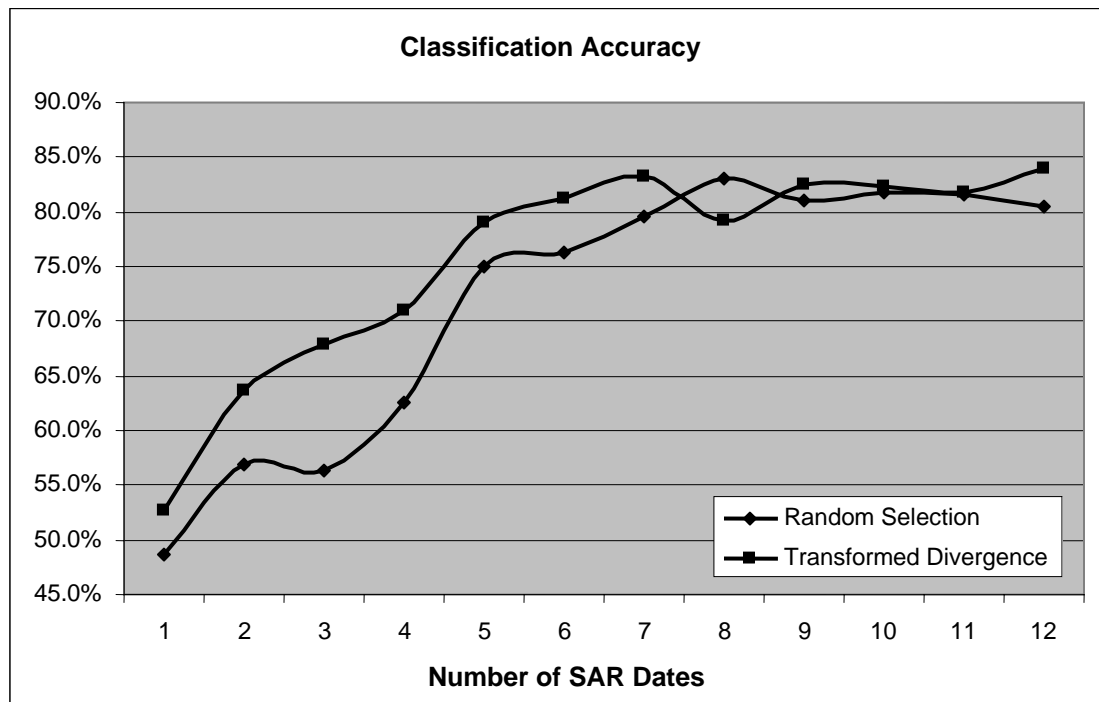


Figure 4.18: Multitemporal SAR GM09 Classified as Multiband Images

greatest improvement is found as the 4th and 5th dates are added either selection process and the greatest value is achieved at the 7th date with transformed divergence selection and the 8th date with random selection. The classification results achieved are comparable to a single Landsat TM dataset with the 6th date when a band selection tool is used and the 8th date with random selection. No further improvement is realized as additional dates beyond the 7th or 8th are added.

The MSI data used in this analysis consisted of Landsat 5 TM data with three visible light bands and three infrared bands. Many imaging systems, especially in the higher spatial resolution sector, have a limited number of spectral bands with three visible and one infrared being common. To assess the value of adding SAR to a limited MSI dataset, DryTM was limited to bands 1-4 and couplings of unfiltered and speckle suppressed (GM09) were added in random date assignments to see at what point multi date SAR images would bring the value of a MSI that consisted of visible plus one IR band up to that of a more comprehensive MSI dataset such as those collected by Landsat TM. The results of this analysis are presented in Figure 4.19.

A classification of DryTM bands 1-4 resulted in a total classification accuracy of 72.8%. As presented in Figure 4.19, a single SAR date (as a 2-band

coupling of unfiltered and GM09 of the same date) brings a limited MSI dataset on par with a 6-band Landsat TM dataset (classification accuracy of ~80%).

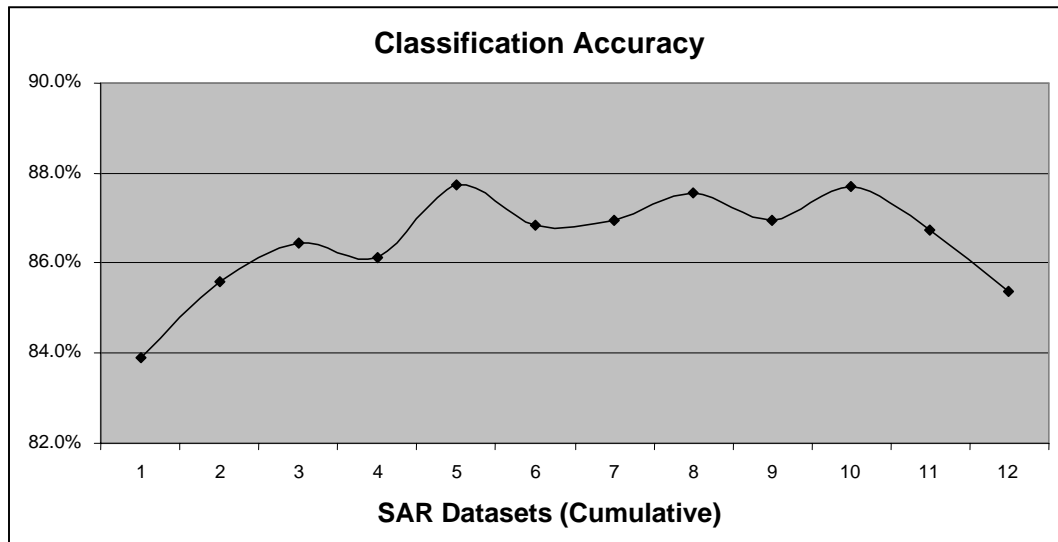


Figure 4.19: DryTM B1-B4, Combined with SAR Couple (Unfiltered, GM09)

Additional SAR dates added in cumulatively improve on the total classification accuracy with five dates providing a maximum benefit. Beyond 11 dates the classification accuracy declines. The additional SAR dates may add a confusion factor rather than an advantage in classification. As presented in Figure 4.18, adding additional SAR scenes beyond eight provided no further value.

The Transformed Divergence separability tool was applied to the collection of unfiltered SAR, speckle suppressed SAR processed with a GM 9x9 kernel, and DryTM and WetTM as a combined dataset. The datasets/bands

identified as the best to use for these land cover categories were then processed as 1 – 12 band combinations. In addition, a combination of the best TM and best GM09 bands were processed as couples to compare the value of the fused data sources. This translates to 2-24 band data series and set of results. Figure 4.20 presents the results of this process. Note that the SAR GM09 Best Dates series was already presented in Figure 4.18 and is repeated here.

The SAR Unfiltered datasets provides a typically low classification accuracy with a steady improvement as dates are added. When processed to suppress speckle (in this case with a GM9x9 filter) the same trend is seen but with significantly better results. The 6th date added provides classification accuracy results equivalent to a single 6-banded MSI dataset such as one provided by the Landsat TM sensor. The TM best bands selection provides excellent results with a best 3-band combination (WetTM band 1(Blue), DryTM band 4(NIR), and DryTM band 5(SWIR)) from two TM dates providing results equivalent to a single 6-banded TM dataset. The significant increase in water surface area in the WetTM scene may explain the value of band 1 from that date. As additional bands are added, the accuracy results improve to a peak of just over 87% for the full 12 bands.

When combining TM bands with speckle suppressed SAR the value of the combination is quickly apparent. The TM SAR GM09 Best Bands data series

surpasses a single TM dataset with the inclusion of two TM bands (WetTM band 4(NIR) and DryTM band 5(SWIR)), combined with two GM09 processed SAR (0401 and 0510, both dry season dates). The peak accuracy is achieved with

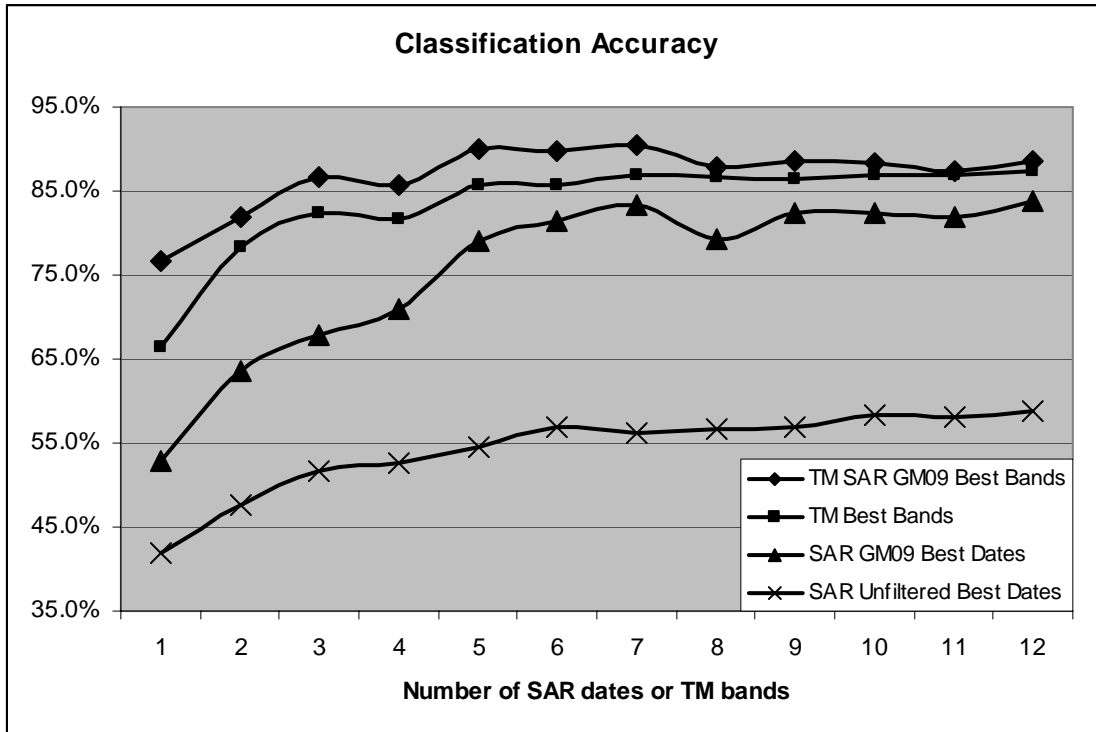


Figure 4.20: Dataset Selection Using Transformed Divergence

between five and seven MSI and speckle suppressed best-band combinations with accuracy results in the area of 90%. The accuracy then tapers off slightly. These results reinforce the value of combining MSI and SAR datasets, especially when multiple datasets are available over an extended time period.

As a final point of investigation, both TM dates were combined with all SAR dates processed to reduce speckle with a GM09 filter and the results assessed. Table 4.40 presents the contingency table of the accuracy assessment for this combination of data. The total accuracy of 91.3% is the highest achieved in this project. Note that the Mangrove class proves to be the most problematic with regards to successful classification.

Table 4.40: DryTM, and All SAR Processed at GM09

	Coppice	Pinelands	Rockland	Saw grass	Mangrove	
Coppice	1249	52	10	0	0	1311
Pinelands	25	2377	2	0	0	2404
Rockland	27	19	552	33	271	902
Saw grass	1	19	0	710	28	758
Mangrove	1	10	0	7	392	410
	1303	2477	564	750	691	5785
Producers Accuracy	95.9%	96.0%	97.9%	94.7%	56.7%	Total
						91.3%

5.0 DISCUSSION AND FUTURE RESEARCH

5.1 DISCUSSION

The value of MSI for land cover characterization is well documented throughout the scientific literature. This study certainly reinforces this fact in that with MSI alone, a decent assessment of land cover was possible for the study site. Multitemporal MSI is clearly even more valuable by providing a means for capturing and assessing phenological differences in vegetation across growing seasons or climate patterns. If weather conditions were never a problem, multi date MSI provides the best source of information for characterizing the surface of the earth. Unfortunately, weather is a significant issue in many regions of the world. This research provides considerable evidence that MSI data can be suitably supplemented with SAR data to effectively assess land cover. This proves to be most useful in instances where a single MSI dataset can be acquired and then fused with SAR datasets collected over time periods that include seasonal changes in vegetation. The particular value of acquiring SAR is the opportunity to exclude issues related to weather conditions and cloud cover.

While this research did not focus on maximizing the value of MSI for land cover characterization, it is likely that improved classification accuracies could have been achieved solely utilizing MSI by applying some basic filtering techniques such as a majority filter to classification results. Furthermore, the use of band ratioing techniques or other transformations may also improve the results of the MSI processing.

Single date SAR datasets do not prove to be of much value for consistently discriminating vegetated land cover categories. The variability in backscatter for similar land covers across individual scenes constitutes a significant barrier to achieving consistent homogenous land cover characterization. This variability is largely due to the presence of speckle. In this study there did appear to be some value to SAR data collected in wet season conditions over that collected in dry season conditions. Whether this was due to the moisture content of vegetation or to a change in the surface matrix (moist soil or increased standing water) of the vegetation classes considered could not be determined and was not the focus of this research. There was no clear value to varying the incident angle of SAR nor a clear difference derived from orbit (ascending collection vs. descending collection). The orbit result was expected but the incident angle results are likely only applicable to this particular study site.

There was a respectable value to SAR data combined into a multitemporal dataset. Time series SAR data should be considered a worthwhile source of

information especially where growing season variations can be leveraged (such as crop calendars) and MSI data are of limited availability. It should be noted that multitemporal data are similar to multispectral data in that individual datasets (bands) record changes in time rather than changes in spectral response. Discrimination may not be precisely as accurate as those achieved with MSI but faced with a data vacuum, multitemporal SAR certainly provides some value. Also of note in this study is the fact that a limited collection of wet season images (eight) proved more valuable than a more extensive set of dry season data (thirteen). This may be because most vegetation growth occurs during the wet season and a sampling of points in time across that season capture appropriate magnitudes of change to characterize the land cover more effectively. During the dry season vegetation senesces or is in a more dormant state so there is limited change over time to leverage.

Processing SAR to suppress speckle is clearly essential to maximizing its value. In this study, speckle suppression using moderate kernels (7x7 and 9x9) proved most valuable. While a number of speckle suppression techniques were tested and the GM was deemed most valuable, any of the five algorithms assessed increased the value of SAR for land cover classification over unfiltered SAR. There was still a great deal of variation between scenes collected with different system parameters on different dates and this variation was not consistent. As such, no conclusions could be drawn on the most appropriate

system parameters (incident angle and orbital path) utilizing speckle suppressed data as was the case with the unfiltered datasets.

Similar to the findings with speckle suppression applied to SAR, texture measures also provide some value improving the classification accuracy of SAR data by utilizing its texture qualities. What was not assessed here was the role of scale when integrating texture measures calculated from SAR. Since texture is a fractal phenomenon, it is possible that more value could be gained by assessing texture at multiple scales (for example a local scale utilizing small kernels and a broader scale utilizing larger kernels). The scale factor is a multidimensional problem that would be difficult to effectively assess due to the combination of scale factors. SAR imagery has a pixel resolution that differs from its spatial resolution (ground sample distance or GSD). Furthermore, the land cover types assessed have textures that manifest at different scales depending on the interaction of SAR GSD and land cover characteristics. The texture of vegetation classes may vary across incident angles given these scale factors as well. Finally, the size of calibration and validation sites factor into appropriate scales at which to assess texture.

One factor that proved interesting though not readily understandable is the fact that a multitemporal speckle suppressed SAR dataset was more valuable than a multitemporal texture measure dataset. This could indicate that for this study site backscatter changes over time (perhaps seasonal variation in

vegetation) while texture does not. It may also indicate that the seasonal changes in SAR return were an indication of vegetation changes rather than surface matrix. Moist soil and more surface pooling of water during the wet season would translate to a significant change in texture that should have permitted a greater discrimination of land cover classes, yet this did not prove to be the case. In any event, texture variations across land cover classes were not substantial enough to provide the degree of value that speckle suppression did.

One of the goals of speckle suppression is to preserve the surface response of SAR data while suppressing the artificial speckle noise inherent in the system. In this study it was determined that while speckle suppressed SAR data are valuable, texture measures calculated on speckle suppressed SAR are definitely not. A single texture measure was utilized in this study (Variance) and there are many others that have been developed and successfully applied to remotely-sensed data. It is possible that the Variance texture measure may not be applied appropriately following speckle suppression. Testing other texture measures following speckle suppression is warranted.

One factor that may contribute to this may be the simple fact of data degradation. From an imagery purist perspective, there is a point at which sending data through a sequence of processes, ostensibly to improve its value, may have the opposite effect. The greater the number of processes applied, the more removed the dataset becomes from its original (actually measured)

condition. In this study data were speckle suppressed, resampled to the MSI spatial resolution, and a texture measure then applied. Such multistage processing should be pursued with caution.

Fusing MSI data with SAR sources does prove to offer some value when attempting to characterize land cover. In this study, the greatest value was achieved using speckle suppressed SAR especially when multiple dates were included. It does indicate that SAR can provide significant value to MSI especially in instances where limited MSI data are available or weather conditions consistently preclude their acquisition. MSI fused with speckle suppressed SAR was consistently valuable while fusion with SAR texture measure was only nominally so and only at small kernel sizes (essentially local texture rather than regional texture).

A notable and interesting discovery in this research was the value of SAR processed as couples. Essentially, this constituted a single unfiltered date of SAR data coupled with a speckle suppressed version of itself as a two-banded dataset. The combination achieved respectable classification accuracies for SAR data when compared to either dataset individually. This value was even more pronounced when the SAR couple was combined with an MSI dataset. The SAR couple proved to be equal in value to a second MSI dataset from an opposing season.

5.2 FUTURE RESEARCH

As is the case with many research projects, while this one has answered many questions it has equally raised a number of questions that warrant further investigation. Chief amongst these is determining the impact of processing SAR data at the system resolution rather than the ground resolution. This is an especially important issue when considered in conjunction with speckle suppression and texture processing. Collins et al., (1998) indicated that texture processing should occur at the pixel spacing scale rather than the ground resolution. It may prove to be more valuable to process SAR data at the pixel resolution and resampling MSI data to match rather than the other way around. The resampling of SAR data to match with a coarser spatial resolution MSI dataset results in a significant amount of data loss. One consideration here may also be the possibility of fusing RADARSAT SAR at its pixel resolution (12.5m) with pan-sharpened Landsat 7 ETM+ datasets.

Also worth pursuing is the relationship among calibration and validation site sizes and SAR filter kernel sizes. It is possible that some of the classification results of filtered SAR datasets especially at broader kernel sizes were impacted by the dimensions of the study sites. It is likely that the size of calibration and validation sites may significantly impact the results of this kind of analysis. As the kernel size expands to be comparable to the size of calibration and validation

sites, any values resulting from a filter process incorporate data falling outside of the calibration/validation sites. As a result, land cover outside of the study sites is impacting values arrived at inside of study sites. This may account for the apparent leveling off of accuracies achieved with the SAR texture processes at greater kernel sizes, as well as the decline in classification results when those datasets were combined with TM data. The hypothesis is that the classification results achieved for single SAR texture measure datasets reflected the smoothing effect of the large kernels and not an inherent texture assessed for the land cover categories. When combined with TM data that retained information characteristic of the land cover categories, the filtered (smoothed) SAR data contradicted the unfiltered MSI and increased confusion between land cover classes resulting in lower classification accuracies as Variance texture measure kernels expanded beyond 13x13.

Resolving this issue would involve ensuring that calibration/validation sites are collected in core areas of the cover type assessed (essentially selecting sites with a buffer of consistent land cover equal to one-half of the largest kernel window utilized), or by using a fully developed land cover dataset for the area of interest for both calibration and validation.

The timing of imagery collection is a very important factor when assessing vegetation. A more extensive dataset could determine precisely the sequence of SAR images and the time spacing that would provide the greatest value,

especially when combined with an MSI dataset as a baseline. Selecting SAR dates tied to phenological patterns would likely be very valuable.

This study focused on the Variance texture measure due to the success achieved applying it in SAR and MSI fusion research in prior studies.

Appropriate combinations of speckle suppression and texture measure algorithms should be investigated more thoroughly to determine if an ideal combination can successfully suppress speckle while preserving inherent surface-related texture in SAR data. Identifying such a combination would be a significant accomplishment especially if applicable to multiple land cover types and in multiple ecotones.

Another aspect of texture that needs to be investigated further is the fractal aspect that may manifest itself at different spatial scales. This could be investigated in a couple of different ways. Data at a consistent spatial resolution could be assessed using texture measures applied at a local scale (smaller kernels) in combination with texture measures assessed at a regional scale (larger kernels). This should also be investigated utilizing different texture measure algorithms to determine if texture at different landscape scales is best assessed using a consistent filter or combinations of different ones. A second method for assessing the fractal dimension of texture is to measure texture across multiple scales of data and combine the results. For example, using texture assessed at the

pixel resolution of SAR data or using a panchromatic band of MSI and combining the result with texture measured at a moderate spatial resolution.

The spatial resolution of SAR and MSI datasets in combination should also be evaluated further. SAR data are collected and delivered at a pixel resolution that is significantly different from its ground resolution. Simply resampling the SAR to its GSD destroys a significant amount of information contained in the dataset. The appropriateness of this process should be fully assessed. Essentially, pixel resolution data contains overlapping samples at the GSD. Appropriate processes applied to these data at the pixel resolution may preserve valuable information that would make these data more appropriately integrated with MSI at a similar scale. For example, fusing SAR at a pixel resolution with pan-sharpened MSI data.

Newer SAR imaging systems are collecting data with a greater diversity of system parameters such as different wavelengths and polarization combinations. As these sensors start collecting data systematically they provide a new and consistent source of data that needs to be fully evaluated. The process used in this study lends itself to evaluation of the usability of these new sources and thoroughly investigating the value of their variables.

Furthermore, this study was applied to a region where climate conditions (subtropical) lend themselves to a multi system approach to land cover assessment. There are many other locations that should be evaluated and could

benefit from multi sensor integration. Applying similar techniques to other biomes and land cover categories is recommended.

Finally, this study focused on determining appropriate processing techniques for fusing SAR and MSI datasets and assessed results in a relative sense. It did not focus on maximizing the information content of these data independently or in combination. One technique that merits further investigation is the value of using band ratios such as NDVI calculations and transformations including PCA and Tasseled Cap (TC) processing to maximize the information content of imagery while minimizing the data volume required for processing. A cursory application of these techniques performed during the early stages of this project provided promising results.

5.3 CONCLUSION

In general, the results of this study prove interesting and valuable. They validate other studies that have tackled similar issues proving that speckle suppression and texture measures are valuable tools to apply when fusing SAR and MSI data. Each incremental step in processing of SAR and MSI/SAR fusion nominally improves classification accuracy. Texture or speckle suppressed SAR is more valuable than unfiltered SAR. MSI fused with SAR is more valuable than MSI alone. MSI fused with speckle suppressed SAR is more valuable than MSI and unfiltered SAR. MSI fused with a single SAR couple is more valuable than

MSI fused with a speckle suppressed SAR and equal in value to a two-date MSI dataset. Finally, multi date MSI combined with multi date SAR provides the greatest value.

REFERENCES

REFERENCES

Adair, M., and B. Guindon, 1989. Methods for evaluation speckle-suppression filters based on edge detection performance. *Canadian Journal of Remote Sensing*, 15(2):100-108.

Ahern, F., D. Leckie, and J. Drieman, 1993. Seasonal changes in relative C-band backscatter of northern forest cover types. *IEEE Transaction in Geoscience and Remote Sensing*, 31:668-680.

Amarsaikhan, D., and T. Douglas, 2004. Data fusion and multisource image classification. *International Journal of Remote Sensing*, 25(17):3529-3539.

Amarsaikhan, D., M. Ganzorig, P. Ache, and H. Blotevogel, 2007. The integrated use of optical and InSAR data for urban land-cover mapping. *International Journal of Remote Sensing*, 28(6):1161-1171.

Anderson, J.R., E.E. Hardy, J.T. Roach, and R.E. Witmer, 1976. A Land Use and Land Cover Classification System for Use with Remote Sensor Data. *U.S. Geological Survey Professional Paper, 964*. U.S. Government Printing Office: Washington D.C., 28 pp.

Anys, H., and D. C. He, 1995. Evaluation of textural and multipolarization radar features for crop classification. *IEEE Transaction in Geoscience and Remote Sensing*, 33(5):1170-1181.

Arai, K., 1991. Multi-temporal texture analysis in TM classification. *Canadian Journal of Remote Sensing*, 17(3):263-270.

Aschbacher, J., and J. Lichtenegger, 1990. Complementary nature of SAR and optical data: a case study in the Tropics. *Earth Observation Quarterly*, 3(1):4-8.

Baghdadi N., R. Pedreros, N. Lenotre, T. Dewez, and M. Paganini, 2007. Impact of polarization and incidence of the ASAR sensor on coastline mapping: example of Gabon. *International Journal of Remote Sensing*, 28(17):3841-3849.

Baldocchi, D., R. Valentini, S. Running, W. Oechel, and R. Dahlman, 1996. Strategies for measuring and modeling carbon dioxide and water vapour fluxes over terrestrial ecosystems. *Global Change Biology*, 2:159-168.

Balztera, H., L. Skinner, A. Luckman, and R. Brooke, 2003. Estimation of tree growth in a conifer plantation over 19 years from multi-satellite L-band SAR. *Remote Sensing of Environment*, 84(2):184-191.

Ban, Y., and P.J. Howarth, 1999. Multitemporal ERS-1 SAR data for crop classification: A sequential-masking approach. *Canadian Journal of Remote Sensing*, 25(5):438-447.

Banner, A. V., and F.J. Ahern, 1995. Incidence angle effects on the interpretability of forest clearcuts using airborne C-HH SAR imagery. *Canadian Journal of Remote Sensing*, 21(1):64-66.

Bauer, M., M. Hixson, B. Davis, and J. Etheridge, 1978. Area estimation of crops by digital analysis of Landsat data. *Photogrammetric Engineering and Remote Sensing*, 44(8):1033-1043.

Beaudoin, A., T. Le Toan, S. Goze E. Nezry, A. Lopes, E. Mougin, C. C. Hsu, H. C. Han, J. A. Kong, and R. T. Shin, 1994. Retrieval of forest biomass from SAR data. *International Journal of Remote Sensing*, 15:2777-2796.

Belhadj, Z., and S. Jebara, 2002. Adaptive speckle reduction using combined multiresolution analysis and prediction technique. *International Journal of Remote Sensing*, 23(11):2263-2282.

Belward, A.S., and T. Loveland, 1995. The IGBP-DIS 1km Land Cover Project: remote sensing in action. *Proceedings, 21st Annual Conference of the Remote Sensing Society*, Southampton, UK, 3:1099-1106.

Bergh, C., F. Lowenstein, R. Myers, J. Snyder, and D. Wade, 2003. Fire management assessment of the Caribbean pine (*Pinus caribea*) forest ecosystems on Andros and Abaco Islands, Bahamas. *The Nature Conservancy*, April 2003.

Bin, Y., 2003. Synergy of multitemporal ERS-1 SAR and Landsat TM data for classification of agricultural crops. *Canadian Journal of Remote Sensing*, 29(4):518-526.

Blaes, X., L. Vanhalleb, and P. Defournya, 2005. Efficiency of crop identification based on optical and SAR image time series. *Remote Sensing of Environment*, 96(3-4): 352-365.

Bloom, A., E. Fielding, and X. Fu, 1988. A demonstration of stereo-photogrammetry with combined SIR-B and Landsat-TM images. *International Journal of Remote Sensing*, 9:1023-1038.

Bonan, G., 1993. Importance of leaf area index and forest type when estimating photosynthesis in boreal forests. *Remote Sensing of Environment*, 43:303-314.

Brisco, B., and F. T. Ulaby, 1984. Improving crop classification through attention to the timing of airborne radar acquisitions. *Photogrammetric Engineering and Remote Sensing*, 50(6):739-745.

Brisco, B., R.J. Brown, and M. J. Manore, 1989. Early season crop discrimination with combined SAR/TM data. *Canadian Journal of Remote Sensing*, 15(1):44-56.

Brisco, B. and R. J. Brown, 1995. Multi date SAR/TM synergism for crop classification in western Canada. *Photogrammetric Engineering and Remote Sensing*, 61(8):1009-1014.

Cao, G., and Y. Jin, 2007. A hybrid algorithm of the BP-ANN/GA for classification of urban terrain surfaces with fused data of Landsat ETM and ERS-2 SAR. *International Journal of Remote Sensing*, 28(2):293-305.

Chan, J. C., N. Laporte, and R. S. Defries, 2003. Texture classification of logged forests in tropical Africa using machine-learning algorithms. *International Journal of Remote Sensing*, 24(6):1401-1407.

Chavez P.S., S.C. Sides, and J.A. Anderson, 1991. Comparison of three different methods to merge multiresolution and multispectral data: TM & SPOT pan. *Photogrammetric Engineering and Remote Sensing*, 57:295-303.

Chenghu, Y. X. Z., 1998. Recognition of flooded area in radar image using texture feature analysis. *19th Asian Conference on Remote Sensing* Manila, Philippines, November 1998.

Chunming, H., G. Huadong, W. Changlin, and F. Dian, 2002. A novel method to reduce speckle in SAR images. *International Journal of Remote Sensing*, 23(23):5095-5101.

Chust G., D. Ducrot, and J. Pretus, 2004. Land cover discrimination potential of radar multitemporal series and optical multispectral images in a Mediterranean cultural landscape. *International Journal of Remote Sensing*, 25(17):3513-3528.

Cimino, J., A. Brandani, D. Casey, J. Rabassa, and S. D. Wall, 1986. Multiple incidence angle SIR-B experiment over Argentina: mapping of forest units. *IEEE Transactions on Geoscience and Remote Sensing*, 24:498-509.

Coburn C. A., and A. C. B. Roberts, 2004. A multiscale texture analysis procedure for improved forest stand classification. *International Journal of Remote Sensing*, 25(20):4287-4308.

Collins, M. J., J. Wiebe, and D. A. Clausi, 1998. The effect of speckle filtering on scale-dependent texture estimation of a forested scene. *IEEE Transaction in Geoscience and Remote Sensing*, 38(3):1160-1170.

Congalton, R. G., and K. Green, 1999. *Assessing the Accuracy of Remotely Sensed Data: Principles and Practices*. Lewis Publishers, New York.

Cook E., L. Iverson, and L. Graham, 1989. Estimating forest productivity with Thematic Mapper and biogeographical data. *Remote Sensing of Environment*, 28:131-141

Correll, D.S. and H. B Correll, 1982. Flora and fauna of the Bahamas archipelago. *Gantner Verlag*, Germany.

Crist, E.P., and R.C. Cicone, 1984. Comparisons of the dimensionality and features of simulated Landsat-4 MSS and TM data. *Remote Sensing of Environment*, 14:235-246.

Davidson G, K. Ouchi, G. Saito, N. Ishitsuka, K. Mohri, and S. Uratsuka, 2006. Single-look classification accuracy for polarimetric SAR. *International Journal of Remote Sensing*, 27(22): 5073-5080.

DeFries R.S., M. Hansen, and J. Townshend, 1998. Global land cover classifications at 8 km spatial resolution: The use of training data derived from Landsat imagery in decision tree classifiers. *International Journal of Remote Sensing*, 19(16):3141-3168.

Dell'Acqua, F., and P. Gamba, 2006. Discriminating urban environments using multiscale texture and multiple SAR images. *International Journal of Remote Sensing*, 27(18):3797-3812.

Dejhan, K., S. Wisetphanichkij, P. Kerdyou, F. Cheevasuvit, S. Mitatha, C. Pienvijarnpong, and C. Soonyeeakan, 2000. Flooded area assessment with fused multi-spectral multi-sensor by using texture feature analysis and neural network classification. *21st Asian Conference on Remote Sensing* Taipei, Taiwan, December 2000.

Dias, J.M., T.A. Silva, and J.M. Leitao, 1998. Adaptive restoration of speckled SAR images. *IEEE Geoscience and Remote Sensing Symposium, Proceedings IGARSS 1998*, 1:19-23.

Dikshit, O., and D.P. Roy, 1996. An empirical investigation of image resampling effects upon the spectral and textural supervised classification of a high spatial resolution multispectral image. *Photogrammetric Engineering and Remote Sensing*, 62(9):1085-1092.

Dobson, M., F. Ulaby, T. Le Toan, T. Beaudoin, E. Kasischke, and N. Christensen, 1992. Dependence of radar backscatter on coniferous forest biomass. *IEEE Transaction in Geoscience and Remote Sensing*, 30(2):412-414.

Dobson, M., E. Wilcox, and F. Ulaby, 1993. Effects of forest structure on radar response to biomass. *IEEE Geoscience and Remote Sensing Symposium, Proceedings IGARSS 1993*, 2:383.

Dobson, M., F. Ulaby, and L. Pierce, 1995. Landcover classification and estimation of terrain attributes using synthetic aperture radar. *Remote Sensing of Environment*, 51:199-214.

Dobson, M., L. Pierce, J. Kellndorfer, and F. Ulaby, 1997. Use of SAR image texture in terrain classification. *IEEE Geoscience and Remote Sensing Symposium. Proceedings IGARSS 1997*, 3:1180-1183.

- Dong, Y., A.K. Milne, and B.C. Forster, 2000. A review of SAR speckle filters: texture restoration and preservation. *IEEE Geoscience and Remote Sensing Symposium, Proceedings IGARSS 2000*, 2:633-635.
- Drieman, J., D. Leckie, and F. Ahern, 1989. Multi-temporal C-SAR for forest typing in eastern Ontario. *IEEE Geoscience and Remote Sensing Symposium, Proceedings IGARSS 1989*, 3:1376-1378.
- Du L., M. R. Grunes, and J. S. Lee, 2002. Unsupervised segmentation of dual-polarization SAR images based on amplitude and texture characteristics. *International Journal of Remote Sensing*, 23(20):4383-4402.
- Duggin, M., R. Rowntree, and A. O'Dell, 1988. The application of spatial filtering methods to urban feature analysis using digital image data. *International Journal of Remote Sensing*, 9(3):543-553.
- Duguay, G., G. Holder, P. Howarth, and E. LeDrew, 1987. Integrating remotely sensed data from different sensors for change detection. *IEEE International Geoscience and Remote Sensing Symposium, Proceedings IGARSS 1987*, 1:333-337.
- Durand, J.M., B.J. Gimonet, and J.R. Derbos, 1987. SAR data filtering for classification. *IEEE Transactions on Geoscience and Remote Sensing*, 25(5):629-637.
- Durieux, L, J. Kropáček, G. de Grandi, and F. Achard, 2007. Object-oriented and textural image classification of the Siberia GBFM radar mosaic combined with MERIS imagery for continental scale land cover mapping. *International Journal of Remote Sensing*, 28(18):4175-4182.
- Fang, Y. C., 1980. Aerial photo and Landsat image use in forest inventory in China. *Photogrammetric Engineering and Remote Sensing* 46(11):1421-1424.

Foody, G. M., 1992. On the compensation for chance agreement in image classification accuracy assessment. *Photogrammetric Engineering and Remote Sensing*, 58(10):1459-1460.

Foody, G.M., G. Palubinskas, R.M. Lucas, P.J. Curran, and M. Honzak, 1996. Identifying terrestrial carbon sinks: classification of successional stages in regenerating tropical forests from Landsat TM data. *Remote Sensing of Environment*, 55:205-216.

Ford, J., and D. Casey, 1988. Shuttle radar mapping with diverse incidence angles in the rainforest of Borneo. *International Journal of Remote Sensing*, 9(5):927-943.

Ford, K., 1997. A description of the ecological communities of North Andros. *Bahamas Journal of Science*, 5(1):29-33.

Gilmer D.S., E.A. Work Jr., and J.E. Colwell, 1980. Enumeration of prairie wetlands with Landsat and aircraft data. *Photogrammetric Engineering and Remote Sensing*, 46(5):631-634.

Gilruth P.T., C.F Hutchinson, and B. Barry, 1990. Assessing deforestation in the Guinea Highlands of West Africa using remote sensing. *Photogrammetric Engineering and Remote Sensing*, 56(10):1375-1382.

Gordon, D.K., and W.R. Philipson 1986. A texture-enhancement procedure for separating orchard from forest in Thematic Mapper data. *International Journal of Remote Sensing*, 7(2):301-304.

Green, K., D. Kempka, and L. Lackey, 1994. Using remote sensing to detect and monitor land-cover and land-use change. *Photogrammetric Engineering and Remote Sensing*, 60:331-337.

Grenier, M., A. Demers, S. Labrecque, M. Benoit, R. A. Fournier, and B. Drolet, 2007. An object-based method to map wetland using RADARSAT-1 and Landsat ETM images: test case on two sites in Quebec, Canada. *Canadian Journal of Remote Sensing*, 33(1):S28-S45.

Guerschman J. P., J. M. Paruelo, C. Bella, M. C. Giallorenzi, and F. Pacin, 2003. Land cover classification in the Argentine Pampas using multi-temporal Landsat TM data. *International Journal of Remote Sensing*, 24(17):3381-3402.

Guo, X., K. P. Price, and J. Stiles, 2003. Grasslands discriminant analysis using Landsat TM single and multitemporal data. *Photogrammetric Engineering and Remote Sensing*, 69(11):1255-1262.

Haack, B.N., 1984. Multisensor data analysis of urban environments. *Photogrammetric Engineering and Remote Sensing*, 50(10):1471- 1477.

Haack B., N. Bryant, and S. Adams, 1987. An assessment of Landsat MSS and TM data for urban and near-urban land-cover digital classification. *Remote Sensing of Environment*, 21(2):201-213.

Haack, B.N., and E.T. Slonecker, 1994. Merged spaceborne radar and Thematic Mapper digital data for locating villages in Sudan. *Photogrammetric Engineering and Remote Sensing*, 60(10):1253-1257.

Haack, B.N., M.A. Bechdol, and L. Isavwa, 1998. Integrating optical and radar data for feature extraction in east Africa. *RADARSAT ADRO Symposium*, Montreal, Canada, Oct. 1998.

Haack, B.N. and M.A. Bechdol, 1999. Multisensor remote sensing data for land cover mapping. *Computers, Environment and Urban Systems*, 23(1):53-69.

Haack, B.N., N.D. Herold, and M.A. Bechdol, 2000. Radar and optical data integration for land-use/land-cover mapping. *Photogrammetric Engineering and Remote Sensing*, 66(6):709-716.

Hagg, W., and M. Sties, 1994. Efficient speckle filtering of SAR images. *IEEE Geoscience and Remote Sensing Symposium, Proceedings IGARSS 1994*, 4:2140-2142.

Haralick, R.M., K. Shanmugan, and I. Dinstein, 1973. Textural features in image classification. *IEEE Transactions on Systems, Man and Cybernetics*, 3:610-621.

Haralick, R.M., 1979. Statistical and structural approaches to texture. *IEEE Proceedings*, 67(5):786-804.

Harris, J. R., R. Murray, and T. Hirose, 1990. IHS transform for the integration of radar imagery and other remotely sensed data. *Photogrammetric Engineering and Remote Sensing*, 56(12):1631-1641.

Hayes, D., and S. Sader, 2001. Comparison of change-detection techniques for monitoring tropical forest clearing and vegetation regrowth in a time series. *Photogrammetric Engineering and Remote Sensing*, 67(9):1067-1075.

Henebry, G. M., and D. R. Rieck, 1996. Applying Principal Components Analysis to image time series: effects on scene segmentation and spatial structure. *IEEE Transaction in Geoscience and Remote Sensing*, 1:448-450.

Herold N. D., B. N. Haack, and E. Solomon, 2005. Radar spatial considerations for land cover extraction. *International Journal of Remote Sensing*, 26(7):1383-1401.

Hill G.J., and G.D. Kelly, 1987. A comparison of existing map products and Landsat for land cover mapping. *Cartography*, 16(1):51-57.

Hoekman, D., F. Amar, and M. Quinones, 1995. Biomass and structure estimation of primary and secondary tropical forests using AirSAR data. *IEEE Geoscience and Remote Sensing Symposium, Proceedings IGARSS 1995*, 1:706-707.

Hoffer, A.M., 1978. Biological and physical considerations in applying computer-aided analysis techniques to remote sensor data, in *Remote Sensing: The Quantitative Approach*, P.H. Swain and S.M. Davis (Eds), McGraw-Hill Book Company, 227-289.

Hollister, J., M.L. Gonzalez, J.F. Paul, P.V. August, and J.L. Copeland, 2004. Assessing the accuracy of national land cover dataset area estimates at multiple spatial extents. *Photogrammetric Engineering and Remote Sensing*, 70(4):405-414.

Hong, T. D., and R. A. Schowengerdt, 2005. A robust technique for precise registration of Radar and optical satellite images. *Photogrammetric Engineering and Remote Sensing*, 71(5):585-593.

Howman A., 1988. The extrapolation of spectral signatures illustrates Landsats' potential to detect wetlands. *IEEE Geoscience and Remote Sensing Symposium, Proceedings IGARSS 1988*, 1:537-539.

Hsu, S., 1978. Texture-tone analysis for automated land-use mapping. *Photogrammetric Engineering and Remote Sensing*, 44(11):1393-1404.

Huang, H., J. Legarsky, and M. Othman, 2007. Land-cover classification using Radarsat and Landsat imagery for St. Louis, Missouri. *Photogrammetric Engineering and Remote Sensing*, 73(1):37-43.

Hussin, Y.A. and R.M. Hoffer, 1990. Swamp forest differentiation with multipolarized and multiple incidence angle l-band radar data. *IEEE Geoscience and Remote Sensing Symposium, Proceedings IGARSS 1990*, 2:573-576.

Imhoff, M., 1995a. A theoretical analysis of the affect of forest structure on synthetic aperture radar backscatter and the remote sensing of biomass. *IEEE Transaction in Geoscience and Remote*, 33(2):341-352.

Imhoff, M., 1995b. Radar backscatter and biomass saturation: ramifications for global biomass inventory. *IEEE Transaction in Geoscience and Remote*, 33(2):510-518.

Imhoff, M., T. Sisk, A. Milne, O. Morgan, and T. Orr, 1997. Remotely sensed indicators of habitat heterogeneity: Use of synthetic aperture radar in mapping vegetation structure and bird habitat. *Remote Sensing of Environment*, 60:217-227.

Israelsson, H., J. Askne, and R. Sylvander, 1994. Potential of SAR for forest bole volume estimation. *International Journal of Remote Sensing*, 15(14):2809-2826.

Jackson M.J., P. Carter, and T.F. Smith, 1980. Urban land mapping from remotely sensed data. *Photogrammetric Engineering and Remote Sensing*, 46(8):1041-1050.

Jensen, J.R., 1996. Introductory digital image processing: A remote sensing perspective, 2nd Edition. Prentice Hall, Upper Saddle River, New Jersey.

Jensen J.R. and D.C. Cowen, 1999. Remote sensing of urban/suburban infrastructure and socio-economic attributes. *Photogrammetric Engineering and Remote Sensing*, 65(5):611-622.

Josse, C., G. Navarro, P. Comer, R. Evans, D. Faber-Langendoen, M. Fellows, G. Kittel, S. Menard, M. Pyne, M. Reid, K. Schulz, K. Snow, and J. Teague, 2003. Ecological Systems of Latin America and the Caribbean: A Working Classification of Terrestrial Systems. NatureServe, Arlington, VA.

Jurgens C., 1997. The modified normalized difference vegetation index (mNDVI) - a new index to determine frost damages in agriculture based on Landsat TM data. *International Journal of Remote Sensing*, 18(17):3583-3594.

Karjalainen, M., H Kaartinen, and J. Hyyppa, 2008. Agricultural monitoring using Envisat alternating polarization SAR images. *Photogrammetric Engineering and Remote Sensing*, 74(1):117-126.

Kasischke, E., 1992. Monitoring changes in above-ground biomass in Loblolly Pine forests using multichannel synthetic aperture radar. Ph.D. thesis, University of Michigan, Ann Arbor.

Kasischke, E., I. Bourgean-Chavez, N. Christenson, and E. Haney, 1994. Observations on the sensitivity of ERS-1 SAR image intensity to changes in above-ground biomass in young loblolly pine forests. *International Journal of Remote Sensing*, 15:3-16.

Kasischke, E., N. Christenson, and I. Bourgean-Chavez, 1995. Correlating radar backscatter with components of biomass in loblolly pine forests. *IEEE Transaction in Geoscience and Remote Sensing*, 30(2):403-411.

Kaup, V.H., W.P. Waite, and H.C. Macdonald, 1982. Incident angle considerations for spacecraft imaging radar. *IEEE Transaction in Geoscience and Remote Sensing*, 20(3):384-389.

Kellndorfer, J.M., H.Xie, F.T. Ulaby, and M. C. Dobson, 1998. Combined multi-temporal ERS-1/JERS-1 imagery for land-cover classification. *IEEE Geoscience and Remote Sensing Symposium, Proceedings IGARSS 1998*, 3:1714-1716.

Kelly N.M., 2001. Changes to the landscape pattern of coastal North Carolina wetlands under the clean water act, 1984-1992. *Landscape Ecology*, 16(1):3-16.

Keys, L.D., N.J. Schmidt, and B.E. Philips, 1990. A prototype example of sensor fusion used for siting analysis. *Technical Papers 1990, ACSM-ASPRS Annual Convention, Image Processing and Remote Sensing*, 4:238-249.

Koeln, G.T., J.D. Dykstra, and D.J. Cunningham, 1999. Geocover and Geocover-LC: orthorectified Landsat TM/MSS data and derived land cover for the world. *International Symposium on Digital Earth*, Nov 29- Dec 2, Beijing, China, Science Press, Beijing.

Kuplich, T. M., P. J. Curran, and P. M. Atkinson, 2005. Relating SAR image texture to the biomass of regenerating tropical forests. *International Journal of Remote Sensing*, 26(21):4829-4854.

Kwarteng, A.Y., V. Singhroy, R. Saint-Jean, and D. Al-Ajmi, 1999. The usefulness of different Radarsat beam modes in the assessment of oil lakes and polluted surfaces in the greater Burgan Oil Field, Kuwait. *Canadian Journal of Remote Sensing*, 25(3):291-301.

Lawrence, W., S., Saatchi, R. DeFries, J. Dietz, R. Rice, L.A. Dietz, M. Siquiera De Araujo, K. Alger, 1995. Utilization of SAR and optical remote sensing data for habitat conservation in the tropical forest of Brazil. *IEEE Geoscience and Remote Sensing Symposium, Proceedings IGARSS 1995*, 2:1480-1482.

Leckie, D. G., 1990. Synergism of synthetic aperture radar and visible/infrared data for forest type discrimination. *Photogrammetric Engineering and Remote Sensing*, 56(9):1237-1246.

Lee, J.H., and W.D. Philpot, 1991. Spectral texture pattern matching: a classifier for digital imagery. *IEEE Transaction in Geoscience and Remote Sensing*, 29(4):545-554. Lee, J.S., 1983. A simple speckle smoothing algorithm for synthetic aperture radar images. *IEEE Transactions in Systematics, Man, and Cybernetics*, 13:85-89.

Lee, J.S., M.R. Grunes, and S.A. Mango, 1991. Speckle reduction in multipolarization, multifrequency SAR imagery. *IEEE Transaction in Geoscience and Remote Sensing*, 29(4):535-544.

Lee, K. S., and R.M. Hoffer, 1990. Analysis of combined Sir-B and TM data for assessing forest biomass. *IEEE Geoscience and Remote Sensing Symposium, Proceedings IGARSS 1990*, 3:1227-1230.

LeToan, T., A. Beaudoin, J. Riom, and D. Guyon, 1992. Relating forest biomass to SAR data. *IEEE Transaction in Geoscience and Remote*, 30(2):403-411.

Lewis A.J., and F.M. Henderson, 1998. Radar fundamentals: The geoscience perspective. In *Principles and Applications of Imaging Radar*, (F.M. Henderson and A.J. Lewis) Wiley, New York, pp 131-181.

Liew, S., 2001. Principles of Remote Sensing. Centre for Remote Imaging, Sensing and Processing (CRISP), National University of Singapore, <http://www.sci-ctr.edu.sg>.

Linke, J. and S. Franklin, 2006. Interpretation of landscape structure gradients based on satellite image classification of land cover. *Canadian Journal of Remote Sensing*, 32(6):367-379.

Lloyd, C., S. Berberoglu, P. Curran, and P. Atkinson, 2004. A comparison of texture measures for the per-field classification of Mediterranean land cover. *International Journal of Remote Sensing*, 25(19):3943-3965.

Lozano-Garcia, D.F., and R.M. Hoffer, 1993. Synergistic effects of combined Landsat-TM and SIR-B data for forest resource assessment. *International Journal of Remote Sensing*, 14(14):2677-2694.

Lu, D., 2005. Above-ground biomass estimation using Landsat TM data in the Brazilian Amazon. *International Journal of Remote Sensing*, 26(12): 2509-2525.

Lu, D., and Q. Wang, 2005. Urban Classification Using Full Spectral Information of Landsat EMT+ Imagery in Marion County, Indiana. *Photogrammetric Engineering and Remote Sensing*, 71(11):1275-1284

Lu, D., M. Batistella, and E. Moran, 2005. Satellite Estimation of Aboveground Biomass and Impacts of Forest Stand Structure. *Photogrammetric Engineering and Remote Sensing*, 71(8):967-974

Lu, Y.H., S.Y. Tan, T.S. Yeo, W.E. Ng, I. Lim, and C.B. Zhang, 1996. Adaptive filtering algorithms for SAR speckle reduction. *IEEE Geoscience and Remote Sensing Symposium, Proceedings, IGARSS 1996*, 1:67-69.

Lu, Y.H., Y.L. Yoh, T.S. Yeo, and C.B. Zhang, 1997. Speckle reduction by wavelet transform. *Asia-Pacific Microwave Conference Proceedings, APMC 1997*, 3:1017-1020.

Luckman, A., A.C. Frery, C.C.F. Yanass, and G.B. Groom, 1997. Texture in Airborne SAR imagery of tropical forest regeneration stage. *International Journal of Remote Sensing*, 18(6):1333-1349.

Lunetta, R., and M. Balogh, 1999. Application of multi-temporal Landsat 5 TM imagery for wetland identification. *Photogrammetric Engineering and Remote Sensing*, 65 (11):1303-1310.

Mejail M. E., J. C. Jacobo-Berlles, A. C. Frery, and O. H. Bustos, 2003. Classification of SAR images using a general and tractable multiplicative model. *International Journal of Remote Sensing*, 24(18):3565-3582.

Miles, V. V., L. P. Bobylev, S. V. Maximov, O. M. Johannessen, and V. M. Pitulko, 2003. An approach for assessing boreal forest conditions based on combined use of satellite SAR and multi-spectral data. *International Journal of Remote Sensing*, 24(22):4447-4466.

Milne, A.K., G. Horn, and M. Finlayson, 2000. Monitoring wetlands inundation patterns using Radarsat multitemporal data. *Canadian Journal of Remote Sensing*, 26(2):133-141.

Miranda, F.P, L.E. Fonseca, J.R. Carr, and J.V. Taranik, 1996. Analysis of JERS-1 (Fuyo-1) SAR data for vegetation discrimination in northwestern Brazil using the Semivariogram Texture Classifier (STC). *International Journal of Remote Sensing*, 17(17):3523-3529.

Mladenoff D.J., G.J. Niemi, and M.A. White, 1997. Effects of changing landscape pattern and USGS land cover data variability on ecoregion discrimination across a forest-agriculture gradient. *Landscape Ecology*, 12(6):379-396.

Morain, S.A., and Budge, A.M. (editors), 1997. *The Manual of Remote Sensing, 3rd edition - Volume 1: Earth Observing Platforms & Sensors*, John Wiley & Sons.

Muñoz-Villers, L. E. and J. López-Blanco, 2007. Land use/cover changes using Landsat TM/ETM images in a tropical and biodiverse mountainous area of central-eastern Mexico. *International Journal of Remote Sensing*, 29(1):71-93.

Myint, S., 2003. Fractal approaches in texture analysis and classification of remotely sensed data: comparisons with spatial autocorrelation techniques and simple descriptive statistics. *International Journal of Remote Sensing*, 24(9):1925-1947.

Nemani, R., and S.W. Running, 1996. Implementation of a hierarchical global vegetation classification in ecosystem function models. *Journal of Vegetation Science*, 7:337-346.

Nezry, E., A. Lopes, and R. Touzi, 1991. Detection of structural and textural features for SAR image filtering. *IEEE Geoscience and Remote Sensing Symposium, Proceedings IGARSS 1991*, 4:2169-2172.

Nezry, E., E. Mougin, A. Loes, J.P. Gastellu-Etchegorry, and Y. Laamonier 1993. Tropical vegetation mapping with combined visible and SAR spaceborne data. *International Journal of Remote Sensing*, 14:2165-2184.

Nicholas, J.M., F. Tupin, and H. Maitre, 2001. Smoothing speckled SAR images by using maximum homogenous region filters: an improved approach. *IEEE Geoscience and Remote Sensing Symposium, Proceedings IGARSS 2001*, 3:1503-1505.

Nyoungui A., E. Tonye, and A. Akono, 2002. Evaluation of speckle filtering and texture analysis methods for land cover classification from SAR images. *International Journal of Remote Sensing*, 23(9): 1895-1925.

Paris, J.F., and H.H. Kwong, 1988. Characterization of vegetation with combined Thematic Mapper (TM) and Shuttle Imaging Radar (SIR-B) image data. *Photogrammetric Engineering and Remote Sensing*, 54(8):1187-1193.

Parmuchi, M. G., H. Karszenbaum, and P. Kandus, 2002. Mapping wetlands using multi-temporal RADARSAT-1 data and a decision-based classifier. *Canadian Journal of Remote Sensing*, 28(2):175-186.

Pierce L., M. H. Xie, M.C. Dobson, and F. Ulaby, 1998. Texture features for classification with ERS/JERS composites. *IEEE Geoscience and Remote Sensing Symposium, Proceedings IGARSS 1998*, 1:324-326.

Plaut, J., B. Rivard, and M. D'Iorio, 1999. Radar: Sensors and case studies, in *Remote Sensing for the Earth Sciences*, A. Rencz (Ed), John Wiley and Sons, Inc., 613-642.

Pohl, C., 1996. Geometric Aspects of multisensor fusion for topographic map updating in the humid Tropics. *ITC Publication No. 39*.

Pohl, C. and J. L. van Genderen, 1998. Multisensor image fusion in remote sensing: concepts, methods and applications. *International Journal of Remote Sensing*, 19(5):823-854.

Pope, K., J. Rey-Benayas, and J. Paris, 1994. Radar remote sensing of forest and wetland ecosystems in the Central American tropics. *Remote Sensing of Environment*, 48(2):205-219.

Price, K. P., X. Guo, and J. M. Stiles, 2002. Optimal Landsat TM band combinations and vegetation indices for discrimination of six grass land types in eastern Kansas. *International Journal of Remote Sensing*, 23(23): 5031-5042.

Proisy C., E. Mougin, F. Fromard, V. Trichon, and M. A. Karam, 2002. On the influence of canopy structure on the radar backscattering of mangrove forests. *International Journal of Remote Sensing*, 23(20):4197-4210.

Raghavawamy, V., N. C. Gautam, M. Padmavathi, and K. V. S. Badarinath, 1996. Studies on microwave remote sensing data in conjunction with optical data for land use/land cover mapping and assessment. *Geocarto International*, 11(4):25-31.

Ranson, K., and Sun, G. 1994. Northern forest classification using temporal multifrequency and multipolarimetric SAR images. *Remote Sensing of Environment*, 47:142-153.

Ranson, K., S. Saatchi, and G. Sun, 1995. Boreal forest ecosystem characterization with SIR-C/X-SAR. *IEEE Transaction in Geoscience and Remote Sensing*, 33(4):867-876.

Rany. K., 1998. Radar fundamentals: Technical Perspective, in *Principles and Applications of Imaging Radar*, F. Henderson and A. Lewis (Eds), John Wiley and Sons, Inc., 9-130.

Rauste, Y., 2005. Multi-temporal JERS SAR data in boreal forest biomass mapping. *Remote Sensing of Environment*, 97(2):263-275.

Rheault, M., R. Simard, C. Garneau, and V.R. Slaney, 1991. SAR Landsat TM – Geophysical data integration utility of value – added products in geological exploration. *Canadian Journal of Remote Sensing*, 17(2):185-190.

Rignot, E., C. Williams, J. Way, and L. Viereck, 1994. Mapping forest types in Alaskan boreal forest using SAR imagery. *IEEE Transaction in Geoscience and Remote Sensing*, 32:1051-1059.

Riou, R., and F. Seyler, 1997. Texture analysis of tropical rain forest infrared satellite images. *Photogrammetric Engineering and Remote Sensing*, 63(5):515-521.

Rogers, R.H. and L. Wood, 1990. The history and status of merging multiple sensor data: an overview. *Technical Papers, ACSM-ASPRS Annual Convention 1990, Image Processing and Remote Sensing*, 4:352-360.

Running, S., R. Nemani, D. Peterson, L. Band, D. Potts, L. Pierce, and M. Spanner, 1989. Mapping regional forest evapotranspiration and photosynthesis by coupling satellite data with ecosystem simulation. *Ecology*, 70(4):1090-1101.

Saatchi, S., J. Soares, and D. Alves, 1996. Mapping deforestation and land use in Amazon rainforest using SIR-C Imagery. *Remote Sensing of Environment*, 59:191-202.

Saatchi, S., and E. Rignot, 1997. Classification of boreal forest cover types using SAR images. *Remote Sensing of Environment*, 60:270-281.

Sader, S., R. Waide, W. Lawrence, and A. Joyce, 1989. Tropical forest biomass successional age class relationships to a vegetation index derived from Landsat TM data. *Remote Sensing of Environment*, 28():143-156

Saxby, G., 2002. *The Science of Imaging*. Institute of Physics Publishing Inc., London .

Schistad, A.H. and A.K. Jain, 1992. Texture analysis in the presence of speckle noise. *IEEE Geoscience and Remote Sensing Symposium, Proceedings IGARSS 1992*, 2:884-886.

Schistad-Solberg, A., A. Jain and T. Taxt, 1994. Multisource classification of remotely sensed data: fusion of Landsat TM and SAR images. *IEEE Transaction in Geoscience and Remote Sensing*, 32(4):768-778.

Schriever, J. R., and R.G. Congalton, 1995. Evaluation seasonal variability as an aid to cover-type mapping from Landsat Thematic Mapper data in the Northeast. *Photogrammetric Engineering and Remote Sensing*, 61(8):321-327.

Sealey, K., 2003. Coastal Zone Classification System. *University of Miami*, unpublished manuscript.

Sheng, Y. and Z.G. Xia, 1996. A comprehensive evaluation of filters for radar speckle suppression. *IEEE Geoscience and Remote Sensing Symposium, Proceedings IGARSS 1996*, 3:1559-1561.

Shimabukuro, Y., R. Almeida-Filho, T. Kuplich, and R. Freitas, 2007. Quantifying optical and SAR image relationships for tropical landscape features in the Amazônia. *International Journal of Remote Sensing*, 28(17):3831-3840.

Shimada, M., 2005. Long-term stability of L-band normalized radar cross section of Amazon rainforest using the JERS-1 SAR. *Canadian Journal of Remote Sensing*, 31(1):132-137.

Smith, A.M., D.J. Major, C.W. Lindwall, and R.J. Brown, 1995. Multi-temporal, multi-sensor remote sensing for monitoring soil conservation farming. *Canadian Journal of Remote Sensing*, 21(2):177-184.

Smith, D. M. 1996. Speckle reduction and segmentation of synthetic aperture radar images. *International Journal of Remote Sensing*, 17(11):2043-2057.

- Solaiman, B., L.E. Pierce, and F.T. Ulaby, 1999. Multisensor data fusion using fuzzy concepts: Application to land-cover classification using ERS-1/JERS-1 SAR composites. *IEEE Transaction in Geoscience and Remote Sensing*, 37(3):1316-1326.
- Stern A.J., P.C. Doralswamy, and P.W. Cook, 2001. Spring wheat classification in an AVHRR image by signature extension from a Landsat TM classified image. *Photogrammetric Engineering and Remote Sensing*, 67(2):207-211.
- Strobl, D., J. Raggam, and M.F. Buchroithner, 1990. Terrain correction geocoding of a multi-sensor image data set. *Proceedings 10th EARSeL Symposium*, Toulouse, France (Paris: European Space Agency), pp. 98-107.
- Stromberg, W.D., and T.G. Farr, 1986. A Fourier-based textural feature extraction procedure. *IEEE Transactions on Geoscience and Remote Sensing*, 24(5): 722-731.
- Suites, G., W. Malila, and T. Weller, 1988. Procedures for using signals from one sensor as substitutes for signals of another. *Remote Sensing of Environment*, 25:395-408.
- Tanaka, S., K. Takasaki, T. Yamanokuchi, and K. Kameda, 1999. Radarsat and TM data fusion for urban structure analysis. *Canadian Journal of Remote Sensing*, 25(1):80-84.
- Thomlinson J.R., P.V. Bolstad, and W.B. Cohen, 1999. Coordinating methodologies for scaling landcover classifications from site-specific to global: Steps toward validating global map products. *Remote Sensing of Environment*, 70(1):16-28.
- Tottrup, C., 2004. Improving tropical forest mapping using multi-date Landsat TM data and pre-classification image smoothing. *International Journal of Remote Sensing*, 25(4): 717-730.

Townsend, P., 2001. Mapping seasonal flooding in forested wetlands using multi-temporal Radarsat SAR. *Photogrammetric Engineering and Remote Sensing*, 67(7):857-864.

Townsend, P. A., 2002. Estimating forest structure in wetlands using multitemporal SAR. *Remote Sensing of Environment*, 79(2-3):288-304.

Treitz, P.M., P.J. Howarth, O.R. Filho, and E.D. Soulis, 2000. Agricultural crop classification using SAR tone and texture statistics. *Canadian Journal of Remote Sensing*, 26(1):18-29.

Uça Z. D., F. Erbek, L. Kuşak, F. Yaşa, and G. Özden, 2006. The use of optic and radar satellite data for coastal environments. *International Journal of Remote Sensing*, 27(17):3739-3747.

Ulaby, F.T., R.Y. Li and K.S. Shanumgan, 1982. Crop classification using airborne radar and Landsat data. *IEEE Transactions on Geoscience and Remote Sensing*, 20(1):42-50.

Van Genderen, J.L, and C. Pohl, 1994. Image fusion, issues, techniques and applications. *Intelligent Image Fusion, Proceedings EARSeL Workshop, Strasbourg France, 11 September 1994*, edited by, J.L. Van Genderen and V. Cappellini (Enschede: ITC), pp. 18-26.

Verhoeve, J. and R. De Wulf, 1999. An image processing chain for land-cover classification using multitemporal ERS-1 data. *Photogrammetric Engineering and Remote Sensing*, 65(10):1179-1186.

Vidal-Pantaleoni, A., and D. Martí, 2004. Comparison of different speckle-reduction techniques in SAR images using wavelet transform. *International Journal of Remote Sensing*, 25(22):4915-4932.

Vogelmann J.E., T. Sohl, and S.M. Howard, 1998. Regional characterization of land cover using multiple sources of data. *Photogrammetric Engineering and Remote Sensing*, 64(1):45-57.

Wakabayashi, H. and K. Arai, 1996. A new method for SAR speckle noise reduction (CST Filter). *Canadian Journal of Remote Sensing*, 22(2):190-197.

Wall S.L., R.W. Thomas, and C.E. Brown, 1984. Landsat-based inventory system for agriculture in California. *Remote Sensing of Environment*, 14:267-278.

Wang, J., J. Shang, B. Brisco, and R.J. Brown, 1998. Evaluation of multi date ERS-1 and multispectral Landsat imagery for wetland detection in southern Ontario. *Canadian Journal of Remote Sensing*, 24(1):60-68.

Wang, L. and D. C. He, 1990. A new statistical approach for texture analysis. *Photogrammetric Engineering and Remote Sensing*, 56(1):61-66.

Wang, Y., F. Davis, J. Melack, E. Kasischke, and N. Christenson, 1995. The effects of changes in forest biomass on radar backscatter from tree canopies. *International Journal of Remote Sensing*, 16:503-513.

Welch, R. and M. Ehlers, 1988. Cartographic feature extraction with integrated SIR-B and Landsat TM images. *International Journal of Remote Sensing*, 9(5):873-889.

Weydahl, D. J., 2002. Backscatter changes of urban features using multiple incidence angle RADARSAT images. *Canadian Journal of Remote Sensing*, 28(6):782-793.

Wigneron, J., D. Guyon, J. Calvet, G. Courier, and N. Bruguier, 1997. Monitoring coniferous forest characteristics using a multi frequency (5-90 GHz) microwave radiometer. *Remote Sensing of Environment*, 60:299-310.

Williams, C., E. Rignot, K. McDonald, L. Viereck, A. Balsler, and J. Way, 1994. An ecological approach to radar mapping of biomass in interior Alaska boreal forests. *IEEE International Geoscience and Remote Sensing Symposium, Proceedings IGARSS 1994*, 4:2140-2142.

Wood, D., H. McNairnb, R. J. Brown, and R. Dixon, 2002. The effect of dew on the use of RADARSAT-1 for crop monitoring: Choosing between ascending and descending orbits. *Remote Sensing of Environment*, 80(2):241-247.

Wu, W., and G. Shao, 2002. Optimal combinations of data, classifiers, and sampling methods for accurate characterizations of deforestation. *Canadian Journal of Remote Sensing*, 28(4):601-609.

Xia, Z.G., 1996. Application of multi-frequency, multi-polarization and multi-incident angle SAR systems in urban land use and land cover mapping. *IEEE Geoscience and Remote Sensing Symposium, Proceedings IGARSS 1996*, 4:2310-2314.

Xiao J., J. Li, and A. Moody, 2003. A detail-preserving and flexible adaptive filter for speckle suppression in SAR imagery. *International Journal of Remote Sensing*, 24(12):2451-2465.

Xie, H., L.E. Pierce, M.C. Dobson and F.T. Ulaby, 1998. Combining orbital SAR and optical data for global classification. *IEEE Geoscience and Remote Sensing Symposium, Proceedings IGARSS 1998*, 3:1599-1601.

Xie, H., F.T. Ulaby, L.E. Pierce, and M.C. Dobson, 1999. Performance metrics for SAR speckle-suppression filters. *IEEE Geoscience and Remote Sensing Symposium, Proceedings IGARSS 1999*, 3:1540-1542.

Xu, B., and P. Gong, 2007. Land-Use/Land-Cover classification with multispectral and hyperspectral EO-1 Data. *Photogrammetric Engineering and Remote Sensing*, 73(8):955-965.

Zaitsev, V.V. and V.V. Zaitsev, 1996. Analysis of MAP speckle suppression algorithms. *IEEE Geoscience and Remote Sensing Symposium, Proceedings IGARSS 1996*, 1:363-365.

Zhu, L., and R. Tateishi, 2000. Integration of multisensor multitemporal satellite data for agricultural vegetation mapping. *21st Asian Conference on Remote Sensing*, Taipei, Taiwan, December 2000.

Zhu, L., and R. Tateishi, 2006. Fusion of multisensor multitemporal satellite data for land cover mapping. *International Journal of Remote Sensing*, 27(5):903-918.

CURRICULUM VITAE

Erwin Villiger holds a Masters of Science in Geographic and Cartographic Sciences and a Bachelor's of Arts in Geography, both from George Mason University. He has worked in the geospatial technologies field in government, academia, and private industry with twenty years of experience. In 1999 he founded Global View Inc., a GIS and remote sensing consulting firm, and serves as president and CEO.